UTS UNIVERSITY OF TECHNOLOGY SYDNEY

VOLATILE FATTY ACID AND WATER EXTRACTION FROM RUMEN FLUID BY FORWARD OSMOSIS

By Jamshed Ali Khan

Thesis submitted in fulfilment of the requirements
for the degree of

Doctor of Philosophy

under the supervision of Professor Long D. Nghiem and
Professor Hokyong Shon

University of Technology Sydney
Faculty of Engineering and Information Technology
April 2021

This thesis is dedicated to my wife

Dr Shabana Ghaffar

For her priceless love and consistent support

Certificate of Original Authorship

I, **Jamshed Ali Khan** declare that this thesis is submitted in fulfilment of the requirements of the award of **Doctor of Philosophy**, in the School of Civil and Environmental Engineering at the University of Technology Sydney.

I also certify that the work in this thesis has not previously been submitted for a degree nor it has been submitted as part of requirements for a degree except as fully acknowledged within the text.

This thesis is wholly my own work unless otherwise reference or acknowledged. Any help that I have received in my research and preparation of the thesis has been acknowledged. Besides, I certify that all information sources and literature used are indicated in the thesis. This research is supported by the Australian Government Research Training Program.

Production Note:
Signature removed prior to publication.

Signature of student

Date: 01 April 2021

Acknowledgements

This dissertation would have not been possible without the guidance and the support of several individuals who, in one way or another, contributed to my PhD journey and the completion of my research work.

First of all, I would like to express my heartiest gratitude and appreciation to my principal supervisor, Prof. Long D. Nghiem for his untiring support and guidance throughout my PhD journey. I found him not only a good supervisor but a great human being and an inspiring mentor who motivated me with his leadership to strive hard for the best outcomes. Besides, his encouragement and immense knowledge helped me a lot to conquer the challenges during my research work and thesis writing. I consider myself extremely lucky to work under his supervision and share this challenging but wonderful expedition with him.

I would like to appreciate and thank my co-supervisor, Prof. Hokyong Shon for his consistent encouragement and support during my PhD studies. I truly admire his valuable feedback on my research work.

I cannot forget to extend my sincere gratitude to the co-authors of my research work including Dr Luong N. Nguyen, Dr Hung C. Duong, Mr Minh T. Vu, and Miss Quynh Anh Nguyen. I want to acknowledge Dr Luong's help in performing ion chromatography analysis while Dr Hung was of great help to improve my technical writing skills. I greatly appreciate Mr Minh's assistance in performing the SEM and EDS analyses and Miss Quynh's support for DNA extraction and 16S rRNA sequencing. The much-needed encouragement from my colleagues; Dr Lei Zheng, Mr Asif Iqbal Khan, and Miss Chelsey Vu is highly appreciated. My heartiest gratitude covers all the laboratory staff for their help and support. I also want to thank the Higher Education Commission, the

University of Wollongong, and the University of Technology Sydney for their financial assistance and support.

Last but not least, I would also like to express my sincere gratitude to all of my family members especially my mother, Noor Jahan and my brother, Noor Ul Islam for their constant encouragement and love during my studies.

Research Outcome Summary

Journal papers

1) **Khan JA**, Shon HK, Nghiem LD. From the Laboratory to Full-Scale Applications of Forward Osmosis: Research Challenges and Opportunities. Current Pollution Reports. 2019;5(4):337-52.
2) **Khan JA**, Nguyen LN, Duong HC, Nghiem LD. Acetic acid extraction from rumen fluid by forward osmosis. Environmental Technology & Innovation. 2020;20:101083.
3) **Khan JA**, Vu MT, Nghiem LD. A preliminary assessment of forward osmosis to extract water from rumen fluid for artificial saliva. Case Studies in Chemical and Environmental Engineering. 2021:100095.

In-preparation Journal Paper

4) **Khan JA**, Nguyen AQ, Vu MT, Shon HK, Nghiem LD. Biofouling characterization and evaluation of membrane cleaning techniques in a forward osmosis process to dewater rumen fluid. Journal of Membrane Science (in preparation)

Table of Contents

List of Figures

List of Tables

List of Abbreviations

Abbreviation	Meaning
AOC	Assimilable organic carbon
CFV	Cross flow velocity
CTA	Cellulose triacetate
DI	Deionized
ECP	External concentration polarization
EDTA	Ethylene diamine tetra-acetic acid
EDX	Energy dispersive X-ray
EPS	Extracellular polymeric substances
FO	Forward osmosis
FTIR	Fourier transformed infrared
gMH	$g/m^2.h$
ICP	Internal concentration polarization
IP	Interfacial polymerization
LMH	$L/m^2.h$
MBR	Membrane bioreactor
MD	Membrane distillation
MED	Multi-effect distillation
MF	Microfiltration
mgMH	$mg/m^2.h$
MPD	M-phenylenediamine
MSF	Multi-stage flash
NF	Nanofiltration
NMP	N-methyle-2-pyrrolidone

PA	Polyamide
PAI	Polyamide-imide
PcoA	Principal coordinates analysis
PEI	Polyethyleneimine
PES	Polyethersulfone
PET	Polyethylene terephthalate
PRO	Pressure retarded osmosis
PSF	Poysulfone
RO	Reverse osmosis
RSF	Reverse solute flux
SEM	Scanning electron microscopy
SRSF	Specific reverse solute flux
TDS	Total dissolved solids
TFC-PA	Thin-film composite polyamide
TMC	Trimesoyl chloride
UF	Ultrafiltration
VFAs	Volatile fatty acids
VS	Volatile solids

Abstract

Nature offers elegant, efficient, and sustainable solutions to most of our problems. One such problem is to convert the most abundant natural resource of lignocellulosic biomass into a fermented solution for subsequent biochemicals extraction. An efficient, economical and eco-friendly technique or system has not been developed yet to address this problem. Nature has offered a robust solution to this problem in the form of ruminant's digestive system where a fermented solution (rumen fluid) is produced from the digestion of biomass in the fore-stomach (or rumen) with the help of diverse microbiota followed by volatile fatty acids (VFAs) absorption from the rumen fluid in the small intestine along with water absorption in the omasum and large intestine. This study aims to replicate the two important processes taking place inside the ruminant's digestive system with a membrane-based forward osmosis (FO) process. First is the use of FO for acetic acid extraction from rumen fluid by mimicking the VFAs absorption in the small intestine and second is employing FO for dewatering of rumen fluid by simulating the water absorption in the omasum and the large intestine. Besides, this study also covers the membrane biofouling that can occur as a result of resource recovery from rumen fluid in a long term FO operation and evaluates the various membrane cleaning strategies for flux recovery.

Unlike other FO applications to extract water and reduce the feed water volume, this study used FO to mimic the ruminant’s small intestine for extracting acetic acid from rumen fluid to a clean matrix with a minimum water flux. Membrane characterisation results showed better separation performance by the thin-film composite polyamide (TFC-PA) membrane in terms of pure water permeability, solute rejection, and structural parameter compared to the cellulose triacetate (CTA) membrane. This was further endorsed by the higher acetic acid transport through the CTA membrane than the TFC-PA membrane.

Increasing the stripping solution pH from 5.5-6.5 to 9.0-10.0 increased the acetic acid transport through both the CTA and TFC-PA membranes. On the other hand, the membrane orientation had no discernible effect on the transport of acetic acid. Under the optimum conditions, the FO process using the CTA membrane exhibited negligible water flux and extracted 27% of the maximum attainable acetic acid from the synthetic solution within 8 hours of operation. The optimised conditions were used to elaborate the FO extraction of acetic acid from a real rumen fluid. Considerably lower extraction rate from the real rumen fluid was observed compared to the synthetic solution.

This study also explored the use of FO for extracting water from the rumen fluid by replicating the dewatering function of the large intestine and omasum in ruminant animals. The reference artificial saliva solution was determined by comparing its osmotic pressure to that of the rumen fluid. The concentrated saliva showed good pH buffering capacity with no significant pH changes during FO operation. High water flux and a low reverse solute flux (RSF) were observed using concentrated artificial saliva as a draw solution and clean water as the feed. However, the water flux decreased and the RSF increased significantly when rumen fluid was used as the feed. Membrane fouling was observed with the deposition of mainly biomolecules from the rumen fluid on the membrane surface and the high temperature of feed solution further exacerbated membrane fouling. Membrane fouling was evidenced by visual examination as well as scanning electron microscope (SEM), energy dispersive X-ray (EDX), and Fourier transformed infrared (FTIR) analysis of the membrane surface.

Membrane biofouling was investigated in a long term FO operation for water extraction from rumen fluid. Three of the possible membrane module configurations were used to assess their effect on the membrane fouling. In the horizontal membrane module configurations, the circulation of the feed solution on top of the membrane cell led to

more severe fouling compared to that from the bottom of the membrane module. The best resistance to fouling was observed in the vertical configuration of the membrane module. The results suggest that fouling is driven mostly by the gravity-driven deposition of foulants on the membrane surface. This was evidenced by the SEM-EDX and FTIR analyses of the fouling layers. The biofouling phenomenon was further characterized using the bioinformatics analysis of the inoculum, feed solution, and fouling layer microbial communities. A distinct biofilm microbial community with lower diversity and different composition from other samples were observed when feed solution was on top in the membrane module, due to the thick and more mature fouling layer. Aerobic and facultatively anaerobic microbial species such as *Pseudomonadaceae, Xanthomonadaceae* and *Arcobacteraceae* that were not detected in the inoculum emerged in the feed and thrived in biofilms under all membrane module configurations. Among these species, *Pseudomonadaceae* and *Xanthomonadaceae* were the most abundant, and both have been previously reported to possess superior attachment and biofilm-forming capacity. Different membrane cleaning techniques including hydraulic cleaning, osmotic backwashing, and chemical cleaning were applied to remove membrane fouling. A combination of chemical cleaning using 0.1% NaOCl and osmotic backwashing using NaCl 1M solution was found to be most effective with 70.0% flux recovery while hydraulic cleaning was the least effective that could only recover 14.1% flux. While the results are still preliminary, they highlight the potential for effective control of membrane fouling during water extraction from rumen fluid by FO.

Chapter 1 Introduction

1.1 Background

As the global population continues to grow, the demand for the earth's resources has increased significantly [1]. A UN report (2019) estimates that the global population will reach 9.7 billion people by 2050. Hence, there is an urgent need for securing essential resources like food, water and energy to support the expected population growth. The worldwide energy demand is increasing due to population expansion, climate change and ever-growing urbanization. Furthermore, the depletion of global fuel reserves (fossil fuels) and the increased pollution from its consumption is making the situation worse. It is a necessity to explore new and renewable resources for the long term sustainability of human life on earth.

Lignocellulosic biomass is a rich resource from which biofuels, biochemicals and other potential by-products can be generated. It is being investigated as a renewable energy resource that can be used to overcome the global energy crisis [2, 3]. Lignocellulosic material is the most abundant biomass available on Earth [4, 5]. It is an exceptional medium that is biocompatible, renewable, biodegradable and environmental friendly [6]. Various chemical and biological approaches can convert lignocellulosic materials to valuable products such as volatile fatty acids (VFAs), methane, ethanol, butanol, and hydrogen [7-9]. VFAs and methane can be recovered by the anaerobic digestion of lignocellulosic feed, where the residual mass can be utilized as a fertilizer [9].

Lignocellulose is a plant-based material that mainly includes grass, hay, and a range of crop and forestry residues [10, 11]. It is composed of cellulose (35-50%), hemicellulose (20-35%) and lignin (10-25%). The remaining fraction includes protein, oil and ash [2]. It is a tough fibrous material with a complex structure that contributes to its hydrolytic stability, structural strength and resistance to microbial degradation [12]. Furthermore,

the cross-linking between cellulose and hemicellulose with lignin via ester and ether linkages makes it resistant to enzymatic, microbial and chemical degradation [13, 14]. Ruminants are the only animals capable of utilising lignocellulose in their diets.

Ruminants are specialist animals that can digest lignocellulosic materials. The rumen in these animals acts as a natural cellulose-degrading system [15]. It accomplishes this task efficiently with the help of its diverse microbiota including bacteria, fungi, protozoa, archaea and viruses [16]. They degrade the lignocellulosic biomass and converts it into proteins and VFAs [17, 18]. Due to this, rumen has attracted immense interest among scientists worldwide. To evaluate the rumen's digestibility, they are investigating the composition and specific function of these complex microbial communities. Rumen as a source of enzymes has also been investigated for its biorefinability and as a model that can lead to revolutionizing metabolic engineering [19].

After rumen fluid formation in the rumen, the ruminant animals absorb the energy-rich VFAs from the rumen fluid in their small intestine to meet the energy requirements of their bodies. Following that, the omasum and large intestine extract the maximum amount of water from the rumen fluid before it is excreted outside in the form of animal waste. Just like rumen fluid formation in the rumen, these two processes of VFAs absorption followed by water absorption have stimulated interest in simulating these processes in vitro. Different membrane and non-membrane based processes have been used for extracting solutes and/or clean water from the wastewater such as sand filtration, bio-flocculation, nanofiltration (NF), and reverse osmosis (RO). However, these processes are either inefficient and/or expensive. Therefore, a more advanced, technically viable, and economically affordable process is needed to process complex solutions like rumen fluid. This study proposes forward osmosis (FO) as the most feasible option to extract acetic acid and water from the rumen fluid.

An emerging membrane technology, FO has gained considerable attention in desalination and wastewater treatment. It has been extensively studied for various processes including wastewater treatment, food processing, pharmaceutical processes and water recovery from drilling mud [20-24]. FO is a process based on the osmotic pressure gradient between two solutions that are separated by a semi-permeable membrane. Unlike conventional membrane technologies, FO uses a naturally generated osmotic gradient as a driving force for transporting water/solutes across the membrane. It does not employ any external energy input for transporting water and/or solutes across the membrane and is therefore economically more viable. Due to the absence of external pressure, there is a lower tendency to membrane fouling and the fouling is easily reversible.

1.2 Economic assessment of lignocellulose conversion to VFAs

This section provides a preliminary economic analysis to illustrate the lignocellulosic biomass as an alternative to fossil resources for the production of VFAs and the potential economic viability of this approach. The material flow of lignocellulosic biomass to VFAs conversion via rumen reactor and subsequent extraction by the FO system is described in Figure 1.1.

Lignocellulose is the most abundant natural resource of biomass on earth. The estimated global lignocellulosic biomass production is 200 billion tons per year [25]. Even at a conservative estimate that only 7% of this biomass is available at an industrial scale for VFA production [25], this would amount to 14 billion tons/year. After collection, the lignocellulosic biomass is pre-treated by physical, chemical, and biological processes to improve its digestibility. Pre-treatment can account for about a 9% loss of the lignocellulosic biomass [26], resulting in 12.7 billion tons/year for VFA production. The volatile solids (VS) content varies for different types of lignocellulosic biomass. For example, the VS content in maize silage is 87.8% [27]. While the VS content in

agricultural residua of other crops can be as high as 90% [28], a more conservative estimate of 80% VS content is selected here for further calculation, resulting in 10.2 billion tons of VS per year. Each kg of VS can produce 438g of VFAs [27]. In other words, about 4.5 billion tons of VFAs can be produced from lignocellulosic biomass per year. For simplification, acetic acid is used to represent VFAs in this preliminary economic assessment. Acetic acid extraction from the aqueous phase (i.e. rumen fluid) can reach about 90% efficiency to produce 4 billion tons/year of acetic acid. This is more than 250 times the current global consumption of acetic acid (of 15 million tons per year; according to a market report from mordorintelligence.com).

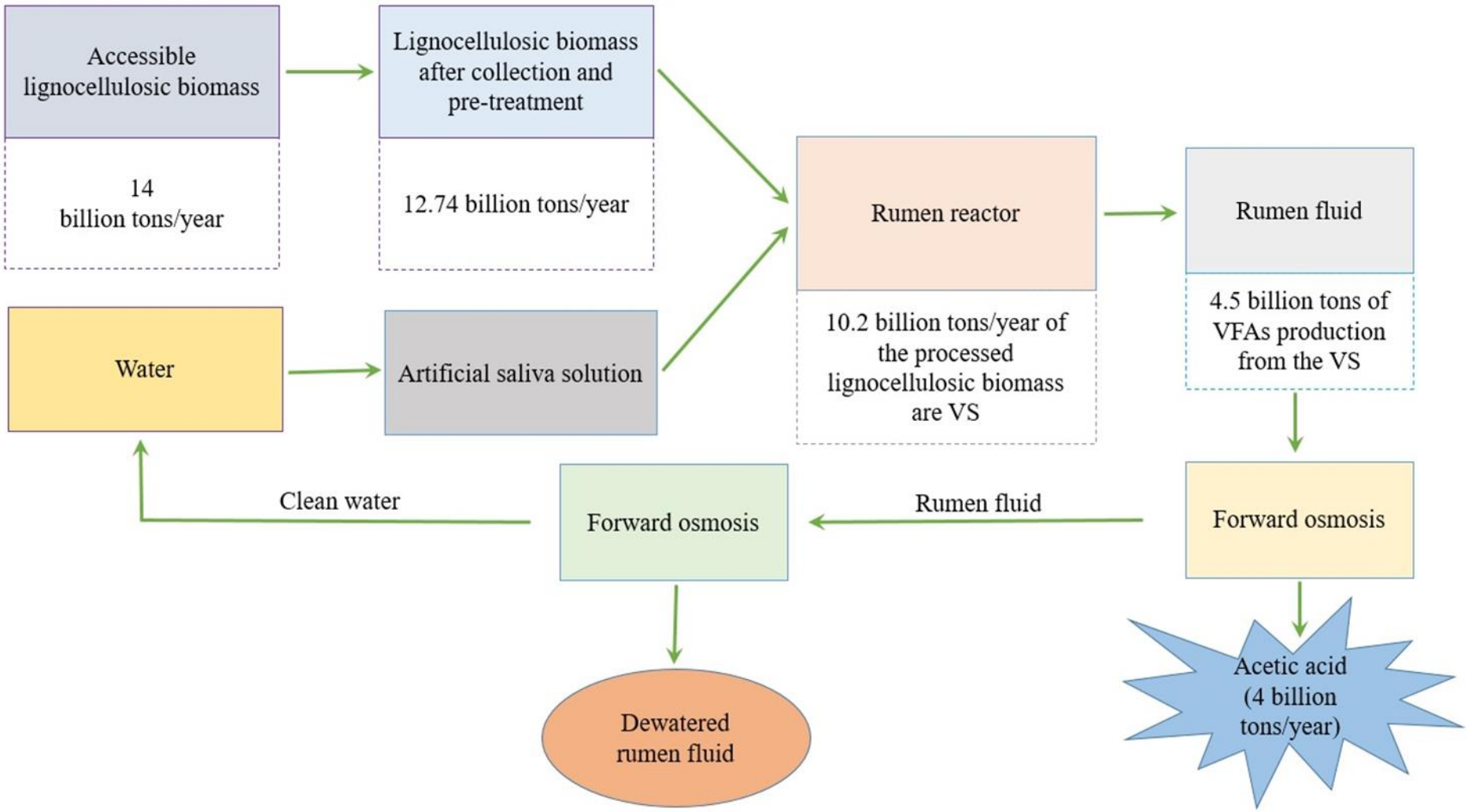

Figure 1.1: Flow chart of VFAs production potential from all the available lignocellulosic biomass and their extraction by the FO system

A hypothetical rumen factory that produces acetic acid with an input capacity of 100,000 tons/yr is used to analyse the economic viability of VFA production from lignocellulosic biomass. The service life of this factory is set at 20 years. Using the same data presented in Figure 1.1, a high-level analysis of the revenue and expenditure of the factor is presented in Table 1.1. According to Figure 1.1, 100,000 tons of processed lignocellulosic material would possess 80,000 tons of VS content which could produce 35,000 tons of acetic acid per year in a rumen reactor. The total VFAs concentration in rumen fluid is about 0.1M or 5 g/L [29]. Therefore, the potential of rumen fluid production per year in a rumen reactor is 7 million tons. This shows that a rumen reactor with a lignocellulosic material processing capacity of 100,000 tons/year would require an FO system with 7 million tons of rumen fluid processing per year capacity. The FO system with 7 million tons of rumen fluid processing capacity would separate 31,400 tons of acetic acid from the rumen fluid annually (Figure 1.1).

The net profit of the extracted acetic acid was calculated by subtracting the total cumulative cost (capital and operational costs) of all the equipment and processes involved in the production and extraction of acetic acid from the total revenue generated by the extracted acetic acid. The price of acetic acid varies significantly depending on the quality and volume of purchase. The value of an asset is normally calculated on the basis of spot price. The spot price is the current market value of an asset available for immediate delivery at the moment of the quote. The spot price of acetic acid is currently $795/ton. Therefore, the price of 31,400 tons of the produced acetic acid is $25 million. Based on the estimated rumen reactor's operational life of 20 years [30], the total revenue potential of acetic acid production over 20 years is estimated to be $500 million.

The total cumulative cost involves the collection and pre-treatment cost of lignocellulosic biomass and the capital and operational cost of a rumen reactor and the two FO systems.

Based on the calculations of an anaerobic digester, the capital cost of a rumen reactor with a capacity of processing 100,000 tons of lignocellulosic material per year is estimated to be almost $20 million with an operational cost of around $1 million/year (5% of the total capital cost) [31, 32]. Thus, the total cost of a rumen reactor for 20 years of operation is $40 million. The collection and pre-treatment cost of lignocellulosic biomass is at least 20% of the rumen reactor's total cost i.e. $8 million [33]. Following the capital and operational cost of 1 million gallons/day (≈3,800 tons/year) feed processing capacity of the FO system, the capital cost of the FO system with 7 million tons of rumen fluid processing capacity per year is estimated to be $44 million and the annual operational cost around $4.2 million [34]. The operational cost of the FO system for 20 years would be $84 million and the total cost of the FO system involving both the capital and the 20 years operational cost would be $128 million. For two FO systems, the total cost would increase to $256 million. The net profit potential of acetic acid production in a rumen reactor followed by the FO system extraction of acetic acid from the rumen fluid comes out to be $196 million over 20 years of operation.

Although it is preliminary, the above analysis confirms that the available lignocellulosic biomass can replace fossil materials as feedstock to produce VFAs. It also shows that an engineered rumen reactor can generate profit at the current spot price of acetic acid.

Table 1.1**:** Economics of acetic acid (with the spot price of $795/ton) production from lignocellulosic biomass in a rumen reactor with 100,000 tons of lignocellulosic material processing capacity per year and acetic acid extraction by FO over 20 years of operation.

Description	**Revenue (million $)**	**Cost (million $)**
Value of 31,400 tons of acetic acid production/year	25	
The revenue potential of produced acetic acid	**500**	
The capital cost of a rumen reactor		20
The operational cost of a rumen reactor		1
Total cost (capital and operational cost) of a rumen reactor		40
The collection and pre-treatment cost of lignocellulosic biomass		8
The capital cost of the FO system		44
The operational cost of the FO system		4.2
The operational cost of the FO system for 20 years		84
The total cost of the FO system		128
The total cost of the two FO systems		256
Total cumulative cost		**304**
Net profit ($)	**196**	

1.3 Objectives

The main objective of this study was to investigate the prospects of using FO for resource recovery from the rumen fluid by mimicking the VFAs and water absorption in the ruminant's small and large intestines, respectively. The specific objectives of this study were to:

- Evaluate the potential of acetic acid extraction from rumen fluid by FO and determine the effect of membrane, pH and membrane orientation on acetic acid extraction.
- Investigate the effectiveness of FO for dewatering the rumen fluid using artificial saliva as a draw solution.
- Characterize the membrane biofouling in a long term FO process and compare the effectiveness of various membrane cleaning techniques.

1.4 Research questions and hypothesis

Besides these specific objectives, this thesis answers some of the key research questions as summarised below:

1. Does FO offer any potential to extract acetic acid from rumen fluid and how the various process parameters can impact the FO performance?
2. Can artificial saliva be effective as a draw solution to extract water from the rumen fluid and what will be the impact of draw solution concentration and feed solution temperature on the rumen fluid dewatering process?
3. What are the morphology, chemical nature and microbial composition of the membrane biofouling layer when FO is operated for water extraction from rumen fluid over a longer period?
4. How can different physical and chemical cleaning techniques be effective and compared to clean the membrane and recover the flux?

It is expected that FO will separate acetic acid from the rumen fluid by reciprocating the natural process of VFAs absorption in the small intestine of the ruminant animals. Different process parameters such as membrane type, stripping solution pH and membrane orientation will significantly affect the acetic acid extraction process. Mimicking another natural process of water separation from the rumen fluid in the

omasum and large intestine of ruminants by FO to dewater the rumen fluid using artificial saliva as a draw solution will potentially show promising results. The long term use of FO for dewatering of rumen fluid will cause biofouling on the membrane surface. Investigation of the biofouling layer (biofilm) will help us in understanding the morphology and chemical nature of the biofilm besides discovering the various details of the microbial communities. The combination of physical and chemical membrane cleaning techniques will be more effective to recover the lost water flux due to membrane fouling.

1.5 Thesis structure

This thesis consists of six chapters in the following sequence (Figure 1.2):

Chapter 1 is an introduction chapter that includes the background, economic assessment of VFAs production from lignocellulosic biomass, research objective, research questions and thesis structure.

Chapter 2 provides an extensive literature review about the recent developments regarding FO, its applications and opportunities.

Chapter 3 focuses on the resource recovery potential of FO by assessing the acetic acid extraction from the rumen fluid.

Chapter 4 is a continuation of the resource recovery potential of FO to extract water from the rumen fluid.

Chapter 5 covers the characterization of membrane biofouling over a longer period of FO operation to concentrate rumen fluid and the effectiveness of various membrane cleaning techniques.

Chapter 6 highlights the conclusions obtained from this study and presents recommendations for future studies.

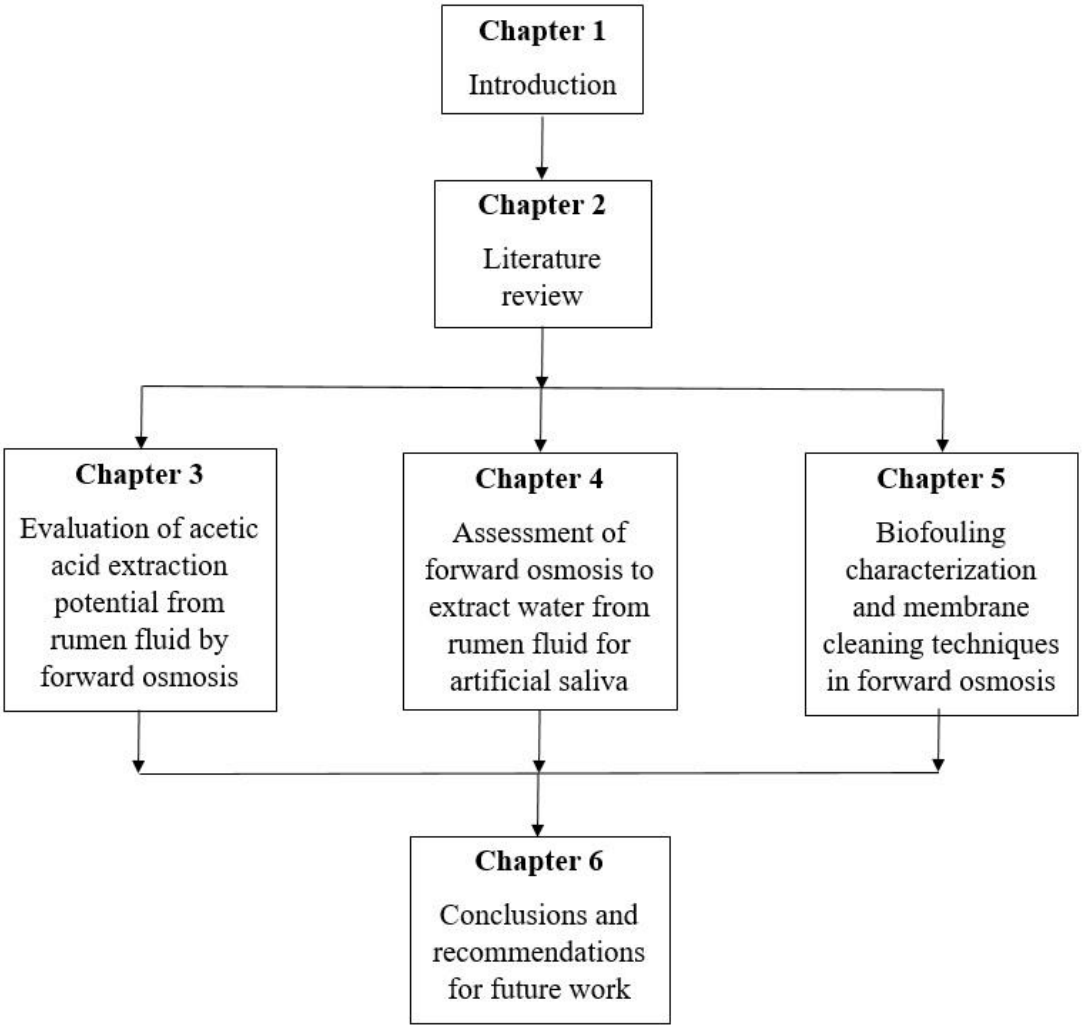

Figure 1.2: Thesis outline

Chapter 2 Literature Review

This thesis chapter is based on the following journal article.

Khan JA, Shon HK, Nghiem LD. From the Laboratory to Full-Scale Applications of Forward Osmosis: Research Challenges and Opportunities. Current Pollution Reports. 2019;5(4):337-52.

2.1 Introduction

Clean water, energy, and raw chemicals are essential resources in our modern society. Freshwater is vital to life on earth. Energy is the bloodline for our society to function. We also rely on just a few simple chemicals currently derived from crude oil and other fossil sources as raw material input for our industry. With a growing global population and significantly improved living conditions, the long-term sustainability of these resources is under threat.

A freshwater resource is for example under immense pressure today due to rapid population increase, rapid industrialization, and improved economic conditions [35]. In many regions, the available freshwater resources have been severely depleted due to increasing demand for domestic, agricultural and industrial consumption. Currently, one-third of the world's population faces water shortage. This number is expected to increase to two-thirds by 2050 [35]. Each year 3.5 million people die due to lack or shortage of water supply and sanitation which shows the immense importance of clean water availability for our mankind [36]. There is a growing need for developing alternative ways and means to cope with the existing issue of water shortages and the aggravating water crisis in our future.

One such alternative is to purify wastewater and desalinate seawater by various thermal and membrane-based processes. Thermal processes like evaporation, multi-stage flash

(MSF), and multi-effect distillation (MED) have been explored for desalination purposes. Water separation in all thermal processes are based on phase change that needs a high amount of energy in the form of heat and are, therefore, costly processes [37]. Membrane-based desalination technologies were developed as a better alternative to the thermal processes. Among membrane-based processes, microfiltration (MF) and ultrafiltration (UF) are less energy-intensive than NF and RO and can concentrate a solution by rejecting particles of sizes 0.01-1 μm like pathogens, organic macromolecules, and minerals. The NF requires more energy than the MF and the UF processes but less than the RO process. The NF can perform further fine filtration and can reject the particles with sizes down to most of the multivalent ions. RO is the most energy-intensive of all the membrane processes with the best results in terms of rejecting the small organic contaminants (such as pharmaceutically active compounds, industrial chemicals, and pesticides), salts, and heavy metals. One common factor among all these membrane processes is the requirement of an external energy source to generate hydraulic pressure for pushing water through the membrane while rejecting the solutes in the process. A more feasible choice can be an FO process as it does not need any external energy source and uses the natural concentration gradient as a driving force to permeate water across the membrane.

FO has recently emerged as a promising alternative to overcome the shortcomings of commercialized pressure-driven membrane processes. Unlike RO that needs an external energy source for its operation, FO operates by utilizing the naturally occurring osmotic gradient between high concentrated draw solution and low concentrated feed solution to drive water out of feed solution into the draw solution across a semi-permeable membrane. Some of the potential advantages of FO include low fouling tendency, high fouling reversibility, and high water recovery along with the most important advantage of no external energy input requirement [31, 38, 39]. In addition to a range of water

purification applications, innovative FO processes to facilitate the transport of VFAs and nutrients (e.g. ammonia) instead of water have also been suggested [40].

By replicating ruminant's digestive system, FO offers an exciting opportunity to extract VFAs and clean water from an engineered rumen reactor with lignocellulosic feed. Production of VFAs from lignocellulosic material followed by their extraction through FO can be a huge success to end our reliance on fossil fuels for the industrial production of various chemicals. Moreover, the use of FO to extract clean water from the rumen rector's fermented solution can be used for the production of artificial saliva, an important component of the rumen reactor system. These concepts are based on the hypothesis that the FO process can be used to simulate the functions of the small intestine to extract VFAs from the rumen fluid as well as mimicking the omasum and large intestine by separating water from the rumen fluid. In ruminant animals, the absorbed VFAs act as energy reservoirs for body functions and growth while the recovered water is recycled for saliva production that helps in chewing the lignocellulosic feed at the start of the digestion process.

To date, most of the research on FO has been carried out at lab-scale with the main focus on exploring and improving the structural and operational features of the process. Very little has been investigated about the barriers in shifting the paradigm from a lab-scale process to large scale applications or to explore new applications beyond the domain of water purification. Given the focus on water purification of the current literature, this chapter aims to highlight the key challenges in the path of FO transformation from a lab-scale process to full-scale applications. Innovative use of FO for non-water purification applications will also be explored wherever possible. Key challenges and issues in the development of the FO process including membranes materials, transport phenomena, draw solute selection, draw solute regeneration and membrane fouling are discussed.

Specifically, this study focuses on recent developments in FO applications, membrane fabrication, concentration polarization, reverse solute flux (RSF), multi-criteria comparison of different draw solutes types, and different forms of membrane fouling along with their respective cleaning and mitigation strategies.

2.2 FO applications

Significant research work has been devoted to the new application prospects of the FO process. Various manufacturing industries have harnessed FO due to its potential advantages over other membrane-based processes. A recent study has evaluated 51 research papers exploring the prospects of FO for industrial applications [41]. All the 51 research papers were based on lab or bench-scale experimental data. These research papers did not include the ones on drinking water production by FO as they did not fit under the umbrella of manufacturing industries. The percentage of publications on different types of industrial applications are shown in Figure 2.1. It shows that the maximum number of FO publications (23%) are related to chemical industry applications. Many research studies were on the applicability of FO in food and beverage industries (dairy and non-dairy) where FO was employed not only to concentrate the food products like milk, juice, whey but also to treat wastewaters.

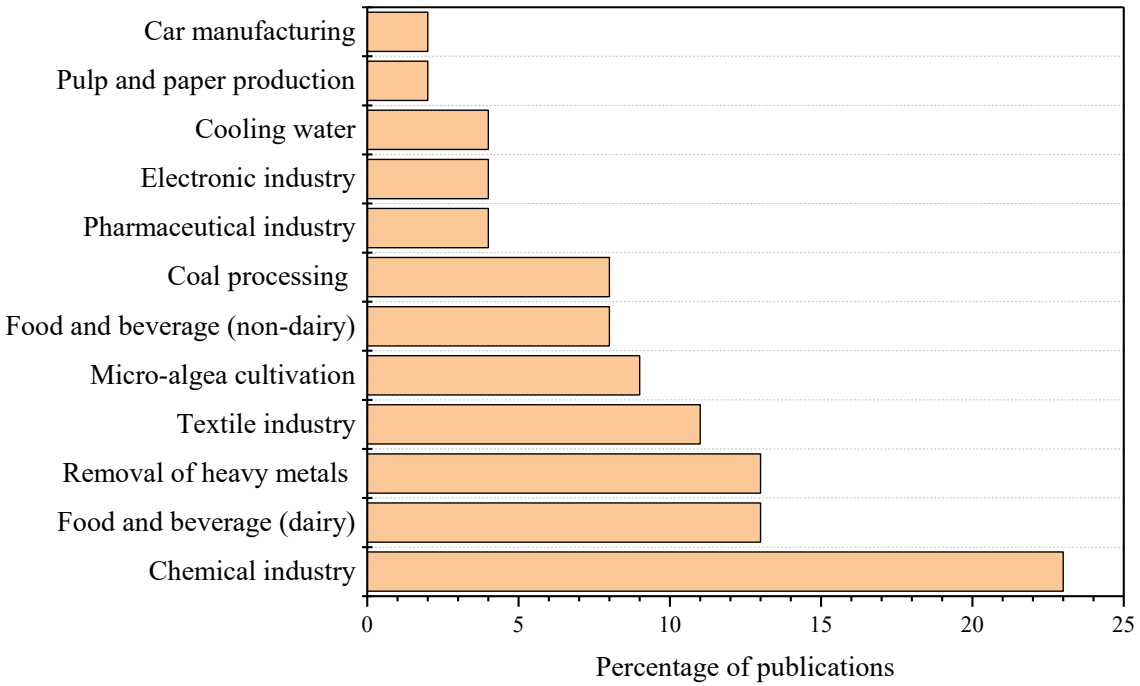

Figure 2.1: The percentage distribution of research papers on various industrial applications [41].

Besides manufacturing industries, FO exhibits vast application prospects ranging from lab-scale experiments to full-scale implementation. It has been investigated for the treatment and processing of challenging water solutions in a range of applications including seawater desalination [42], wastewater treatment [43], agricultural use for fertigation [44], microbial fuel cells [45], and emergency water supply with so-called hydration bags [46]. FO has a potential role to play in wastewater treatment with applications such as osmotic membrane bioreactor (MBR) [43], treatment of drilling fluid, landfill leachate, and fracking wastewater for water reuse [47, 48], and pre-concentration of digested sludge for nutrient recovery [49]. Other potential applications of FO include water reuse during long term space missions and regeneration of dialyzing fluid for kidney failure treatment [50].

Although FO has been used in a wide range of water purification applications as stated above, FO application to extract cleaning water and volatile fatty acids in an artificial

rumen system could also be an exciting possibility. Rumen fluid is a resource-rich fermented solution that is produced inside the rumen of the ruminant animals (such as cows, sheep, and goats) as a result of lignocellulosic material biodegradation. Recent work has demonstrated the potential for an engineered rumen reactor to convert a renewable, eco-friendly, energy-rich and the most abundant resource of lignocellulosic biomass into volatile fatty acids [51]. In such a reactor, a major challenge to the operation is the ability to continuously extract clean water and volatile fatty acids from rumen fluid. Rumen fluid is enriched in useful biomolecules such as VFAs, carbohydrates, proteins, and phospholipids. VFAs are the main constituents with acetic acid as the predominant VFA that make the most of biomolecules in the rumen fluid. VFAs are valuable biochemicals that can replace petroleum-based chemicals for the production of pharmaceuticals, plastics, and other products of the modern economy [52, 53].

Several membrane-based and non-membrane based methods have been proposed and investigated for recovering VFAs from the fermented solutions. These methods include ultrafiltration [51], nanofiltration [54], liquid-liquid extraction [55], absorption [56], ion exchange [57], pervaporation [58], and electrodialysis [59]. However, all of these methods need input energy to separate the VFAs from the rest of the solution which makes these processes expansive and, therefore, practically prohibitive. Some of these processes like adsorption and ion-exchange are chemically more intensive that can cause serious environmental problems. FO pitches itself as a better alternative to all these processes that can operate without any input energy for the separation processes. There have been some recent attempts to concentrate fermented solutions by FO for subsequent VFAs extraction [60-62]. However, these studies have focussed on dewatering of the fermented solution by FO that will need another process for VFAs extraction from the dewatered mixture. An innovative and more feasible approach can be to mimic the ruminant's digestive

system processes by employing FO at both the steps; first by extracting VFAs from the rumen fluid by FO followed by water extraction from the rest of the rumen fluid by the same FO process.

2.3 Membrane development

Most FO work until the early 2000s was conducted using membranes fabricated for RO applications [63]. The development of membranes specific for FO applications has only commenced over the last two decades thanks largely to breakthroughs in fabrication techniques. These breakthroughs in membrane fabrication techniques have also resulted in a surge in the number of FO related journal publications. Of the total number of over 1700 FO related journal publications to date, over 99% of them were reported since 2005 (Figure 2.2). This upsurge in FO research signifies the rapidly growing interest in this technology platform in recent years.

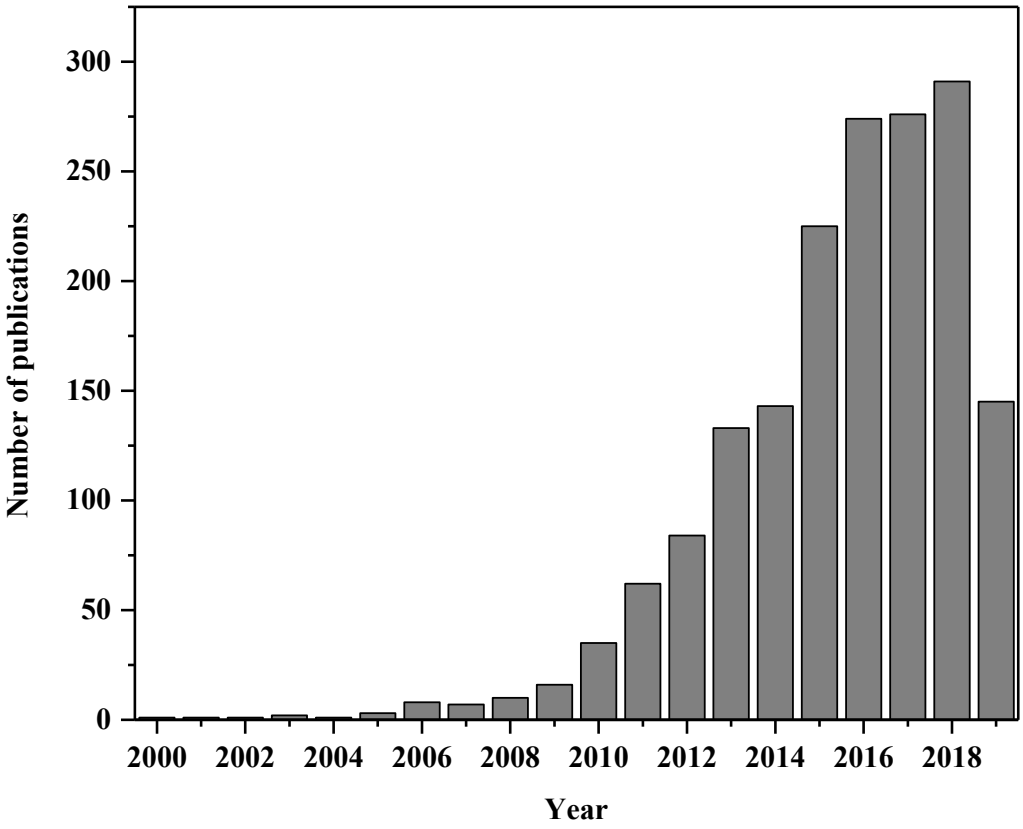

Figure 2.2: FO journal publications since 2005 (According to Web of Science).

A typical FO membrane consists of two layers namely the active skin layer and the support layer [64]. This structural arrangement of the FO membrane is required to safeguard key properties namely water permeation, solute separation and mechanical strength [65]. In the FO membrane, the active skin layer allows for water permeation under an osmotic gradient between the draw and feed solution while preventing the transport of draw solutes and contaminants. The skin layer is designed to be as thin as possible to minimize mass transfer resistance to water. The thin skin layer does not have adequate mechanical strength for self-support, thus, an adequately thick but porous layer is required to provide mechanical support to the active layer. They can be made of either the same or different polymeric materials, corresponding to asymmetric or thin-film

composite polyamide (TFC-PA) membranes. Figure 2.3 illustrates a typical TFC-PA FO membrane with an ultrathin skin on a porous supporting layer.

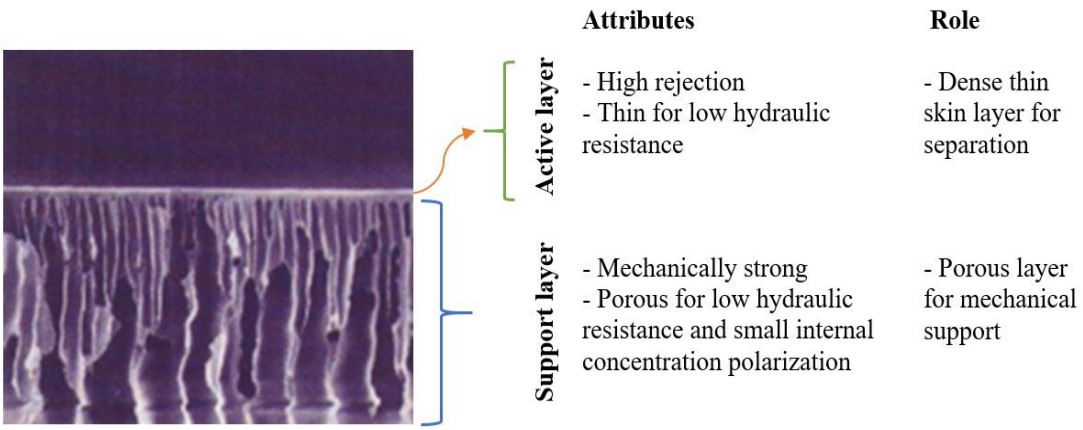

Figure 2.3: Active and support layers of the FO membrane.

A variety of membrane materials and fabrication techniques have been explored for the preparation of FO membranes (Table 2.1). The newly developed FO membranes can be broadly classified into four categories depending on the method of preparation. These categories are cellulose triacetate (CTA) membranes, TFC-PA membranes, chemically modified membranes, and 3D printed membranes.

Table 2.1: Recent developments in FO membrane fabrication.

Category	Year	Membrane	Materials †	Preparation methods	Ref.
CTA membrane	2005	Capsule wall	Cellulose acetate	Dip-coating, phase inversion	[66]
	2008	Flat sheet	Cellulose acetate	Phase inversion and then annealing at 80–95 °C	[67]
	2010	Flat sheet double-skinned	Cellulose acetate	Phase inversion, and then annealing at 85 °C	[68]
	2010	Double dense-layer	Cellulose acetate	Phase inversion	[69]
	2011	Flat sheet composite	Cellulose acetate cast on a nylon fabric	Phase inversion	[70]

Category	Year	Membrane	Materials †	Preparation methods	Ref.
TFC-PA membrane	2010	Flat sheet TFC-PA	PSF support, PA active layer	Phase inversion and IP	[71]
	2011	Flat sheet TFC-PA	PES/sulfonated polymer substrate, PA active layer	Phase inversion and IP	[72]
	2011	Nanoporous PES	PES cast on PET fabric	Phase inversion	[73]
	2011	Flat sheet TFC-PA	PES nanofiber support, PA active layer	Electrospinning and IP	[74]
Chemically modified membrane	2011	Positively charged flat sheet	PAI substrate treated by PEI	Chemical modification	[75]
	2013	PSFN-TFC-PA	PSF/Zeolite	Chemical modification	[76]
	2017	Aquaporin based TFC-PA	Aquaporin embedded in PA active layer, PEI/NMP support with Lithium chloride as an additive	Chemical modification	[77]
3D printed membrane	2018	3D printed membrane feed spacer	Polypropylene	3D printing	[78]
	2018	3D printed membrane feed spacer	Biopolymer polylactic acid	3D printing	[78]

† PSF = polysulfone; PA, polyamide PES = polyethersulfone; PET = polyethylene terephthalate; IP = interfacial polymerization; PAI = polyamide-imide; PEI = polyethyleneimine; NMP = N-Methyl-2-pyrrolidone

CTA membrane was first commercially manufactured by Hydration Technologies Incorporation [79]. Phase inversion is the most common preparation method for preparing asymmetric CTA membranes. This technique involves the formation of an asymmetric membrane structure by a controlled process of polymer transformation from a liquid phase (homogeneous polymer solution) to a solid phase (membrane) [80]. The solvent

(e.g. acetone) in the polymer solution is highly volatile which evaporates quickly during the process to form a dense polymeric membrane.

Work on TFC-PA FO membranes started in 2010 when Yip et al. [81] and Wang et al. [82] reported techniques to prepare flat sheet and hollow fibre TFC-PA membranes, respectively. A typical TFC-PA membrane consists of a porous substrate/support layer formed by phase inversion and a thin PA active layer formed by IP. The most common IP technique is achieved by the cross-linking reaction between M-phenylenediamine (MPD) and trimesoyl chloride (TMC). In addition to phase inversion, electrospinning has also been reported in the literature to develop a nano-fibrous support layer of the TFC-PA membrane [74]. The most common IP technique is achieved by the cross-linking reaction between MPD and TMC (Figure 2.4).

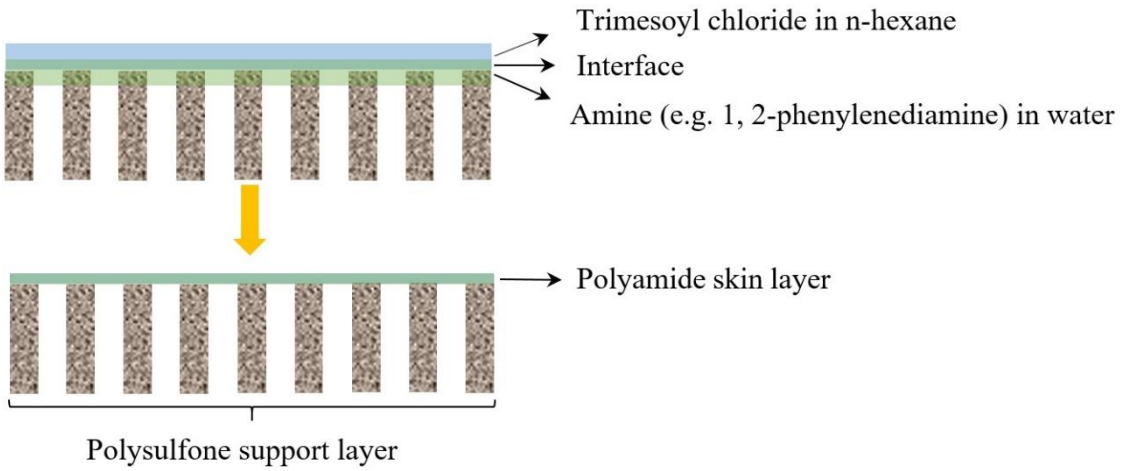

Figure 2.4: IP of PA skin layer

CTA and TFC-PA membranes both have their advantages and disadvantages. Some key advantages of the CTA membrane include the lower fouling tendency due to its smooth surface and nearly neutral surface charge, high resistance to chlorine, lower cost and high hydrophilicity [80, 83]. They are fabricated in a relatively easy and one-step process. CTA membranes also have some major drawbacks such as intrinsically low water permeability

due to thick membrane active layer, narrow temperature range (30–35 °C), low salt rejection, and high structural parameter value due to use of high polymer concentration, and the annealing process during their fabrication [83, 84]. Comparing to CTA, TFC-PA membranes have shown higher water permeability, lower RSF, and more resistance to hydrolysis and biodegradation [83, 85]. On the other hand, TFC-PA membranes can have a high vulnerability to chlorine attack and ICP because their support layers are mainly composed of hydrophobic polymers such as PSF and PES [84, 86]. Although the literature suggests that the TFC-PA membrane is superior to the CTA membrane in terms of its operation over a wider pH range, a more recent study has reported the stability of CTA membrane in higher pH (pH 11) environment [48].

There have been some promising attempts to improve FO performance by chemical modification. The inclusion of several materials such as carbon nanotubes [87], silica and titanate nanoparticles [88], and zeolites [76] in the support layer of FO membranes have been reported in the literature. Qiu et al. [75] modified the PA-imide micro-porous substrate embedded with woven fabric chemically using a PEI polyelectrolyte solution to reduce the thickness of the substrate to 55 μm and enhance the mechanical strength of the membrane. Setiawan et al. [89] induced a positive charge to the active layer of the membrane with post-treatment of PEI polyelectrolyte. They reported that the induced positive charge reduced the salt transport across the membrane due to double charge repulsion [89]. Following nature's model of aquaporin role as a water transporting channel in the cell membrane, aquaporin incorporated TFC-PA membranes have been developed which showed excellent results in terms of high water flux and reduced solute rejection [84]. Li et al. [77] demonstrated the increase in water flux from 3.6 to 7.6 $L/m^2.h$ (LMH) by embedding aquaporin into the PA active layer of the TFC-PA membrane.

The 3D printed membrane is the most novel idea to revolutionize the potential of membranes for various desalination applications. The recent advancements in 3D technology are paving the way for developing 3D printed membranes. Owing to the increasing resolution power of 3D technology and its ability to create a complex shape of almost any geometry, 3D printed membranes are expected to show improved performances in terms of reduced concentration polarization, reduced pressure drop, and low fouling [90]. Different printing materials such as PA composites, acrylonitrile butadiene styrene, polypropylene, and natural polylactic acid have been suggested to prepare membrane feed spacers using 3D technology [78]. Although membrane feed spacers and other membrane module components have been prepared successfully using the 3D printing technique, fabrication of FO membrane using this technique has not been reported yet in the literature [90]. This is mainly because the resolution power of 3D printing technology is currently not advance enough to match the resolution range required for membrane manufacturing [90]. There are several challenges for developing this technology further to get in line for membrane manufacturing. Some of these challenges include the low-resolution power of the current 3D technology, long printing time, material requirements, the need for technical expertise and facilities, and the high cost of 3D printers [90].

FO membrane properties can affect their dewatering characteristics and overall performance. There is a great scope in improving membrane performance by altering the membrane structural features. For example, the ICP is mainly dependent on the porous support structure while solute rejection and RSF are largely governed by the thin active layer of the FO membrane [83]. Studies have shown the reduction in ICP and improvement in water flux by reducing the tortuosity and increasing the porosity and hydrophilicity of the FO membrane support layer [83, 91, 92]. Doubling the active layers

of cellulose acetate membrane, instead of reducing the water flux due to increased resistance, increased the water flux due to reduced ICP in the porous support structure [68].

Membrane development has come a long way since its inception. The development journey covers different membranes starting from the earliest use of animal bladder as a membrane to the latest use of 3D technology for membrane fabrication. Although these developments were aimed to improve the performance indicators of membranes such as water flux, RSF, membrane fouling, and cost of fabrication, no membrane has shown excellent performance in all the key areas. Among all the developed membranes, reported so far, aquaporin based TFC-PA membranes and TFC-PA membranes with nanoparticles embedded into the active and support layers have shown unbeaten performance in terms of high water flux, high rejection capability, and small structural parameter.

2.4 Draw solution

In the FO process, a concentrated solution that can generate a high osmotic pressure is used to induce the driving force for water transport. It is crucial to select a high-performance draw solute for efficient operation and the overall cost reduction of the FO process. The main criteria for the selection of a draw solute include high osmotic pressure, low RSF, easy regeneration, scaling up potential, low toxicity and cost [93]. Draw solutes can be classified as organic, inorganic, volatile and thermo-responsive (Table 2.2).

Table 2.2: Types of draw solutions and some corresponding examples used in FO ([#] at osmotic pressure difference between the feed and draw solution of 2.8 MPa).

Type	Draw solution	Water flux (LMH)	Feed solution	Membrane	RSF ($g/m^2.h$ (gMH))	Regeneration process	Application examples	Ref.
Organic	Glucose	0.37	tomato juice	TFC-PA	Not reported	Direct application, low-pressure RO	Seawater desalination, tomato juice concentration	[94]
	Sucrose	12.9	Deionized (DI) water	Cellulose acetate	Not reported	NF	Wastewater treatment	[95]
	Sodium acetate	9	DI water	CTA flat sheet	2.73[#]	RO	Wastewater treatment	[96]
Inorganic	Sodium chloride	9.65	DI water	CTA flat sheet	7.2[#]	RO, distillation/RO, direct application	Algal biodiesel production, seawater desalination	[97]
	Potassium bicarbonate	8.1	DI water	CTA flat sheet	1.4[#]	RO process	Desalination	[93]
	Magnesium sulfate	5.54	DI water	CTA flat sheet	1.2	NF	Desalination	[93]
	Sodium nitrate	20.54	DI water	Cellulose acetate	85.07	Direct application	Direct fertigation	[98]

Type	Draw solution	Water flux (LMH)	Feed solution	Membrane	RSF ($g/m^2.h$ (gMH))	Regeneration process	Application examples	Ref.
	Ammonium phosphate	15.66	DI water	cellulose acetate	37.01	Direct application	Direct fertigation	[98]
Volatile	Ammonium bicarbonate	7.34	DI water	CTA flat sheet	18.2[#]	Heating - decomposition into NH_3 and CO_2	Seawater desalination	[93]
	Dimethyl ether	2.12–2.91	0.5 wt.% NaCl solution	SW30 membrane	Not reported	Exposure to air	Desalination	[99]
Thermo-responsive	Thermo-responsive oligomer with a glycerol	1.56	Milli-Q water	CTA flat sheet	1.08	Low-pressure RO	Desalination	[100]
	Polymer hydrogels	0.55 -1.1	2000 ppm NaCl solution	CTA-FO	Not reported	Heating and pressurization	Seawater desalination	[101]

Organic draw solutes are mainly non-electrolyte organic compounds such as glucose and sucrose. They must be soluble in water and can generate adequate osmotic pressure for FO [102]. Most organic draw solutions can be readily regenerated by RO and in some cases even NF.

Most inorganic draw solutes are strong electrolytes. They have been used in FO applications that require high osmotic pressure. These inorganic draw solutes can be recovered by RO [93] and a thermal desalination process such as membrane distillation (MD) [103].

Volatile draw solutes change their states with changing temperature. They can be traced back to the early 1960s when Neff first proposed the concept of using a mixture of ammonia and carbon dioxide as a draw solution for seawater desalination [104]. A mixture of ammonium hydroxide (NH_4OH) and ammonium bicarbonate (NH_4HCO_3) is a common example of volatile draw solution. Ammonium carbonate shows good results in terms of the generated osmotic pressure and ease of regeneration by a simple thermal process [105].

Thermo-responsive draw solutes can be either polyelectrolytes or hydrogels; specifically developed for FO applications. These solutes have properties superior to other types of draw solutes in terms of lower RSF and less energy-intensive recovery processes [106]. However, there are some key challenges in the form of complex synthetic procedures, high concentration polarization, low water flux and reduction in water recovery efficiency after reuse of recycled draw solutes [106]. Zhao et al. [107] reported a high water flux of 4 LMH using a thermoresponsive copolymer, poly sodium styrene-4-sulfonate-co-n-isopropyl acrylamide as a draw solute for seawater desalination. It is noteworthy that Zhao et al. performed their study on a small scale using a TFC-PA membrane of area 2 cm^2 [107], thus further work is necessary to scale up this approach. Kim et al. [108] used poly tetra-butyl-phosphonium-styrene-

sulfonates as thermo-responsive draw solutes with TFC-PA membrane of area 0.79 cm^2. They reported a water flux of 14.5 LMH and RSF of only 0.14 gMH [108].

Despite the many different draw solutes evaluated for FO at the lab-scale level, to date, there have only been six pilot-scale FO studies (Table 2.3). The small number of pilot-scale demonstrations highlight the need for further research and development of commercially practical draw solutes. Inorganic draw solutes (i.e. NaCl and seawater) were used in most of these pilot studies. Sodium polyacrylate (ionic organic draw solute) and ammonium carbonate have also been evaluated as draw solutes at the pilot-scale level. However, no pilot-scale study using a thermo-responsive draw solute has been reported so far. The size and duration of these pilot-scale studies range from membrane area of 0.3 to 59.4 m^2 and operation time from 51 days to 180 days respectively. As an example, an NH_3/CO_2 draw solute based FO pilot-scale plant employing a membrane with an effective area of 59.4 m^2 was operated to desalinate brine having 180 ± 19 g/L total dissolved solids (TDS). With four months operation period, there was a substantial decrease in TDS to 300 ± 115 mg/L of the produced water with 57% less energy consumption than the estimated value for an open cycle evaporator [109]. Some of the pilot-scale studies have reported the different problems faced/overcome during the operation. Phuntsho et al. have reported the diffusion of feed and draw solute through the CTA membrane and management of feed concentrate due to the presence of nitrogen as the main problems in the operation of the FO plant [110]. Kim et al. overcame the problems of pipeline blockage due to salt formation from ammonia and carbon dioxide reaction, the supply of absorbent for the recovery process, and bypassing the draw solution [111]. Wang et al came across cake enhanced concentration polarization and limitations of ammonium recovery as the main problems in their study.

Table 2.3: Pilot-scale FO studies reported to date in the literature.

Study	Draw solutes	Membrane area (m^2)	Duration (days)	Key Findings
Phuntsho et al. [110]	Ammonium sulfate	20.2	180	Water flux was restored by hydraulic cleaning without any chemical cleaning. No fouling was observed with NF-post treatment.
Corzo et al. [112]	Magnesium sulfate, sodium polyacrylate, and potassium pyrophosphate.	1.3	Not reported	The optimal operating osmotic pressure for the draw solution was 10 bars. The best performance was obtained with the TFC-PA flat sheet membrane.
Kim et al. [111]	Ammonium bicarbonate	17.6	Not reported	High recovery and separation efficiency (> 99%) was observed. A diluted draw solution was used as an absorbent for DS recovery.
Wang et al. [113]	Sodium chloride	0.3	51	48.1 % of ammonium and 67.8% of total nitrogen rejection were achieved.
McGinnis et al. [109]	Ammonia/ carbon dioxide	59.4	120	The TDS concentration of product water was 300 mg/L. 57% less energy was used than the estimated value of 633 kWh/m^3.
Hancock et al. [114]	Synthetic sea salt	1.58	90	Trace organic compounds were rejected by 99%. Membrane fouling contributed to the higher rejection of trace organic compounds.

Draw solution regeneration is an important prerequisite for the efficient performance of FO. It can be carried out by coupling it with another process to produce clean water. Depending upon the type of draw solute and the nature of FO application, different coupling processes have been evaluated such as RO, NF, UF, MD, and heating. These processes are generally energy-

intensive in the form of hydraulic pressure and heating. Therefore, more research is needed to minimize the energy consumption of the draw solution recovery process and the overall cost of the FO process.

A multi-criteria comparison for different types of draw solutes is shown in a radar chart (Figure 2.5). Each criterion is ranked from low (0) to high (5) level of suitability. The scores for osmotic pressure, RSF, and ease of regeneration are based on data in Table 2.2. The scaling-up potential is based on the number of pilot or full-scale systems reported in the literature (Table 2.3). Toxicity is also based on the literature data, in this case, apart from ammonium carbonate (volatile draw solute), no report of toxicity has been identified for all other categories of draw solutes. Although this is a subjective assessment, Figure 2.5 highlights that no current draw solute can adequately meet all key performance criteria for large scale FO operation. Each type of draw solute manifests its strengths and shortcomings. For example, inorganic draw solutes are good at producing high osmotic pressure but are less advantageous with RSF. On the other hand, organic draw solutes are good at lowering the RSF but generate less osmotic pressure than inorganic draw solutes.

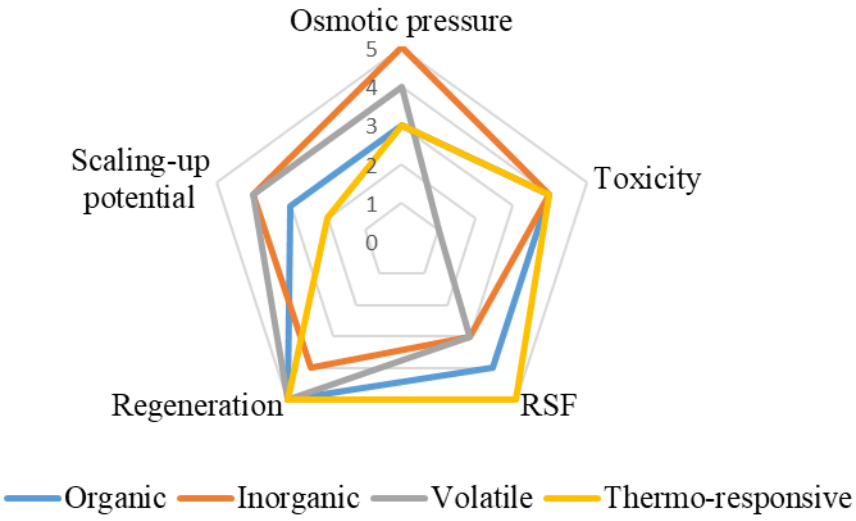

Figure 2.5: Multi-criteria comparison for different types of draw solutes.

Draw solution is one of the most crucial and decisive components for a successful FO operation. Many draw solutes have been investigated to check their suitability in FO but they have fallen short in one or more criteria of an ideal or perfect draw solute. Although draw solute selection mainly depends on the nature of FO application, inorganic and thermo-responsive draw solutes seem to be more competitive and efficient than others as their overall performance in all five criteria is better than the rest. Most recent work on draw solutes has been carried out at a lab scale. Very few pilot-scale studies employing mainly inorganic draw solutes have been reported here. Further research is needed to identify or develop suitable draw solutes that can be evaluated at a pilot scale to determine their commercial viability.

2.5 Transport phenomena

2.5.1 Reverse solute flux

RSF - the transport of draw solutes through the membrane - is a problematic but inherent phenomenon in the FO process. The transport of draw solutes from the draw to the feed solution occurs because the draw solute concentration is much higher in draw solution than feed solution to induce water transport while the membrane is imperfect and cannot offer 100% rejection.

Two important factors which can affect RSF are membrane structural characteristics and physicochemical properties of the draw solution [115]. Therefore, the selection of membrane and draw solute plays a key role in curtailing this phenomenon.

RSF is considered to be a significant impediment in FO [116]. Transport of draw solute across the membrane reduces the osmotic pressure difference between the draw and feed solution, thus reducing the water flux [117]. Moreover, draw solution replenishment to compensate for the loss of draw solute can also increase the operational cost. RSF is also a major problem in several FO applications where it is crucial to keep draw solution completely separate from feed solution e.g. food and drug processing applications [118]. Issues may also arise in more common applications like wastewater treatment and seawater desalination especially concerning FO concentrate management and disposal [119].

Several control measures including the selection of draw solute and advanced membrane fabrication and modifications have been suggested to reduce the RSF. Unlike draw solutes with divalent ions such as calcium and magnesium, draw solutes with monovalent ions such as sodium and potassium can permeate easily through the FO membrane [120]. Therefore, it may be feasible to employ divalent ion solutions having lower diffusion coefficients in all those applications which aim at high rejection [63]. However, divalent ions may aggravate membrane fouling by interfering with feed solution foulants after reverse diffusion [97]. The development of new membranes can significantly reduce RSF. The average value of specific reverse solute flux (SRSF) i.e. the ratio of RSF to water flux for commercial CTA membrane has been reported as 0.60 ± 0.32 g/L while the lowest value (0.10 g/L) of SRSF was obtained using a non-woven flat sheet CTA membrane [121]. In the case of commercial TFC-PA membranes, the average value of SRSF was 0.44 ± 0.32 g/L [121]. Novel TFC-PA membranes with different substrate compositions such as polyketone, nylon 6, 6 microfiltration membrane, cellulose acetate propionate, and polytriazole-polyoxadiazole have been reported to reduce

SRSF. The lowest value (0.035 g/L) of SRSF was obtained using a nylon 6,6 microfiltration membrane support layer [122]. Modifying the FO membrane surface can also help in reducing the RSF. Zou et al. [123] have reported the coating of commercial TFC-PA membrane with zwitterion functionalized carbon nanotubes which reduced the RSF by 83.3%. The reduction in RSF can be attributed to the generation of electrostatic repulsive forces induced by the charged functional groups of Z-CNTs.

2.5.2 Concentration polarization

Concentration polarization is the formation of concentration gradients inside the supporting layer and immediately at the membrane external surfaces during the FO process. Concentration polarization increases the concentration and osmotic pressure of the feed solution while simultaneously decreasing the concentration and osmotic pressure of the draw solution at the membrane active layer [83]. In other words, concentration polarization lowers the effective osmotic pressure difference across the membrane than the bulk osmotic pressure difference across the membrane resulting in a reduced water flux across the membrane [83]. Depending upon the location of the concentration profile, concentration polarization can be classified into external concentration polarization (ECP) and internal concentration polarization (ICP) (Figure 2.6).

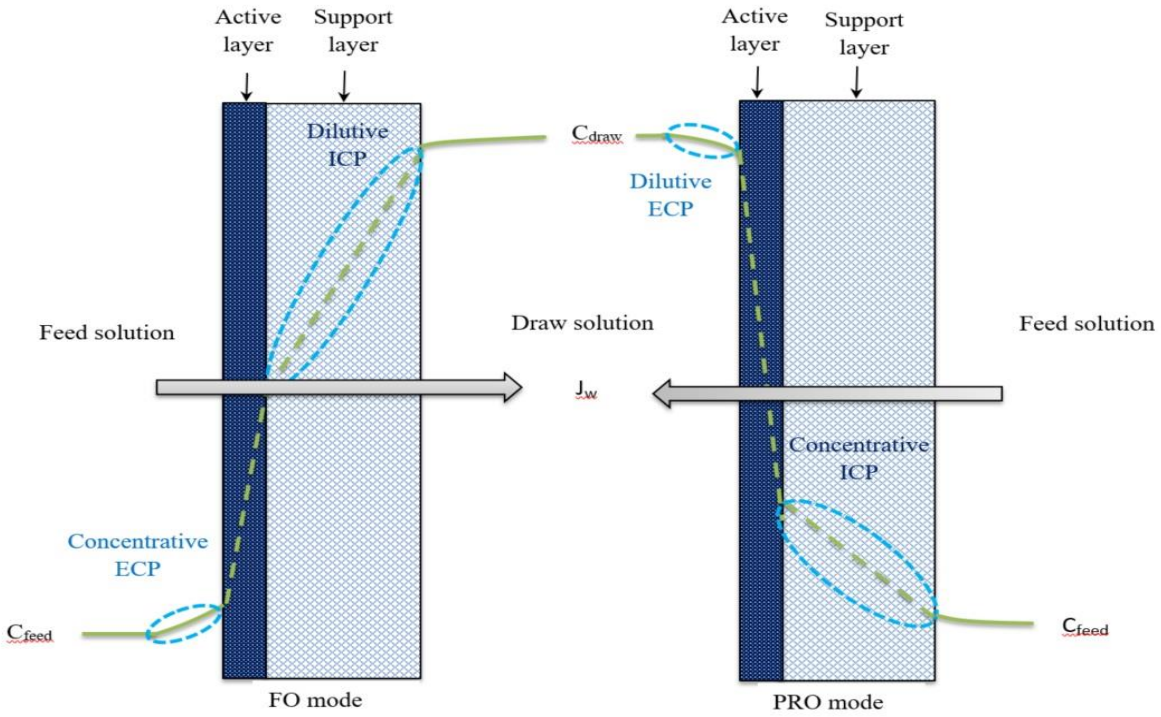

Figure 2.6: Illustration of ICP and ECP in the FO and PRO modes. C_{feed}, C_{draw}, and J_w represent the feed solution concentration, draw solution concentration and water flux, respectively.

ECP occurs at the interface between the bulk solution and the membrane active layer. Depending upon membrane orientation in the FO processes, it can be called either concentrative or dilutive ECP. The positioning of the FO membrane active layer towards the feed solution results in concentrative ECP due to water permeating towards the draw solution causing an increase in solute concentration at the active layer. Alternatively, positioning of FO membrane active layer towards the draw solution results in dilutive ECP at the active layer due to water entering from the feed solution causing solutes dilution at the active layer. ECP reduces the net driving force by increasing the osmotic pressure at the interface of membrane-active layer mode in FO mode i.e. when the membrane active layer faces the feed solution (FO mode) and vice versa in pressure retarded osmosis (PRO) mode i.e. when the membrane active layer is positioned towards draw solution (PRO mode). It has been reported that the negative effects

of ECP can be minimized by altering hydrodynamic conditions such as increasing the flow velocity and optimizing the water flux [50].

ICP takes place inside the porous support layer of the membrane. Depending upon the orientation of the membrane, two types of ICP namely dilutive ICP and concentrative ICP can take place within the support layer of the membrane. Dilutive ICP takes place when the membrane support layer is in contact with the draw solution (FO mode) and water permeating from the feed solution dilutes the porous support layer. Alternatively, when the support layer is directed towards the feed solution (PRO mode), concentrative ICP takes place due to water leaving the support layer through the membrane resulting in the increased solute concentration in the support layer. Unlike ECP, ICP cannot be moderated or diminished by changing the hydrodynamic conditions since it takes place within the support layer. Previous studies have shown that ICP is the major cause of the decline of water flux [124]. However, a recent study demonstrated the effectiveness of ultrasound in reducing the ICP [125]. An 81% increase in water flux was observed with an ultrasound frequency of 25 kHz.

RSF and concentration polarization are the major challenges in FO operation. RSF can be reduced by a suitable draw solute selection and advancement in membrane development. Among all types of draw solutes, thermos-responsive draw solutes have been reported with the lowest RSF. New membranes have been investigated to reduce RSF and the lowest RSF, reported so far, was obtained using nylon 6, 6 microfiltration membrane as TFC-PA membrane support layer. Concentration polarization is the major cause of water flux reduction across the membrane. ICP is a more serious challenge than ECP because it cannot be reduced by altering the hydrodynamic conditions. However, recent studies suggested that ICP effects can be significantly alleviated with ultrasonication [125]. More work is needed to validate the efficiency of ultrasonication and explore other viable options to counter the effects of ICP.

2.6 Membrane fouling and cleaning

2.6.1 Membrane fouling

Membrane fouling is the accumulation/deposition of dissolved and suspended components of the feed solution on the membrane surface [126]. The feed stream components such as microbes, organic, inorganic and extracellular polymeric substances (EPS) which cause fouling can be termed as foulants (Figure 2.7) [127]. When water from the feed solution permeates through the membrane to the draw solution, foulants in the feed solution start accumulating on the membrane surface resulting in the formation of a fouling layer. The fouling layer does not only cause an increase in the resistance to water permeation but also the concentration polarization [128]. Membrane fouling can also decrease the life span of the membrane and consequently increasing the operational and maintenance cost of the FO process [129]. Membrane fouling can be broadly categorized into organic fouling, inorganic fouling (or scaling), biofouling, and cake formation. Organic fouling is the adsorption of organic matter such as proteins, humic substances, and grease on the membrane surface [130]. Scaling or inorganic fouling is the deposition of mineral salts from the bulk solution along with their direct crystallization on the membrane surface [131]. Biofouling is the adhesion and growth of the microbial community on the membrane surface with the help of EPS [132]. Cake formation is caused by the accumulation of a variety of colloidal particles and dissolved organic matter in the form of NOM, EPS, proteins, clay, calcite, and silicates on the membrane surface [133].

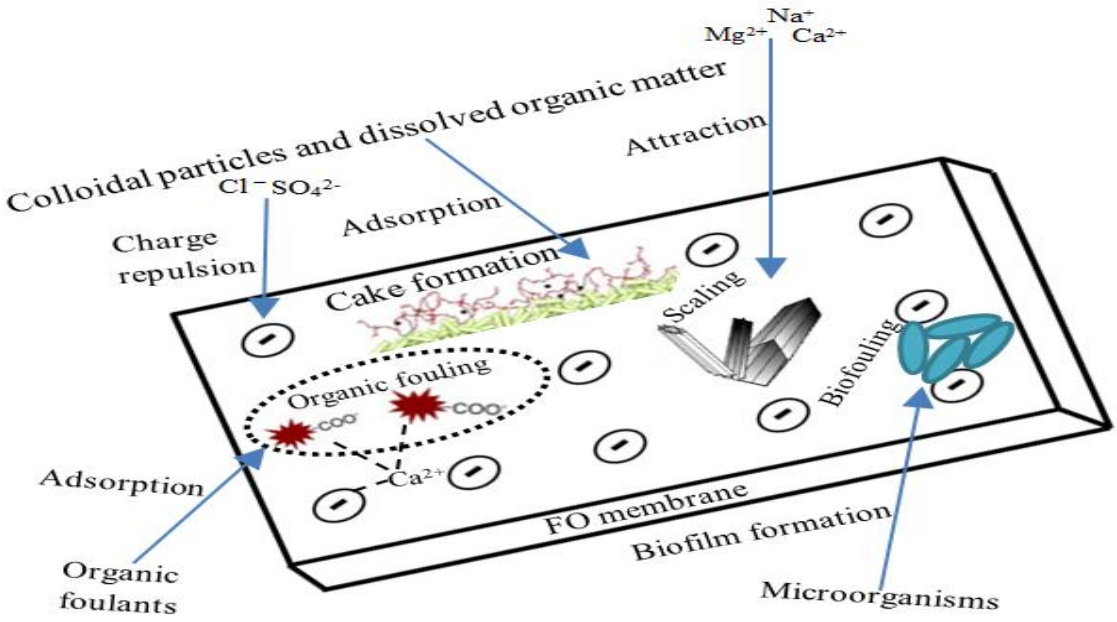

Figure 2.7: Membrane fouling during FO operation.

The comparison between FO and RO in terms of reversibility and water cleaning efficiency has been broadly covered in the literature [134]. FO has a lower fouling tendency in comparison to RO due to the difference in driving force [134]. In RO, water flux is generated by a large hydraulic pressure resulting in the formation of a compact fouling layer which is not easy to remove by hydraulic means. On the other hand, FO is driven by the naturally created driving force due to the concentration gradient across the membrane resulting in a less dense fouling layer that is easy to remove by hydraulic means. Lee et al. demonstrated that membrane fouling is almost reversible in FO and is irreversible in the case of RO [135].

Membrane fouling can influence the rejection of both organic and inorganic contaminants in FO processes. Linares et al. have suggested that organic fouling could improve the negative charge propensity and hydrophilicity of the membrane active layer [136]. Consequently, the absorption efficiency of the membrane could be increased which can inflate the removal of contaminants like trace organic compounds.

Membrane fouling becomes more significant during a resource recovery FO process from a biomolecules rich digestate feed. One good example of digestate is a rumen fluid that can be a potential source for VFAs. Processing rumen fluid for VFAs and water extraction by FO can result in severe membrane fouling as it is a complex fluid containing several other biomolecules such as carbohydrate molecules, amino acids, phospholipids, dicarboxylic acids, glycerides, and cholesterol esters. These biomolecules can be sensitive to the changing conditions in the FO process e.g. temperature and can exacerbate membrane fouling. Studies have shown the aggravated membrane fouling from similar biological-based feed solutions. For example, increasing the rumen fluid temperature in feed to 30 °C and 40 °C exacerbated membrane fouling [137]. Membrane fouling was found as a major obstacle in a seawater-driven FO process for pre-concentrating the digested sludge centrate [49]. Another study on determining the permeation characteristics of VFAs solution demonstrated significant fouling during FO operation [61]. Membrane fouling caused a sharp decline in water flux during the dewatering of the organics rich wastewater by FO for subsequent VFAs recovery [138].

2.6.2 Membrane cleaning and other fouling mitigation strategies

Previous bench-scale FO studies have shown that membrane fouling is readily reversible in comparison to pressure-driven membrane processes such as NF and RO [139]. These studies reveal that the low hydraulic pressure in FO results in a less compacted fouling layer compared to pressure-driven membrane processes. Consequently, a less compacted fouling layer leads to better fouling reversibility [127]. FO membrane cleaning can be achieved either physically or chemically.

Common physical techniques for FO membranes cleaning include osmotic backwashing, high cross-flow velocity (CFV), ultrasonication, air scouring, and hydraulic cleaning [140]. The basis of these techniques is to create strong hydrodynamic conditions or disturbances to dislodge the fouling layer from the FO membrane surface. Osmotic backwashing is an effective

technique to detach foulants from the membrane surface by switching the water flow direction from feed - draw solution to draw - feed solution through the membrane [141]. High CFV is a cleaning method that involves the flushing of the feed channel with fresh water to remove the foulants from the membrane surface [142]. Ultrasonication has also been reported to mitigate membrane fouling using sound energy in the kHz range [143]. It causes cavitation which involves erosion on the membrane surface, dispersing the foulants and/or increasing the dissolution rate of a surface film [143]. Air scouring can be performed under both low and high aeration. Air scouring performed under high aeration results in less biofilm formation whereas low aeration cannot stop significant biofouling [144]. However, aeration is more energy-intensive and therefore a costly process which can be a serious drawback to the economic sustainability of FO. Hydraulic cleaning is performed with the circulation of DI water on the feed side of the membrane. Due to the less compact fouling layer in FO, it can be an effective cleaning strategy and can restore up to 100% of the water flux with 24 - 48 hours of operation [145].

Chemical cleaning involves the use of one or several chemical substances. Normally, a combined cleaning strategy is adopted which involves the dissolution of fouling matrix by chemicals followed by the removal of foulants by mechanical means [127]. Table 2.4 summarizes the commonly used chemicals. The consumption and subsequent disposal of these chemicals, however, can be a potential environmental issue, especially since some of them such as ethylene diamine tetra-acetic acid (EDTA) have been identified as major water pollutants [146]. It is, therefore, important to understand the chemical-foulant, foulant-foulant and foulant-membrane interaction at the molecular level to develop an effective membrane cleaning strategy [127]. The efficiency of chemical cleaning depends on exposure time, hydraulic condition (mixing), the concentration (or strength) of the cleaning chemicals and pH [147]. Acidic cleaning agents such as citric acid and nitric acid are designed to solubilize inorganic

foulants whereas alkaline agents such as NaOH are designed to solubilize organic foulants. Besides, chelating agents such as EDTA can be used to immobilize metal ions, thus, preventing them from interacting with other organic and inorganic constituents in the feed to cause fouling and scaling, respectively [148]. Chemical cleaning with an oxidant like NaOCl has also been reported to be more effective especially for membranes with high hydrophobicity and roughness [149]. Other oxidants like hydrogen peroxide have also been efficiently used as disinfectants in pre-treatment processes [150]. However, their use in membrane disinfection is limited due to the risk of membrane damage or degradation due to chemical attacks.

Table 2.4 Major chemicals used for cleaning different types of membrane fouling

Category	**Chemicals**	**Types of fouling**
Acid	Citric acid [151], nitric acid [152]	Scaling
Alkali	Sodium hydroxide [152], potassium hydroxide [153]	Organic fouling
Chelating agent	EDTA [149], citric acid [152]	Scaling and organic fouling
Oxidant	Sodium hypochlorite [149], hydrogen peroxide [150]	Biofouling and organic fouling

Another effective way to mitigate membrane fouling is to pretreat the feed water. Pretreatment processes like MF and UF consume high energy and therefore have high operating costs. Conventionally, dual media and sand filters are employed as pretreatment processes in large scale desalination plants but their performance is limited and is far below the satisfactory level [154].

The membrane surface properties play a key role in fouling layer formation. Changing the membrane surface with the help of different membrane surface modification techniques can

help in controlling the membrane fouling [155]. Two common strategies for FO membrane surface modification are coating and grafting [155]. The fundamental aim of these strategies is to improve the fouling resistance of the membrane which can be achieved by increasing membrane surface hydrophilicity, decreasing the roughness of membrane surface, adding steric repulsion effect to the membrane and introducing negatively charged surface groups [156].

Biofouling is inevitable in long term operation even at low nutrient concentrations. Biofouling control and mitigation strategies have not been studied in detail. To date, the literature about actual biofouling in FO is scarcely available since biofouling can only start forming during long-term FO operation. As a substitution, reviewing the literature about biofouling in membrane processes like RO and NF can provide some insight into biofouling in the FO processes. In the case of RO and NF, a significant amount of research has been carried out over the past twenty years to understand the process of biofouling and develop techniques for monitoring and control [157]. Different preventive and control strategies to mitigate biofouling include biocide treatment, nutrient control, inhibition of quorum sensing process, and membrane surface modification.

Biocides or antimicrobial substances can be added to feed water as a biofouling prevention strategy. The main factors contributing to the effectiveness of biocides include type and concentration of biocide, level of bioactivity in the system, frequency of dosing, pH, contact time and concentration of organic and inorganic substances in the feed water [158]. A comprehensive literature study reveals that biocides can be broadly categorized into oxidizing and non-oxidizing biocides [157].

Among oxidizing biocides, chlorine is the most commonly used disinfectant in water treatment but it cannot be used for treating all types of membranes because, unlike CTA membranes, PA membranes are sensitive to chlorine [159]. Chlorine also results in the formation of assimilable

organic carbon (AOC) in large quantities which augments bacterial growth [160]. As an alternative to chlorine, the use of chlorine dioxide, chloramines, and potassium ferrate have been suggested [157]. All these agents have high biocidal effectiveness, however, like chlorination; chloramination may lead to the formation of harmful byproducts such as trihalomethanes, haloacetic acids and N-nitrosodimethylamine which can permeate through the membrane. Ozone is a powerful oxidizing agent and can be used for microbial deactivation but has not been widely investigated for FO membrane cleaning due to the potential to form carcinogens and the production of AOC materials as by-products of ozonation [161]. UV irradiations can be effective biocides for water disinfection as they inhibit microbial growth by the production of hydroxyl radicals [162].

Non-oxidizing biocide like formaldehyde, glutaraldehyde and quaternary ammonium compounds have been used in the water treatment industry however they are not suitable for portable applications [163]. They are biologically effective, membrane compatible, cost-effective, suitable for discharge and are used intermittently with a low dose.

Limiting nutrients such as phosphorus in feed water can inhibit microbial growth. It can be achieved by chemical precipitation [164], biological phosphorus removal [165], adsorption [166], and crystallization [167]. Chemical precipitation is a widely used method that involves the use of different coagulants such as iron and aluminum salts, lime, and polyelectrolytes [164]. Chemical precipitation is an effective and flexible approach to precipitate phosphorus out and can be applied at different stages during wastewater treatment. However, its maintenance cost is high, handling and disposing of sludge is problematic, and the treated water needs to be neutralized [164]. Biological phosphorus removal is based on the phenomenon of “luxury uptake” in which favourable conditions are developed for activated sludge to take up phosphorus in the excess amount[165]. No chemicals are used in this method and sludge production in large quantities can be avoided. However, it is more complicated in terms of

complex plant configuration and the operation protocol. Adsorption of phosphorus is carried out with the help of different adsorbents such as dolomite, red mud, blast furnace slag and fly ash [168]. These adsorbents do not produce any additional sludge and do not affect the wastewater pH but they can be costly and have low phosphorus removal efficiency [169]. Phosphorus removal by crystallization is carried out in a fluidized reactor where calcium and magnesium phosphate crystals namely hydroxyapatite and struvite respectively are formed [167]. Unlike chemical precipitation, this method does not involve any sludge handling problem.

Inhibition of quorum sensing can be an effective way to control biofouling [170]. Quorum sensing is a coordination process among microbes for their communal behaviour such as biofilm formation, motility, and EPS production. Kim et al. demonstrated the production of quorum sensing molecules by 60% of the collected bacterial species from fouled RO membrane to justify that biofilm formation can be effectively controlled by inhibition of quorum sensing [171]. Use of furanone [172], vanillin [173], acyl-homoserine lactones and inhibitors like acylase I [174], bacteriophages [175] and nitric oxide [176] have been reported for inhibition of quorum sensing.

Increasing the bacteriostatic properties of the membrane through surface modifications can effectively inhibit microbial growth. Membrane surface modifications can be carried out by polymer blending [177], coating [157], grafting [178] and the addition of inorganic and antimicrobial agents [179]. A promising way to control and mitigate biofouling can involve inducing anti-adhesion and anti-microbial properties to the surface of a membrane [180].

Organic fouling, inorganic fouling and cake formation along with their cleaning techniques have been widely investigated in the literature. The selection of fouling mitigation strategy depends on the type of FO application and scale of FO operation. Of all the FO membrane

fouling types, biofouling is the least investigated phenomenon. Studies on actual biofouling in FO processes and its respective cleaning strategies are hardly available in the literature. Further research is needed to understand biofouling in long term FO operation.

2.7 Full-scale FO plants

As key hurdles to the practical realization of FO at full scale are being addressed, more pilot-scale evaluations and even full-scale trials of FO have recently emerged. In addition to several pilot-scale studies summarized in Table 2.3, in September 2019, Forward Water Technologies Pty Ltd has recently reported a full-scale trial of their FO technology at a wastewater treatment plant in Airdrie, Alberta, Canada [181]. Due to commercial sensitivity, the details of some full-scale trials are not always readily available. The Airdrie full-scale FO plant and several other pilot-scale FO systems are shown in Figure 2.8.

Figure 2.8: Pictures of (a) A full-scale FO plant in Airdrie, Alberta (Canada) [181] (b) A pilot FO plant at Nagasaki (Japan) (c) A pilot FO plant at University of Technology Sydney [110]; and (d) A pilot FO plant at the Quyang Municipal Wastewater Treatment Plant (WWTP), Shanghai (China) [182].

2.8 Conclusion

The transition of FO from laboratory research to large scale applications requires further development in several key areas which include membrane fabrication, draw solute development and membrane fouling mitigation strategies. A prospective FO application of acetic acid and water extraction from rumen fluid produced in an engineered rumen reactor from lignocellulosic biomass can be of great significance due to the potential economic and environmental benefits. The deployment of FO to separate acetic acid and

water from rumen fluid by mimicking the ruminant's digestive system can revolutionize the biochemicals industrial processes with a paradigm shift from fossil resources to a renewable resource of lignocellulosic materials. The focus of membrane development should revolve around high water permeability, low reverse salt flux and ICP, high resistance to fouling, and superior mechanical strength and stability of the membrane. More research is required to develop new draw solutes and to select among the already available ones which are economical, non-toxic, and compatible with the membrane, can generate high osmotic pressure and be easily generated. The number of pilot-scale FO studies and full-scale FO demonstrations is still limited. Inorganic draw solutes were used in most of these pilot and full-scale reports. Results corroborated from this chapter heighten the need for more research work to develop suitable draw solutes for pilot and full-scale FO applications. Membrane fouling is also a major obstacle to the commercialization of the FO process. To date, the literature on biofouling in FO is scarcely available and future research is needed to investigate the underlying mechanisms and develop suitable mitigation techniques.

Chapter 3 Evaluation of Acetic Acid Extraction Potential from Rumen Fluid by Forward Osmosis

This thesis chapter has been published as the following journal article.

Khan JA, Nguyen LN, Duong HC, Nghiem LD. Acetic acid extraction from rumen fluid by forward osmosis. Environmental Technology & Innovation. 2020;20:101083.

3.1 Introduction

Ruminant animals such as cows, sheep, and koalas have a unique digestive system that allows them to acquire nutrients and energy from a plant-based (lignocellulose) diet. Their stomach consists of four compartments instead of one like in other animals. The first compartment, often called the fore-stomach or rumen, contains a complex microbial community of bacteria, archaea, fungi, and protozoa to break down cellulosic materials under anaerobic conditions [15, 183]. The breaking down of cellulosic material leads to the formation of rumen fluid mainly composed of VFAs, phospholipids, amino acids, inorganic ions, dicarboxylic acids, gases, carbohydrates, glycerides, and cholesterol esters [184]. Amongst these constituents, VFAs are vital as they provide energy and nutrient for ruminant animals after diffusing through their intestine [15]. In other words, the unique microbes in the rumen convert lignocellulosic biomass that is indigestible by other animals to beneficial VFAs. This unique capacity of ruminant animals has spurred scientific interests to mimic their rumen for producing VFAs from lignocellulosic material such as crop residues and other lignocellulosic waste [51].

VFAs production from lignocellulosic feed might play an important role in industrial development in the coming years. VFAs are valuable biochemicals that can replace petroleum-based chemicals for the production of pharmaceuticals, plastics, and other products of the modern economy [52, 53]. Each year, about 150 billion metric tons of lignocellulosic biomass is generated, mostly as a by-product of agriculture and forestry

activities [25]. Therefore, VFAs production from the lignocellulosic feed in engineered rumen reactors can obviate the current dependence on crude oil and other fossil resources for raw chemicals. A major technical challenge in the design and development of engineered rumen reactors is the extraction of VFAs from the rumen fermented broth (i.e. commonly known as rumen fluid) like the process inside the ruminant animals' intestine. In this context, we propose to explore FO to mimic the ruminant intestine to extract VFAs from rumen fluid in engineered rumen reactors to promote the realisation of VFAs production from lignocellulosic material.

FO has emerged as a versatile technology platform for the treatment of various impaired waters that are deemed challenging to other treatment processes. Unlike the pressure-driven membrane processes (e.g. NF and RO), FO does not require an externally applied hydraulic pressure but harnesses the intrinsic osmotic gradient between two solutions to facilitate the transport of water and/or solute across the membrane [185]. Driven by the osmotic gradient, the FO process embodies several superior attributes such as low membrane fouling, fouling reversibility, and simple operation. Given these notable attributes, the FO process has been demonstrated for a wide range of applications including wastewater treatment [24, 186, 187], phosphorus recovery from wastewater and digested sludge [21, 22, 103], water recovery from drilling mud [23, 47], and food processing [20, 188]. Most of these FO applications involve the dewatering of the less concentrated feed solution by the high concentrated draw solution with a focus on increasing the water flux and reducing the RSF.

In this study, the FO process was harnessed to promote the extraction of acetic acid from rumen fluid prior to its enrichment and utilisation. The enrichment of acetic acid can be performed by several methods such as distillation, liquid-liquid extraction, and crystallization [189-191]. In other FO applications, water is extracted from the feed to the

draw solution under the osmotic gradient caused by the difference in the feed and draw solution concentrations. Despite the high selectivity of the FO membrane, water flux always coincides with the reverse transport of solute from the draw solution to the feed. Unlike water, which permeates through the membrane from a low concentrated solution to a high concentrated solution, the solutes permeate through the membrane in the opposite direction i.e. from a high concentrated solution to a low concentrated solution following the natural concentration gradient. This solute transport or the RSF has been dealt as a major impediment in the development of FO technology and many attempts have been made to mitigate it [115-117]. This study, however, aimed at using the transport of solute through the FO membrane as a means to promote the extraction of acetic acid from rumen fluid while maintaining minimum water flux. The negligible hydraulic pressure and the minimum water flux applied might render the FO process resistant to the high fouling propensity of the rumen fluid that might be a serious challenge to other pressure-driven membrane processes. The decreasing osmotic pressure difference between the two solutions due to acetic acid transport across the membrane can be neutralized or slowed down by taking the stripping solution volume in bulk or constant dilution of stripping solution. Moreover, the dilution of rumen fluid due to water flux can be reversed by the dewatering process using FO system as explained in the next chapter. Given the abovementioned purpose, this study systematically examined the influence of membrane type, membrane orientation, pH of the stripping solution, and the rumen matrix on the acetic acid extraction of the FO process. The broader idea is to develop an engineered rumen reactor to produce VFAs from lignocellulosic biomass and then extract the produced VFAs from fermented solution by FO.

3.2 Materials and methods

3.2.1 The FO system and the feed and stripping solutions

The lab-scale FO system used in this study consisted of a membrane module, two gear pumps, two flow meters, and two beakers for feed and stripping solutions (Figure 3.1). The membrane module had a flat-sheet FO membrane coupon sandwiched between two identical and symmetrical acrylic semi-cells having flow channels with length, width, and depth of 7.6, 2.6, and 0.3 cm, respectively. The effective area of the membrane was 19.76 cm^2. Two gear pumps (Cole-Parmer, 75211-15) were used to circulate the feed and stripping solution, while two acrylic flow meters (Cole-Parmer, 32461-42) were placed before the inlets of the FO membrane module to measure the feed and stripping solution flow rates. The feed beaker was placed on a digital balance (Adam Equipment, PGL 8001) connected to a computer to allow for the record of change in the solution beaker mass after every 60 minutes. The pH of the feed and the stripping solution was measured every hour using two pH meters (Hach, HQ40d).

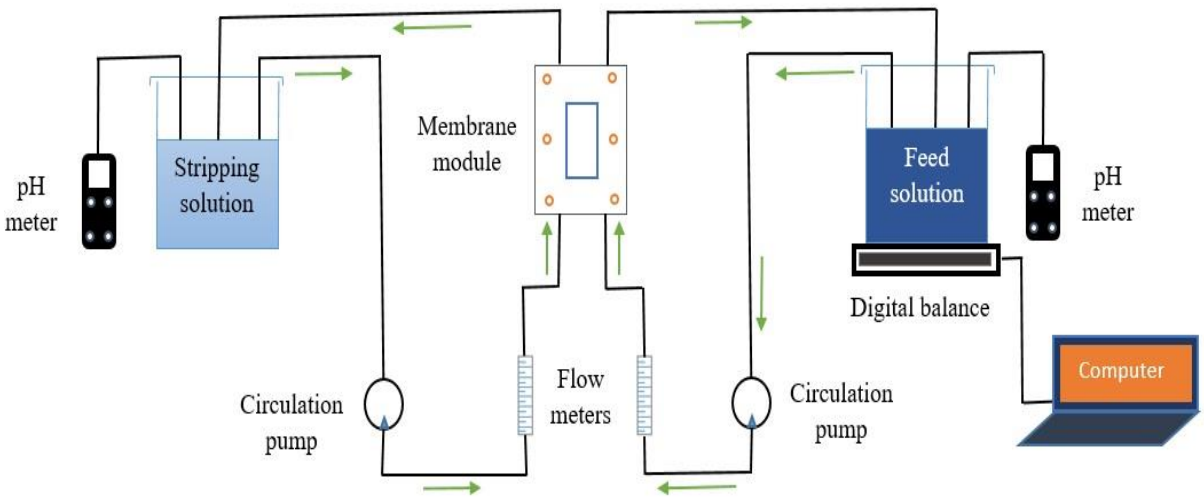

Figure 3.1**:** Schematic diagram of the lab-scale FO system.

Two types of non-commercial FO membranes including TFC-PA and CTA were used in this study. The TFC-PA membrane is a proprietary FO membrane from Hydration

Technology Innovation (Albany, OR), while the CTA membrane is from Fluid Technology Solutions Inc., USA. The TFC-PA membrane is fabricated via interfacial polymerisation having a thin PA active layer with a porous polysulfone support layer. The CTA membrane is prepared from the CTA along with an embedded support layer using the phase inversion method. The pore sizes of the CTA and TFC-PA membrane are in the range of 0.29−0.30 nm. These two membranes have been selected for their contrasting properties in terms of fouling resistance, water permeability, and particularly RSF. Recent results suggest that the CTA FO membrane is less susceptible to fouling but exhibits lower water permeability and higher RSF than the TFC-PA one [80, 192, 193]. Therefore, it is necessary to elucidate the effect of these two membranes with different RSF on the FO extraction of acetic acid from rumen fluid.

A synthetic solution and real rumen fluid were used as feed solutions in this study. The synthetic acetic acid 50 mM solution was prepared by dissolving lab-grade acetic acid (>99% purity from Sigma-Aldrich) in DI water. This low acetic acid concentration was deliberately selected to minimise the water flux while ensuring a sufficient transport rate of acetic acid through the FO membrane. DI water was used as the stripping solution to capture acetic acid transferred through the FO membrane from the feed. Rumen fluid from a twelve years old fistulated cow was also used to replicate the real rumen matrix. Coarse matters in the rumen fluid were removed by straining it through a two-layered cheesecloth followed by a two-layered mesh filter [194]. The obtained rumen fluid was kept at 4 °C in the dark before the extraction experiment. The rumen fluid contains acetic acid as one of the main VFAs but we could not analyse the rumen fluid to find its acetic acid concentration. Therefore, synthetic acetic acid was added to the rumen fluid to obtain a concentration of at least 50 mM.

3.2.2 Analytical methods

The concentration of acetate ions in the stripping solution was analysed using Ion chromatography (Thermo Scientific, Dionex Integrion RFIC) with an anionic column (Dionex IonPac^{TM} AS15) and NaOH 38 mM solution as eluent. The stripping solution samples (i.e. 1 mL each) were collected every hour during the FO acetic acid extraction experiments. Before analysing the samples, the standard curve with an R^2 value of 0.994 was developed using 0.5, 2.0, 5.0, 7.5, and 10.0 mM acetic acid solution as standard solutions (Figure 3.2). Each sample took 30 minutes to develop a chromatogram. The peak curve for acetate ions appeared between 7 and 8 minutes in each chromatogram. It is necessary to note that with the NaOH 38 mM eluent, all acetic acid in the stripping solution has conversed into acetate ions.

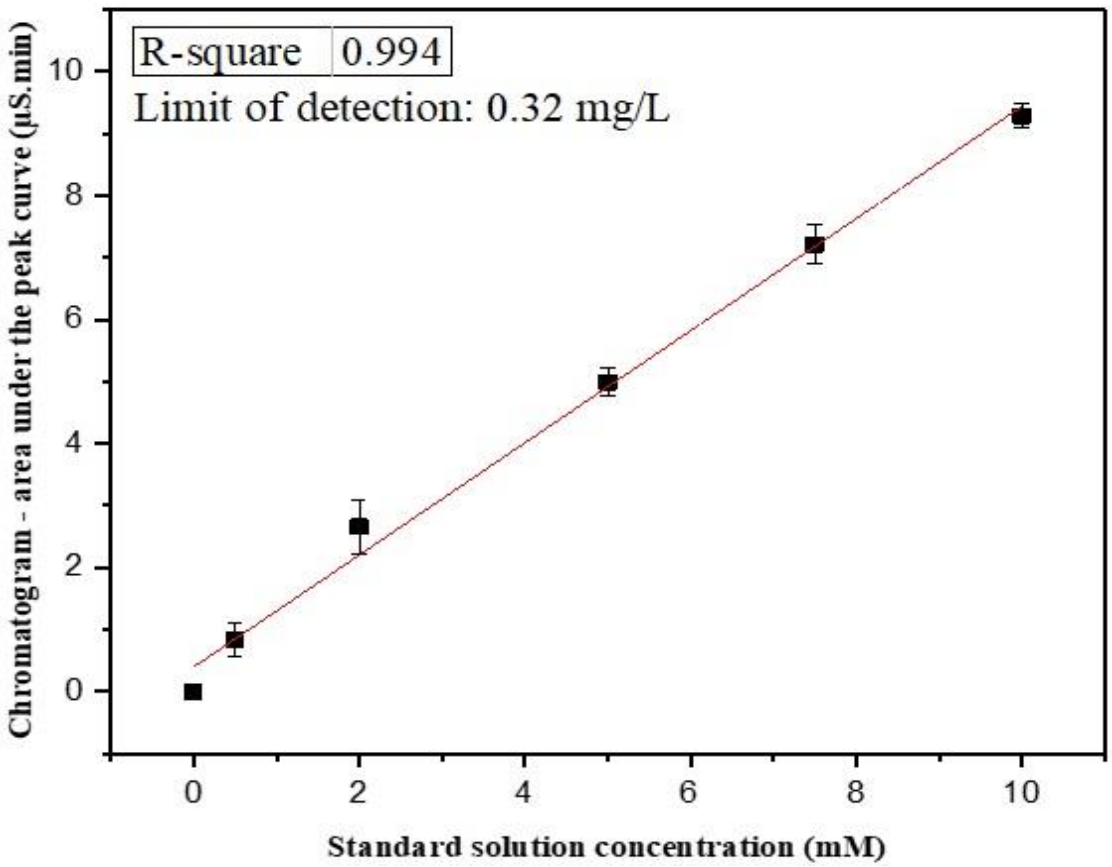

Figure 3.2**:** Standard curve for quantitative analysis of acetate ions in the stripping solution.

The acetic acid recovery from the feed solution was calculated based on its changing concentration in both solutions. The initial concentration of acetic acid was 50 mM on the feed side and zero on the stripping solution side. As the experiment proceeded, the transport of acetic acid from the feed to the stripping side resulted in a gradual decrease in the acetic acid concentration on the feed side and a simultaneous increase on the stripping side. Theoretically, the maximum possible acetic acid concentration on the stripping side will be 25 mM when the equilibrium point is reached between the two solutions. Calculation of acetic acid concentration in the stripping solution were performed with reference to the maximum acetic acid extraction possible.

3.2.3 Characterisation of FO membranes

Membrane transport characteristics including the pure water permeability coefficient (A), salt permeability coefficient (B), and structure parameters were determined using the standard protocol described in the previous studies [195, 196]. A and B values were determined by a cross-flow RO system using DI water and NaCl 34 mM respectively as the feed [197]. The RO system was stabilised for at least one hour at the transmembrane pressure (ΔP) of 10 bar and a cross-flow velocity (CFV) of 25 cm/s before the water flux (i.e. J_{RO} for the process with DI water feed and J_{NaCl} with the NaCl solution feed) was recorded. To determine the B value, feed and permeate samples were collected to determine the observed NaCl rejection (R_{ob}). The A and B values were determined as [197]:

$$A = \frac{J_{RO}}{\Delta P} \tag{3-1}$$

$$B = J_{NaCl}\left(\frac{1 - R_{ob}}{R_{ob}}\right)exp\left(-\frac{J_{NaCl}}{k_f}\right) \tag{3-2}$$

where k_f was the mass transfer coefficient of the cross-flow RO membrane cell. k_f was calculated using the salt concentration at the membrane surface with the thin-film theory for concentration polarisation:

$$k_f = \frac{J_{NaCl}}{ln\left[\frac{\Delta P}{\pi_b - \pi_p}\left(1 - \frac{J_{NaCl}}{J_{RO}}\right)\right]} \tag{3-3}$$

In Equation 3, π_b and π_p were the feed and permeate osmotic pressures and can be determined by their corresponding salt concentrations according to the Van't Hoff equation.

The membrane structural parameter (S) determines the degree of ICP. The S value is defined as below [197]:

$$S = \frac{l\tau}{\varepsilon} \tag{3-4}$$

where l is the thickness of the supporting layer, τ is the tortuosity of the supporting layer, and ε is the porosity of the supporting layer.

Here, the S value was experimentally determined using the cross-flow FO system mentioned above with NaCl 0.5 M as the draw solution and clean water as the feed solution. The membrane active layer was in contact with the feed solution. The FO system was stabilised for one hour before recording the water flux (J_{FO}) to determine the S value using [195, 197]:

$$S = \frac{D_s}{J_{FO}} ln\left(\frac{B + A\pi_{D,b}}{B + J_{FO} + A\pi_{F,m}}\right) \tag{3-5}$$

In Equation 5, D_s is the bulk solution diffusivity of the draw solute, $\pi_{D,b}$ is the bulk osmotic pressure of the draw solution, and $\pi_{F,m}$ is the osmotic pressure at the membrane surface on the feed side.

3.2.4 FO extraction of the acetic acid from the synthetic solution and rumen fluid

All experiments were carried out using a lab-scale FO system for at least 8 hours at room temperature (25±1 ºC). The volumes of feed solution and stripping solution were 2.0 L. The CFV of both the feed and stripping solution was constant at 10.6 cm/s with a co-current configuration. An aliquot sample (1 mL) was taken from stripping solution every hour for acetate ions concentration analysis.

Two ranges of stripping solution pH were applied in this study to assess the impact of stripping solution pH on the acetic acid transport across the FO membrane. One was the pH range of DI water (5.5-6.5) and the other was a pH of 9.0-10.0 achieved by adding 0.2 mL of NaOH 0.1 M solution to the stripping solution after every 8-10 minutes.

3.3 Results and discussions

3.3.1 Membrane characterisation

The membrane characterisation results allow for the comparison between the CTA and TFC-PA membranes with respect to mass transfer across the membrane. Consistent with the literature, the CTA membrane exhibited a lower A value but significantly higher B and S values than the TFC-PA membrane under the same testing conditions (Table 3.1). It is noteworthy that while the water permeability of the CTA membrane was only one-fourth of that of the TFC-PA membrane, its salt permeability was 4.5-fold higher than the salt permeability achieved by the TFC-PA membrane. The markedly high salt permeability/water permeability ratio of the CTA membrane might favour the extraction of acetic acid with minimised water flux from the rumen fluid during the FO process compared to the TFC-PA one.

Table 3.1: Key transport parameters of the CTA and TFC-PA FO membranes.

Parameters	CTA	TFC-PA
Pure water permeability – A value (L/m^2hbar)	0.84	2.10
NaCl permeability – B value (m/s)	8.96×10^{-8}	1.96×10^{-8}
Structural parameter – S value (mm)	0.58	0.30

3.3.2 Acetic acid extraction from the synthetic solution

In the FO process with the synthetic solution feed, the impacts of membrane fouling and complex feed compositions on the transport of acetic acid through the membrane could be excluded, allowing for the accurate evaluation of the influences of FO membrane properties and process operating conditions on the acetic acid extraction. The experimental results shown in Figure 3.3 confirmed the advantage of the CTA membrane over the TFC-PA membrane with respect to the extraction of acetic acid. Under the same operating conditions of both membrane orientations and the stripping solution pH values of 5.5-6.5 and 9.0-10.0, the acid acetic extraction rate of the FO process with the CTA membrane was higher than that with the TFC-PA membrane, demonstrated by its higher acetate ions concentration in the stripping solution at the same operating time. The higher acetic acid extraction rate of the CTA compared with the TFC-PA membrane was consistent with its higher salt permeability reported in section 3.1. Indeed, previous studies have demonstrated that the CTA membrane exhibits lower salt rejection and higher reverse salt flux than the TFC-PA membrane [196, 198].

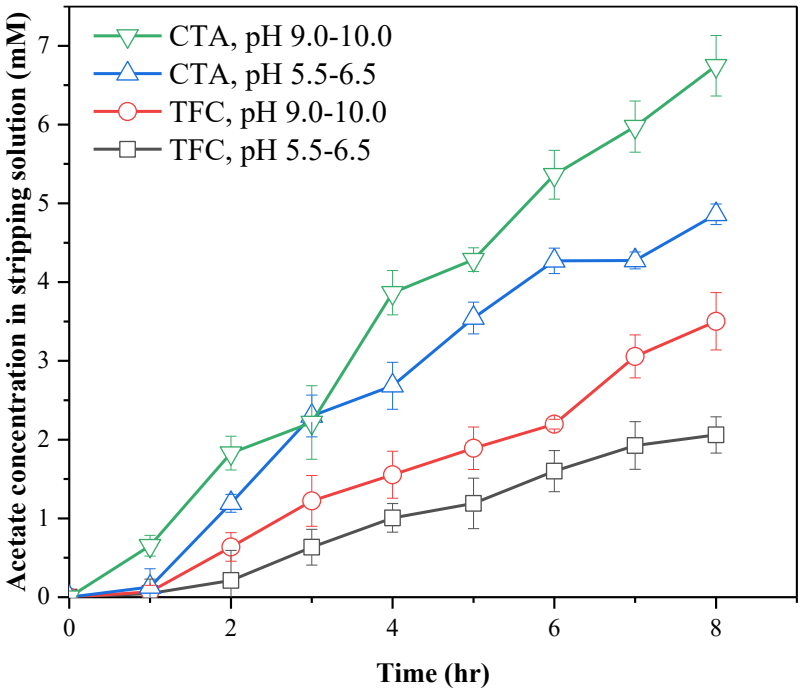

Figure 3.3: Effect of membrane and pH on acetic acid permeation. Experimental conditions were as follows: acetic acid 50 mM solution feed, FO mode, feed and stripping solution CFV =10.6 cm/s. The error bars represent the standard deviation of data obtained from two independent experiments.

It is noteworthy that the membrane pore sizes might not be the prominent factor affecting the transport of acetic acid through the FO membranes. The CTA and TFC-PA membranes used in this study have pore sizes in the range of 0.29−0.30 nm while the calculated molecular diameter of an acetic acid molecule is approximately 0.45 nm. The diffusion of acetic acid through the FO membrane might be controlled by the Donnan effect, not the size exclusion. Indeed, a recent study has found that the electrostatic interaction between the solute molecules and the membrane rather than the size of solute molecules affects the transport of solutes through the membrane [187].

Moreover, the transport of acetic acid through the membranes during the FO process of the synthetic solution feed was primarily driven by the acid concentration difference between the feed and the stripping solution. This is demonstrated by the discrepancy in

the acetic acid transport rate through the membranes when the stripping solution pH was elevated from 5.5-6.5 to 9.0-10.0. At the elevated stripping solution pH, more acetic acid was extracted from the synthetic solution through the FO membranes, leading to higher acetate ion concentration measured in the stripping solution (Figure 3.3). It is necessary to note in both feed and stripping solutions acetic acid dissociated into negatively charged acetate ion and proton: $CH_3COOH \leftrightarrow CH_3COO^- + H^+$ (pKa = 4.76). This equilibrium strongly depended on the pH of the solutions. The synthetic solution feed was highly acidic (i.e. pH = 3); thus, acetic acid existed mainly as neutral molecules in the feed. On the other hand, 80% and almost 100% of all permeated acetic acid molecules from feed to the stripping solution existed in the form of acetate ions at pH of 5.5-6.5 and 9.0-10.0, respectively. The higher acetic acid concentration difference across the FO membranes at the stripping solution pH of 9.0-10.0 rendered more acetic acid transferred through the membranes, leading to the higher measured acetate ion concentration in the stripping solution compared to the stripping solution pH of 5.5-6.5.

The linear relationship between the measured acetate ion concentration of the stripping solution and the operating time shown in Figure 3.3 might be attributed to the excessively high acetic acid concentration of the synthetic solution feed (50 mM) compared with that of the stripping solution (i.e. <1 mM after 8 hours of extraction). If the FO process with the synthetic solution feed was extended, more acetic acid from the feed would transfer to the stripping solution, hence reducing the driving force for the acetic acid extraction from the feed. The acetate ion concentration curves shown in Figure 3.3 would flatten when the driving force dwindled with extended operating time. Theoretically, acetate ion concentration in the stripping solution can increase to 25 mM when the system is at equilibrium with an extended operating time. Nevertheless, as demonstrated in Figure 3.3, after 8 hours of the FO operation, the CTA can achieve 27% and 19% of the

maximum extraction potential at pH of 9.0-10.0 and 5.5-6.5, respectively. Over the same experimental period, the TFC-PA membrane can only achieve 14% and 8% of the maximum extraction potential at the respective pH of 9.0-10.0 and 5.5-6.5.

The effect of membrane orientation was evaluated for both the membranes at the selected stripping solution pH values (Figure 3.4). The TFC-PA membrane orientation had a negligible effect on the acetic acid permeation to the stripping given the inbuilt feature of this membrane to hinder solutes transport across the membrane [199]. The acetate ion concentrations in the stripping solution during the FO process of the synthetic solution feed using the TFC-PA membrane were similar when the membrane orientation was reversed (Figure 3.4a). On the other hand, for the FO process using the CTA membrane, the stripping solution acetate ion concentration increased by 14% when the membrane active layer facing the feed solution (6.7 mM) compared with that obtained when the membrane active layer facing the stripping solution (5.8 mM) (Figure 3.4b). This slight increase could be attributed to the less ICP effect when the membrane active layer facing the feed solution than facing the stripping solution (i.e. the feed acetic acid concentration was much higher than that of the stripping solution). It is worth reminding that the CTA membrane had a higher *S* value than the TFC-PA membrane (Table 3.1); therefore, the negative effect of ICP on the acetic acid extraction during the FO process with the CTA membrane was more severe than that with the TFC-PA membrane. Thus, the effect of membrane orientation on the acetic acid extraction rate was more noticeable for the CTA compared to the TFC-PA membrane.

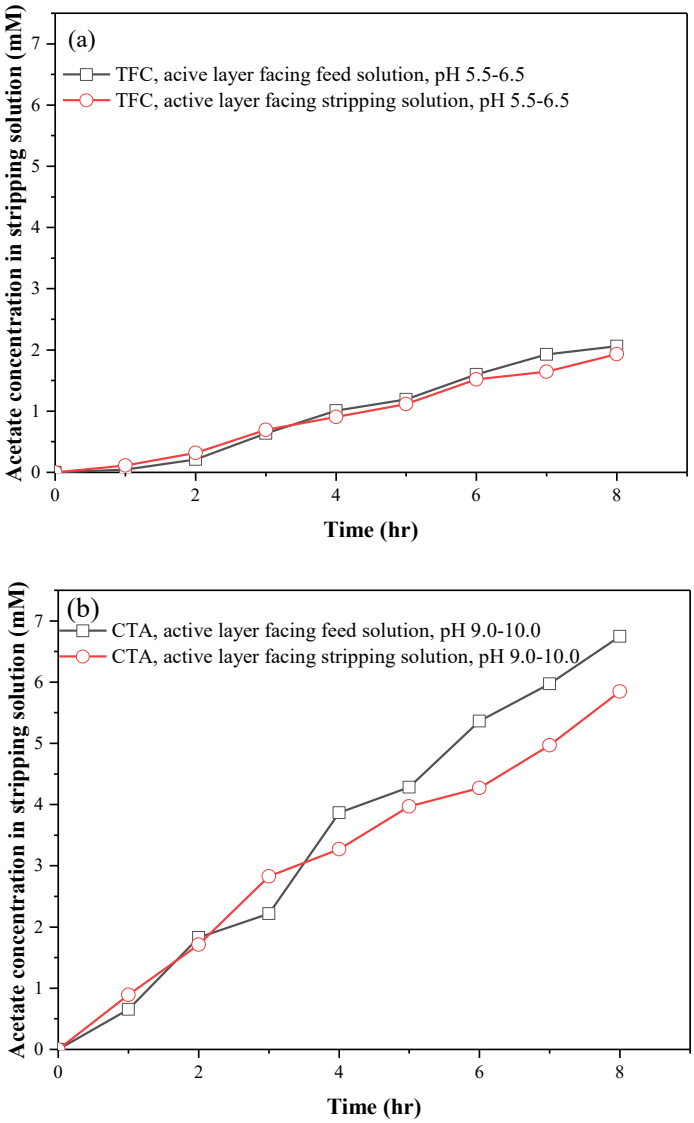

Figure 3.4**:** Effect of membrane orientation on acetic acid permeation when (a) membrane was TFC-PA and stripping solution pH was 5.5-6.5, and (b) membrane was CTA and stripping solution pH was 9.0-10.0. Experimental conditions were as follows: synthetic acetic acid 50 mM solution feed, feed and stripping CFV = 10.6 cm/s.

3.3.3 Acetic acid extraction from rumen fluid

The FO process using the CTA membrane with the active layer facing the feed solution was used to evaluate the acetic acid extraction potential from the real rumen fluid at two stripping solution pH values (Figure 3.5). The acetate ion concentration in the stripping solution increased gradually at both of the stripping solution pH values. A maximum of

3.65 mM acetate ion concentration in the stripping solution was observed after 8 hours of the experiment which is equivalent to ~15% of the maximum attainable concentration (25 mM). In comparison, after 8 hours, acetic acid extraction from the synthetic solution was 27% of the maximum attainable concentration.

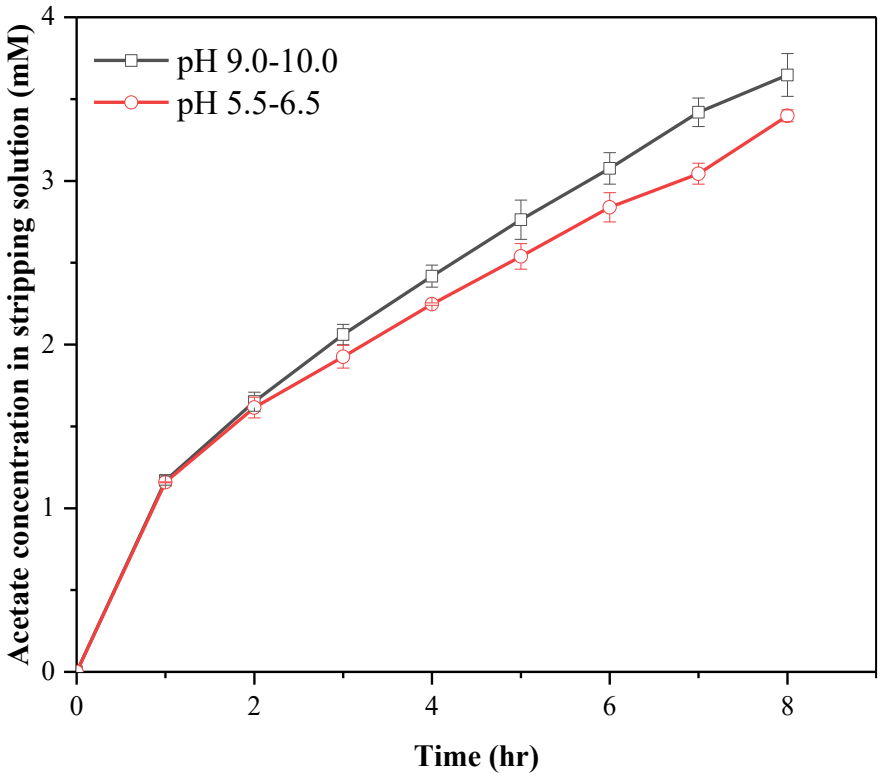

Figure 3.5: Acetic acid permeation from a rumen fluid at two different pH values. Experimental conditions were as follows: rumen fluid with acetic acid 50 mM as the feed, CTA membrane, FO mode, feed and stripping CFV = 10.6 cm/s. The error bars represent the standard deviation of data obtained from two independent experiments.

The lower acetic acid extraction potential of the FO process with the real rumen fluid compared to the process with the synthetic solution could be attributed to complex constituents of the rumen fluid that might lead to membrane fouling. The real rumen fluid contained various constituents including phospholipids, inorganic ions, amino acids, dicarboxylic acids, volatile and non-volatile fatty acids, glycerides, carbohydrate, and cholesterol esters [184]. These constituents hinder the flow of acetic acid from rumen

fluid to the stripping solution. They also act as a source of possible transportation of other small solutes across the membrane, thus creating competition for acetic acid molecules and significantly reducing the effective osmotic pressure across the membrane.

Unlike in the FO process with the synthetic solution feed, in the process with the real rumen fluid, stripping solution pH exerted an indiscernible influence on the acetic acid transport across the membrane. The acetate ions concentration increased from 3.40 mM to only 3.65 mM when the stripping solution pH was elevated from 5.5-6.5 to 9.0-10.0. It can be due to the high pH (~5.6) of the rumen fluid feed. At this pH value, approximately 80% of the acetic acid molecules were in the form of acetate ions and only the remaining 20% acetic acid molecules were available for transport across the membrane. Therefore, even when the stripping solution pH was increased from 5.5-6.5 to 9.0-10.0, the increase in acetate ion concentration in the stripping solution was unnoticeable due to the limited availability of acetic acid molecules in the feed solution. This is consistent with the lower acetic acid extraction potential of the FO process with the real rumen fluid compared with the process using the synthetic solution feed discussed above.

3.3.4 Water transfer between the feed and stripping solutions

Water flux from the stripping to the feed solution was measured by monitoring the changing weight of the feed solution. Negligible water flux was observed when either the synthetic solution or the real rumen fluid was used as the feed (

Figure 3.6). The type of membranes, membrane orientation, and the stripping solution pH showed an indiscernible effect on water flux. For the synthetic solution, water flux was highest (i.e. 1) at the beginning of the experiment, then gradually decreased toward zero with the operating time. These results were expected due to the low transmembrane

osmotic pressure gradient generated by a small difference in acetic acid concentrations between the feed and stripping solution (<50 mM).

When rumen fluid was used as the feed solution, the water flux from the stripping solution to the feed solution was more noticeable at around 3 L/m^{2}h. The higher water flux observed with the rumen fluid feed could be attributed to the increased transmembrane osmotic pressure gradient because of the high concentration of the rumen fluid. Besides acetic acid (>50 mM), the real rumen fluid contained other solutes and hence offered a higher osmotic pressure than the synthetic acetic acid 50 mM solution. As a result, the driving force for water transport from the stripping solution to the rumen fluid feed was higher than that of the synthetic solution feed.

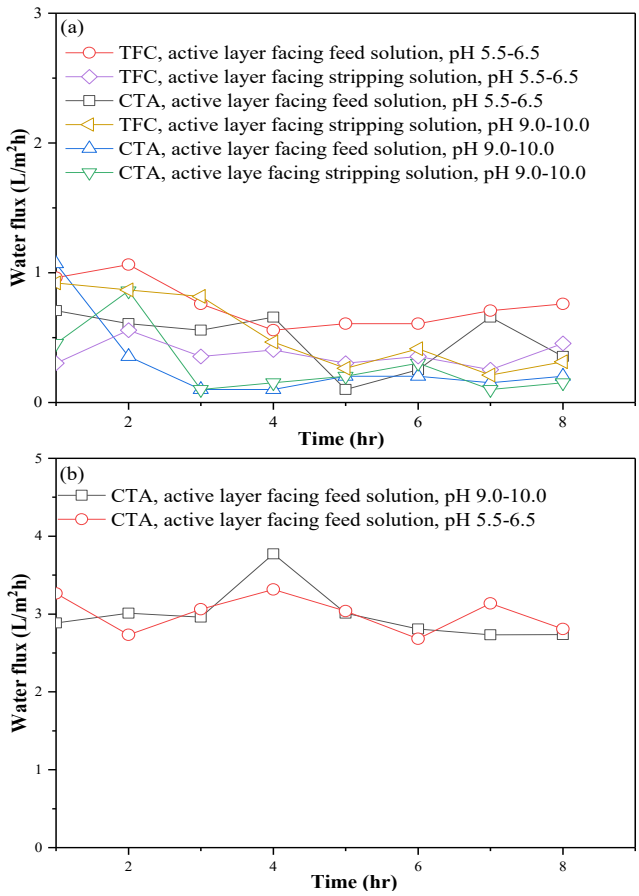

Figure 3.6: Changes in water flux as a function of extraction time when (a) the synthetic acetic acid 50 mM solution and (b) rumen fluid with acetic acid 50 mM was used as the feed.

3.3.5 The pH of feed and stripping solution

Changes in pH of the feed and stripping solutions were recorded after every hour of each experiment. pH values of the synthetic solution and rumen fluid were constant during all FO experiments (Figure 3.7). Both feed solutions acted as the bulk solution for acetic acid and therefore the continuous outflow of acetic acid molecules into the stripping solution did not alter the acidic environment of the feed solutions. The initial and final pH values (~5.7) for rumen fluid was much higher than those for the synthetic solution (~3.0). The higher pH value of rumen fluid could be explained by the presence of organic solutes and inorganic ions resulting in a high buffering capacity.

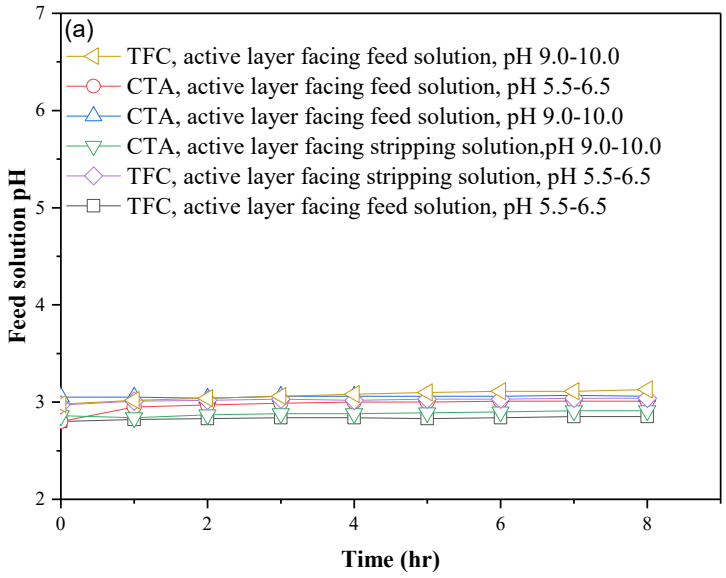

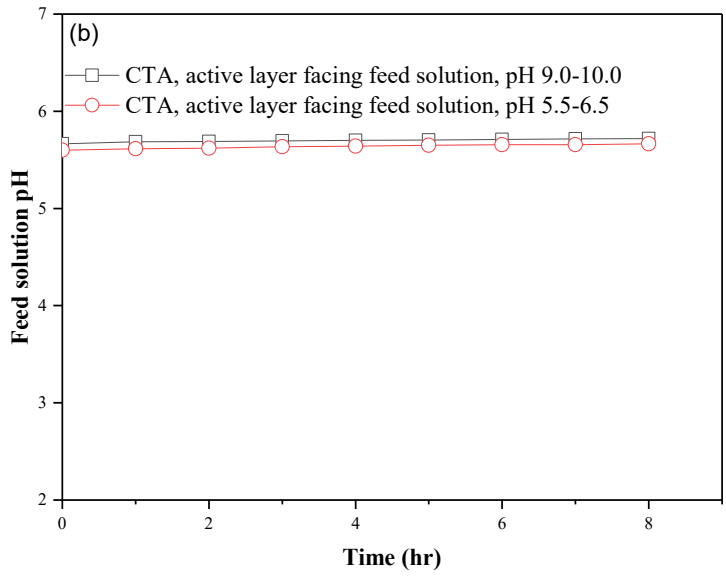

Figure 3.7: Changes in feed solution pH as a function of extraction time when (a) the acetic acid 50 mM solution and (b) rumen fluid with acetic acid 50 mM was used as the feed.

Unlike the feed solution pH, a notable decrease in the stripping solution pH was observed at the beginning of all extraction experiments (Figure 3.8). The observed pH decrease was attributed to the influx of acetic acid from the feed solution. The pH drop was more significant in the first hour and became gradual in the remaining seven hours of the experiments.

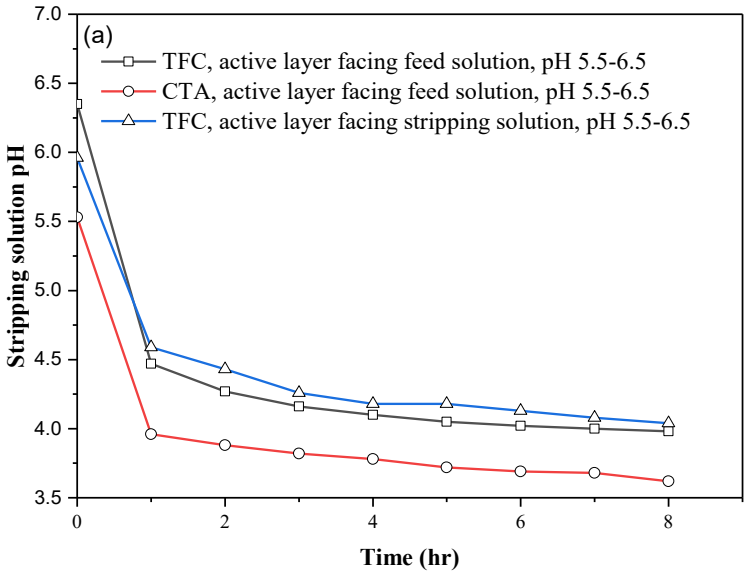

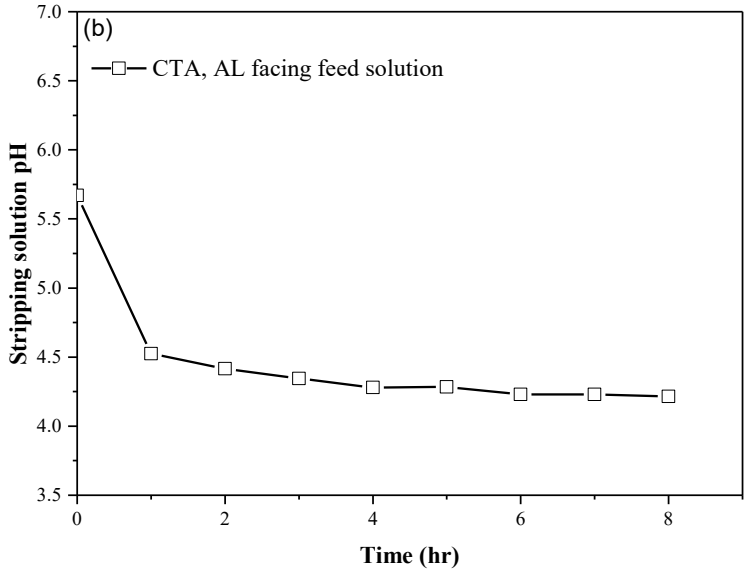

Figure 3.8: Changes in stripping solution pH as a function of extraction time when (a) acetic acid 50 mM solution (b) rumen fluid with acetic acid 50 mM was used as the feed.

3.4 Conclusion

This study provides preliminary but new insight into the potential of acetic acid extraction from the rumen fluid by FO. The membrane characterisations showed better separation performance by the TFC-PA membrane in terms of pure water permeability, solute rejection, and structural parameter compared to the CTA membrane. However, the CTA membrane allowed more acetic acid transport through the membrane than the TFC-PA one under the same experimental conditions. Moreover, the acetic acid transport through the membrane increased as the stripping solution pH was elevated from 5.5-6.5 to pH 9.0-10.0 for both membranes. The effect of membrane orientation on acetic acid transport was insignificant for both TFC-PA and CTA membranes. The highest acetic acid permeation to stripping solution was achieved with the CTA membrane having the active layer facing the feed solution and at the stripping solution pH of 9.0-10.0. The optimised condition was used to evaluate the extraction of acetic acid from the real rumen fluid. Considerably lower acetic acid extraction rate was observed compared to the synthetic solution. Thus, further work is required to improve the extraction rate in a realistic condition involving the complex rumen fluid matrix.

Chapter 4 Assessment of Forward Osmosis to Extract Water from Rumen Fluid for Artificial Saliva

This thesis chapter has been published as the following journal article.

Khan JA, Vu MT, Nghiem LD. A preliminary assessment of forward osmosis to extract water from rumen fluid for artificial saliva. Case Studies in Chemical and Environmental Engineering. 2021:100095.

4.1 Introduction

Ruminant animals such as cows, sheep and goats can rely exclusively on a diet of only lignocellulosic biomass. Their digestive system has evolved to include a four-compartment stomach, namely rumen, reticulum, omasum, and abomasum. The rumen or fore-stomach is the largest compartment acting as a fermenter to convert solid lignocellulosic materials (e.g. grass and hay) to soluble volatile fatty acids (VFAs) using a consortium of anaerobic microbes. The liquid inside the rumen is commonly called rumen fluid. The produced VFAs are the primary nutrient source for ruminant animals to acquire energy and growth [194]. The reticulum is a small, pouch-like compartment to receive heavy or dense feed that cannot be digested for disposal. The omasum is a globe-shaped structure containing leaves of tissue just like flat sheet membranes to absorb water and other substances from the rumen fluid [200]. The abomasum compartment is lined with glands to release enzymes to assist the digestion process [201]. In addition to the omasum, water is also reabsorbed by the large intestine of a ruminant animal before the remaining material is released to the environment as dehydrated manure [202].

Water recovered by the omasum and the large intestine is reused by ruminant animals as saliva to add to the lignocellulosic feed during the chewing process. Each day, a cow produces about 100 litres of saliva to add to the feed [203]. The ruminant saliva is essentially a concentrated salt solution to supplement necessary nutrients and minerals to

the carbon-rich lignocellulosic feedstuffs and to buffer the rumen fluid at near-neutral pH [27]. The composition of ruminant saliva has been studied and defined in the literature. Key minerals in ruminant saliva include sodium, potassium, magnesium, calcium, bicarbonate, phosphate, and chloride [27].

Lignocellulosic biomass is a renewable resource. It is also the most abundant waste material in our modern economy. The potential to utilise this biomass for the production of VFAs is therefore enormous. VFAs are essentially the building blocks of the modern bio-chemical industry as they can replace raw materials from fossil-based materials, such as crude oil and coal [204]. Not surprisingly, significant scientific efforts have been devoted to the development of an engineering rumen reactor that can replicate the ruminant digestive system to convert lignocellulosic materials into VFAs at an industrial scale.

The three most important challenges to develop an engineering rumen reactor are to simulate the fermentation of lignocellulosic feedstuffs to produce VFAs and to extract VFAs and re-adsorb water from the rumen fluid in a way that replicates the function of the small and large intestine, respectively. Several studies have explored the use of anaerobic digester for the production of VFAs from the lignocellulosic biomass. Encouraging results with VFAs yield of 438 mg/g substrate per day have been recently reported to demonstrate the successful production of VFAs from the lignocellulosic feed using an MBR [27]. Lukitawesa et al. [205] have reported 0.8 g of VFAs/g of volatile solids production from food wastes at inoculum to substrate ratio of 1:3 and pH 6. A recent pilot-scale study has demonstrated the biogas production composed of 10% hydrogen and 55% methane along with 0.13 g VFAs per g of total volatile solids production from the agro-waste [206]. A proof of concept demonstration using the forward osmosis (FO) process to extract acetic acid (a representative of VFAs) from

rumen fluid has also been reported [207]. In this case, the small intestine functions similar to a biological membrane and acetic acid can be transferred by osmosis.

Several methods including both membrane-based and non-membrane based have been applied to recover VFAs from the fermented solutions. These methods include ultrafiltration [51], nanofiltration [54], liquid-liquid extraction [55], absorption [56], ion exchange [57], pervaporation [58], and electrodialysis [59]. These methods have high energy demand to separate the VFAs from the aqueous phase, rendering them expensive, and therefore, impractical. Some of these processes (e.g. adsorption and ion exchange) are also chemical-intensive. FO is potentially a better alternative to all of these processes since FO can operate without any input energy for the separation processes.

The use of FO for VFAs and water extraction from the rumen fluid instead of other membrane or non-membrane based processes can reduce the carbon footprints and operational cost of these processes. Production of VFAs from lignocellulosic biomass followed by their extraction through FO can be a huge success to end our reliance on fossil fuels for the industrial production of various chemicals. The replacement of fossil fuels with lignocellulosic materials will not only help in cutting down the huge carbon emissions which is the main cause of climate change but it will also help in a paradigm shift from the non-renewable resources of fossil fuels to a renewable, sustainable, and the most abundant resource of lignocellulosic biomass [4, 5]. The extracted VFAs from the rumen fluid can facilitate the production of bio-chemicals rather than petro-based chemicals. Moreover, the clean water extracted from the rumen fluid after VFAs extraction by FO can be recycled to prepare the saliva solution which is a prerequisite for the breakdown of lignocellulosic feedstuffs in the rumen reactor. In the ruminant animals, the absorbed VFAs act as energy reservoirs for body functions and growth while the recovered water is recycled for saliva preparation that helps in chewing the lignocellulosic

biomass at the start of the digestion process. Thus, by using a draw solution consisting of concentrated synthetic saliva, the FO process can mimic part of the ruminant digestive system.

In the FO process, water is transported across a semi-permeable membrane by an osmotic gradient between the feed solution and a concentrated salt solution, commonly known as the draw solution. Due to the osmotic pressure-driven mass transfer in FO, it does not require any external energy input apart from a small amount of energy for circulating the feed and draw solutions. The absence of an external hydraulic pressure makes the FO process more attractive due to low fouling propensity and easy fouling reversibility.

FO is an excellent process for dewatering complex and challenging solutions. Using a highly concentrated phosphate solution as a draw solution, Nguyen et al. [103] demonstrated that they can concentrate the nutrient-dense sludge 6 times within 15 hrs FO operation. The digested sludge, produced in wastewater treatment plants, is rich in nutrients (i.e. phosphorous and nitrogen) and requires dewatering to reduce its volume and stabilize the organic material before final disposal. FO has been successfully employed to concentrate shale gas drilling flowback fluids [23]. FO has also shown promising results to concentrate digested sludge centrate [49].

The performance of an FO process can be evaluated in terms of water flux, reverse solute flux and resistance to solutes diffusion within the membrane support layer. These parameters are intrinsic properties of an FO membrane. In combination with other factors, such as hydrodynamic conditions on the membrane surface, type and concentration of draw and feed solutions, they govern the performance of the FO process. Therefore, standard methods were developed to measure and compare the performance of FO membranes. These methods focus on measuring the three intrinsic properties of an FO

membrane, i.e. the pure water permeability (A), the solute permeability (B), and the structural parameter (S). The A and B values describe the water and solutes transport across the membrane active layer while the S value is a measure of the resistance to solutes diffusion within the membrane support layer. There are two commonly used standard methods for measuring the A, B, and S values including the pressurized method and a non-pressurized method also known as the single-step FO method [208].

This study aims to evaluate the use of FO to concentrate the rumen fluid and assess the impact of two important process parameters, i.e. temperature and draw solution concentration on the FO performance. The effects of feed solution temperature and draw solution concentration on the rumen fluid concentrating process were evaluated in terms of water flux and reverse solute flux. This research task is the third component of a broader effort to simulate the key steps of ruminant's digestive system by developing an engineered rumen reactor for VFAs production from lignocellulosic biomass, followed by the extraction of the produced VFAs from fermented solution by FO, and finally, concentrating the remaining fermented solution by FO to recycle its water content for preparing the saliva solution. In this context, a novel draw solution in the form of artificial saliva that can offer a buffering capacity to keep pH stable, and reduce the reverse diffusion of draw solutes to the feed solution was introduced.

4.2 Materials and methods

4.2.1 FO membrane

A TFC-PA membrane from Aquapoten Company Ltd (Beijing, China) was used in this study. Similar to other TFC-PA membranes, this membrane was fabricated via interfacial polymerisation to form a thin polyamide active layer on top of an ultra-microporous supporting layer. The membrane was selected and prioritized over the cellulose triacetate (CTA) membrane due to its higher water flux and lower reverse solute flux [185].

4.2.2 Feed and draw solutions

Rumen fluid was collected from a 12-year-old fistulated cow. The rumen fluid was first filtered by a two-layered cheesecloth to remove the coarse material. The coarse filtration was followed by a fine filtration with the help of a two-layered mesh filter [194]. After filtration, the rumen fluid was stored in the fridge at 4 °C before being used in the experiments.

Artificial saliva was used as a draw solution in this study. Artificial saliva derived from the McDougall's saliva composition has been used to control pH in the rumen simulation system due to its great buffering ability [209]. Artificial saliva can also offer less solutes flowing to the feed solution across the membrane in the form of reverse solute flux (RSF), therefore preserving the solutes composition of the feed solution. The artificial saliva was made by mixing the McDougall's saliva recipe containing Na_2HPO_4, $NaHCO_3$, NaCl, KCl, $MgCl_2$, and $CaCl_2$ in deionized (DI) water.

4.2.3 FO system

Figure 4.1 shows a picture and a schematic diagram of the FO system. The FO system consisted of a membrane module, two circulation pumps, two flow meters, a refrigerated water bath, and a hot water bath. The membrane module was comprised of two symmetric and identical acrylic semi cells for counter-current flows of feed and draw solutions. The cross-flow FO unit offered flow channels of 7.6 cm length, 2.6 cm width, and 0.3 cm depth corresponding to an effective membrane area of 19.76 cm^2. The feed and draw solutions were circulated simultaneously in a closed loop using Cole-Parmer gear pumps (75211-15). The flow rate of both solutions was monitored by two acrylic flow metres (Cole-Parmer, 32461-42). A hot water bath (Thermoline, TWB-12D) and a refrigerated water bath (Thermoline, BL-30) were used to keep the feed and draw solution temperature constant at 30/40 ± 1 °C and 20 ± 1 °C, respectively. A dead-end unit (Sterlitech HP4750)

with a membrane area of 14.6 cm^2 and feed volume of 300 mL was used to determine the A and B values. The dead-end unit is a 316 stainless steel high pressure stirred cell

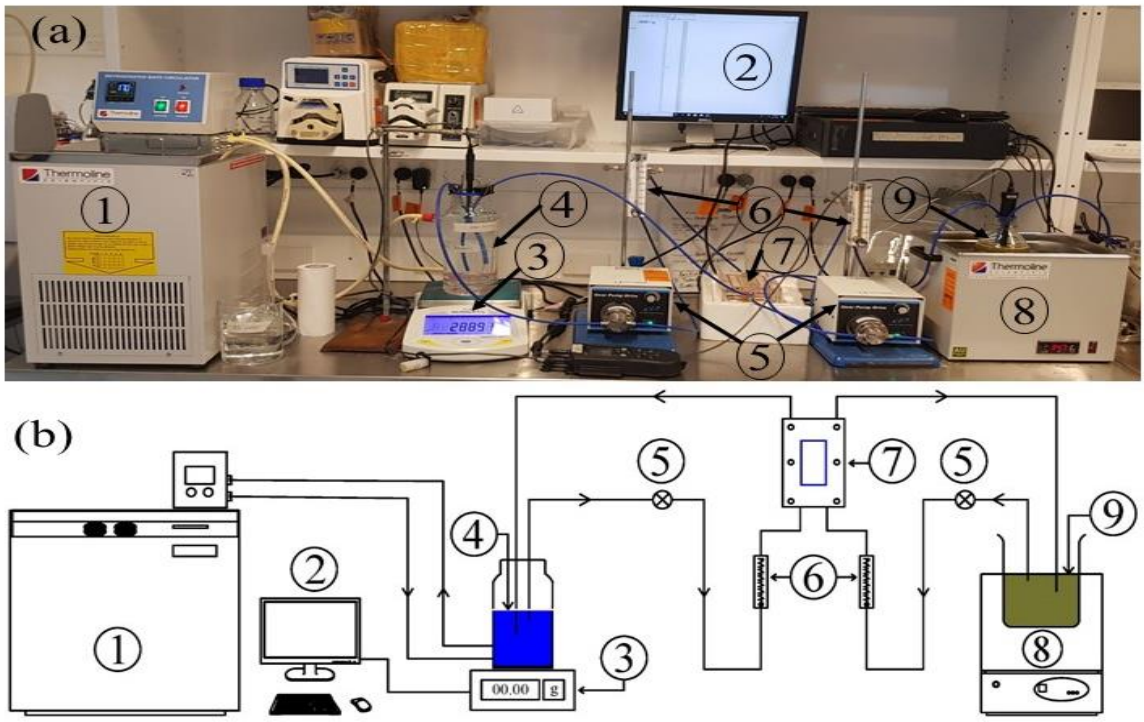

designed for performing a variety of membrane separation operations.

Figure 4.1: Lab-based FO system (a) FO system (b) schematic diagram of the FO system. 1. Refrigerated water bath 2. Computer system 3. Digital balance 4. Draw solution in a double-walled jacketed bottle 5. Gear pumps 6. Flow meters 7. Membrane module 8. Hot water bath 9. Feed solution.

4.3 Experimental methodology

4.3.1 FO membrane characterization

The FO membrane was characterised using a standard method previously reported by Cath et al. [210]. First, the A and B values were determined using a pressurized system in the form of a dead-end filtration cell. Then, the S value was determined using the FO system. All experiments were conducted twice to assess the reproducibility and calculate the standard deviations.

Before the pressurized test, the TFC-PA membrane was compacted for a minimum of 1 hr at 5 bar. The pressure was applied on the active layer side of the membrane. DI water was used as a feed solution. The system was operated at 5 bar using a pressurised nitrogen cylinder. The experiment was performed for two hours. The permeated water was collected in a small beaker and changes in mass were recorded every 10 minutes to measure the water flux. The A value was calculated by dividing the water flux (J_w) with the applied pressure (P) as given in equation 1:

$$A = \frac{J_w}{P} \tag{4-1}$$

The B value was determined by replacing the DI water in the feed with 2 g/L NaCl solution using the same pressurized test. The experiment was performed for 5 hrs. The changes in the mass of permeate were recorded to find the water flux. The conductivity of the feed and permeate were also measured to determine the solute rejection "R" as given below:

$$R = 1 - \frac{C_p}{C_f} \tag{4-2}$$

Where C_p and C_f are the conductivity of permeate and feed, respectively. The value of B was calculated using equation 3.

$$B = J_w \left[\frac{1-R}{R}\right] \exp\left[-\frac{J_w}{k}\right] \tag{4-3}$$

Where k is the solute diffusion coefficient. The S value was determined experimentally using a non-pressurized FO system with NaCl 0.5 M as the draw solution and DI water as a feed solution. The FO system was stabilised for one hour before recording the J_w to determine the S value using the following equation:

$$S = \frac{D}{J_w} \ln\left\{\frac{B + A\pi_{D,b}}{B + J_w + A\pi_{F,m}}\right\} \tag{4-4}$$

In Equation 4, D is the bulk solution diffusivity of the draw solute, $\pi_{D,b}$ is the bulk osmotic pressure of the draw solution, and $\pi_{F,m}$ is the osmotic pressure of the feed solution (0 for DI water).

4.3.2 Rumen fluid dewatering by FO

All FO experiments were performed using the lab-scale system (section 2.3) for at least 8 hrs. The initial volumes of both feed and draw solutions were 1 L during all experiments. The system was operated in the counter-current FO configuration (active layer facing feed solution) with a circulation flow rate of 0.5 L/min (corresponding to a cross-flow velocity of 10.6 cm/s). Changes in pH and conductivity of the feed solution and pH of the draw solution were measured and recorded every hr.

A series of experiments were performed with changing parameters. Initially, the water flux of artificial saliva and rumen fluid were determined separately using DI water as feed at room temperature (24 ± 1 °C). With the water flux of both the solutions resulting in the same range, the concentration of artificial saliva was doubled to find the reference saliva concentration. This concentration of draw solution was used as a benchmark for all the follow-up experiments. The concentration of draw solution was further increased to four times and six times to determine the effect of increasing draw solution concentration on dewatering of the rumen fluid. Next phase of experiments focussed on varying the temperatures of feed solution to assess the impact of changing temperature on the FO performance. First, both feed and draw solutions were operated at room temperature (24 ± 1 °C). Then, the feed solution temperature was increased to 30 ± 1 °C and 40 ± 1 °C with the draw solution temperature kept constant at 20 ± 1 °C.

4.3.3 Analytical Methods

Conductivity and pH were measured by a portable pH and conductivity meter (Hatch - HQ40D).

After the FO experiment, the membrane was taken for scanning electron microscope (SEM) and energy-dispersive X-ray (EDX) spectroscopy analyses. The membrane sample was dried in a desiccator for at least 24 hrs, then coated using a carbon sputter. The SEM (Zeiss, EVO LS15) was used to examine the membrane morphology. The SEM was also equipped with an EDX (Bruker, SDD XFlash 5030) for elementary composition analysis of the deposition on the membrane surface.

One piece of the membrane sample along with a pristine (clean) membrane specimen were also characterized by Fourier transformed infrared (FTIR, Bruker V70) spectrometer to identify organic foulants of the membrane surface. The wavenumber range was 500–4000 cm^{-1}.

4.4 Results and discussion

4.4.1 Transport characteristic of FO membrane

The characterization of the FO membrane provided an insight into the key transport characteristics i.e. the A, B, and S values of the membrane. These values of the TFC-PA membrane used in this study were compared with the values of the other TFC-PA and CTA membranes from the literature (Table 4.1). Luo et al. [196] reported the better performance of the TFC-PA membrane with higher A value and lower B and S values compared to the CTA membrane. The other three studies also demonstrate the superiority of the TFC-PA membrane over the CTA membrane in terms of A, B, and S values [113, 211, 212]. These values of the selected TFC-PA membrane consistently indicate better water transport and lower reverse salt flux compared to the CTA membrane. These values demonstrate the TFC-PA membrane with higher water flux, lower reverse solute flux, and less prone to internal concentration polarization in comparison to the CTA membranes. These results validate the selection of the TFC-PA membrane for dewatering the rumen fluid rather than the CTA membrane, which was previously used for VFAs

extraction. Results in Table 4.1 also show that the properties of the Aquapoten FO membrane are consistent with those of commercially available TFC-PA membranes.

Table 4.1: A, B, and S values of the FO membranes. The error values represent the standard deviation of at least two replicate experiments.

Parameter	**This study**	**Literature (TFC-PA)**	**Literature (CTA)**	**Ref**
Water permeability coefficient - A ($L/m^2.h.bar$)	1.93 ± 0.05	2.50 ± 0.25	0.84 ± 0.03	[196]
		-	0.70 ± 0.07	[113]
		1.78 ± 0.23	-	[212]
		-	0.724	[211]
Solute permeability coefficient - B ($L/m^2.h$)	0.12 ± 0.02	0.19 ± 0.03	0.32 ± 0.06	[196]
		-	0.53 ± 0.03	[113]
		0.34 ± 0.07	-	[212]
		-	0.651	[211]
Membrane structural parameter - S (μm)	440 ± 30	245 ± 35	575 ± 28	[196]
		-	296 ± 26	[113]
		710 ± 140	-	[212]
		-	397.9	[211]

4.4.2 Reference artificial saliva solution

The water flux from feed to draw solution is driven by the osmotic pressure difference between the two solutions. In turn, the osmotic pressure is governed by the concentration of electrolytes or mobile ions in the solution. The artificial saliva and rumen fluid are both complex solutions involving many solutes in their composition. The McDougall artificial saliva in this study is composed of inorganic salts (Section 2.2), which are all strong electrolytes. In addition to inorganic salts intrinsic to ruminant saliva (similar to those in the artificial saliva but at lower concentrations), the rumen fluid also contains a complex mixture of biomolecules, such as VFAs, phospholipids, amino acids, carbohydrates, cholesterol esters, and casein hydrolysate [213]. These organic molecules are weak

electrolytes, thus, they are not expected to contribute to the osmotic pressure of the rumen fluid.

The reference artificial saliva solution was determined by comparing its osmotic pressure to its counterpart, i.e. the rumen fluid. The reference artificial saliva and the rumen fluid were both used as draw solutions to extract water from DI water feed using the FO process. The water flux of both draw solutions was measured separately. The results were used to determine the composition of the reference artificial saliva solution as summarised in Table 4.2. The water fluxes of artificial saliva and rumen fluid show almost identical trends over 8 hrs of FO operation. The average water flux of artificial saliva was 4.36 L/m2.hr (LMH) which was similar to the average water flux of rumen fluid (4.67 LMH) (Figure 4.2).

Table 4.2: Composition of the artificial saliva solution.

Chemicals	Na_2HPO_4	$NaHCO_3$	NaCl	KCl	$MgCl_2$	$CaCl_2$
Concentration (g/L)	3.69	9.8	0.47	0.57	0.06	0.04

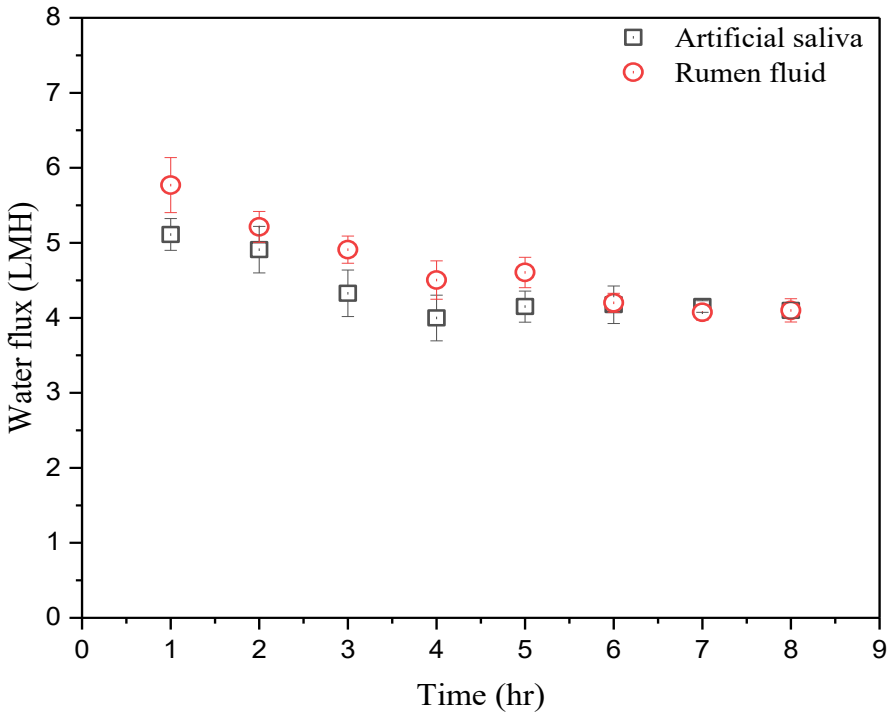

Figure 4.2: Water flux of artificial saliva and rumen fluid as draw solutions with DI water as feed at room temperature of 24 ± 1 °C. The error bars represent the standard deviation of two replicate experiments.

4.4.3 Artificial saliva draw solution

To remove water from the rumen fluid, a more concentrated artificial saliva solution is required compared to the reference solution determined above. Water flux was obtained from artificial saliva solutions as the draw solution at the referencing and twice the referencing concentration (Figure 4.3a). For comparison purposes, DI water was used as the feed solution. The results indicate that the water flux increased when the artificial saliva concentration increased. This observed increase in water flux is attributed to the increase in the draw solution osmotic pressure. It is, however, notable that the increase in water flux (approximately 75%) was less than the increase in the artificial saliva concentration (double or 100% increase). This observation can be attributed to both the internal and external concentration polarisation phenomena that are inherent to the FO

process. As reported in Table 4.1, the FO membrane used in this study has a moderate S value. Thus, considerable internal concentration polarisation was expected.

An increase in the artificial saliva draw solution concentration also increased the RSF (Figure 4.3b). It also shows that the loss of inorganic salts from artificial saliva is insignificant (approximately 1% per m^2 of membrane over one hour). Strictly speaking, this is not a loss as these inorganic salts are simply transferred into the rumen fluid. By doubling the draw solution concentration, the RSF showed a little increase to 16.1 mg/m2.hr (mgMH). Similar to water flux, the increase in RSF (from an average of about 10 to 16 mgMH or 60% increase) was also less than the increase in the artificial saliva concentration (100% increase). As a whole, the results in Figure 4.3 show a trade-off between water flux and RSF. A lower water flux increase is offset by a lower RSF increase when the artificial saliva solution concentration is increased to remove water from the rumen fluid.

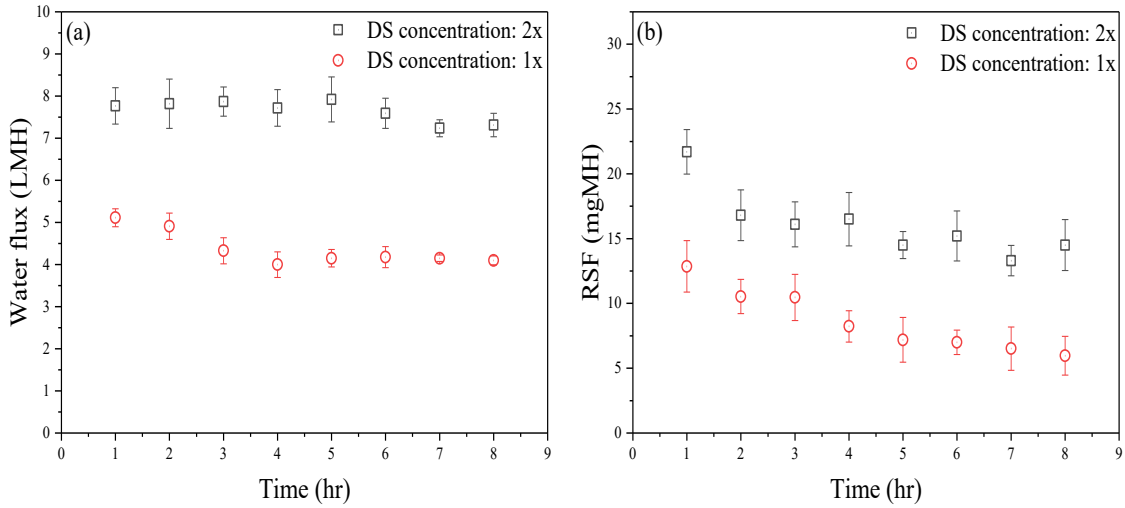

Figure 4.3: Effect of draw solution concentration on (a) water flux and (b) RSF with DI water as a feed solution at room temperature of 24 ± 1 °C. The error bars represent the standard deviation of two replicate experiments (Note: DS stands for draw solution).

Figure 4.4 shows the removal of water from rumen fluid and changes in the RSF values when using different artificial saliva strengths as the draw solution. The artificial saliva was 2, 4, and 6 times more concentrated than the reference value obtained from section 3.2. As expected, an increase in both the water flux and RSF can be observed as the artificial saliva draw solution concentration increases. Increasing the draw solution concentration from 2x to 4x increased the water flux by 68% from 3.56 LMH to 5.99 LMH. Further increase in concentration from 4x to 6x increased the water flux only by 16% equivalent to 6.93 LMH. A trade-off between water flux and RSF increase can also be observed when using real rumen fluid as the feed solution. Dewatering of VFAs solutions using FO has been reported in the literature. Bona et al. [60] have reported a maximum water flux of 4.4 LMH during dewatering of synthetic aqueous solution of VFAs using NaCl 1M as a draw solution. A maximum water flux of 11 LMH was recorded in another study that employed highly concentrated NaCl 5M solution as a draw solution and a fermented broth of different concentrations as a feed solution [61]. Dewatering of activated sludge was performed with a water flux of 8 LMH using a TFC-PA membrane and $MgCl_2$ 2.2M solution as a draw solution [138].

Of particular note is the significant increase in RSF when the feed solution is rumen fluid rather than DI water. Comparing Figure 4.4a and Figure 4.3a, at the same artificial saliva draw solution concentration of 2x, water flux decreases by half but the RSF increase by almost 10 times. The observed decrease in water flux when rumen fluid is used as the feed solution (as opposed to DI water) can be explained by the inherent osmotic potential of the rumen fluid itself. On the other hand, the significant increase in RSF is likely attributed to the external concentration polarization phenomenon, which may be further enhanced by membrane fouling. In fact, there is a gradual but more prominent water flux decline with time when the feed solution was rumen fluid (Figure 4.4a) rather than DI

water (Figure 4.3a). The high RSF observed in Figure 4.4b can significantly reduce the economic potential of FO to remove water from rumen fluid. Future research is necessary to control membrane fouling, hence, reducing the RSF to the value reported in the previous section.

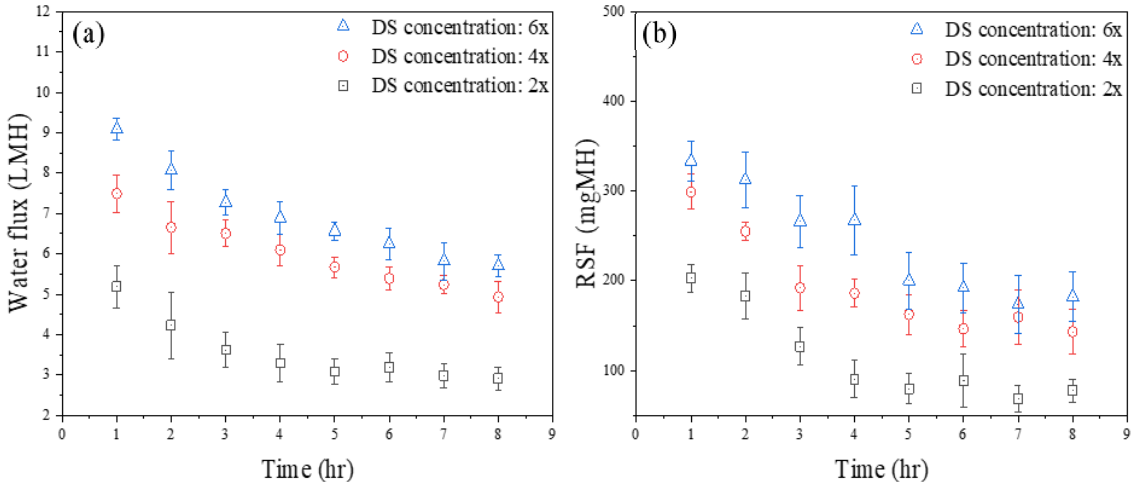

Figure 4.4: Effect of draw solution concentration on (a) water flux and (b) RSF with rumen fluid as feed at room temperature of 24 ± 1 °C. The error bars represent the standard deviation of data obtained from two replicate experiments.

Changes in feed and draw solutions pH were recorded to assess the buffering capacity of the concentrated saliva solution (Figure 4.5). Two different feed solutions were assessed for their impact on the buffering ability of the draw solution. With DI water as feed and concentrated (2x) saliva solution as a draw solution, the pH of the feed solution increased from 6.48 to 7.96 over 8 hrs of FO operation while the draw solution pH showed a slight increase from 8.82 to 9.04 (Figure 4.5a). The significant increase in pH of the feed solution was mainly due to the RSF from the draw solution into the feed solution. However, the draw solution dilution with the water permeation from the feed did not cause any significant changes in the draw solution pH. This observation confirms the pH buffering capacity of the concentrated saliva solution. When DI water was replaced with

rumen fluid in the feed, the increase in feed solution pH was only 0.59 (from 7.22 to 7.81) which was much less than 1.48 (from 6.48 to 7.96) for the DI water (Figure 4.5b). This shows the pH stability of the rumen fluid due to the presence of various phosphates, sulphates, and chlorides salts despite the RSF from the draw solution. The (2x) concentrated saliva solution on the draw side showed a great buffering capacity as its pH increase of 8.68 to 8.97 was not significant. The further increase in the saliva concentration by 4x and 6x with rumen fluid in the feed resulted in the enhanced buffering capability of the draw solution as the draw solution pH only increased by 0.11 (from 8.57 to 8.66) and 0.13 (from 8.56 to 8.69) with 4x and 6x concentration increase of the saliva solution, respectively (Figure 4.5c and Figure 4.5d). These findings demonstrate that the saliva solution offers good pH buffering capacity and acts as a shock absorber to resist any significant pH variations.

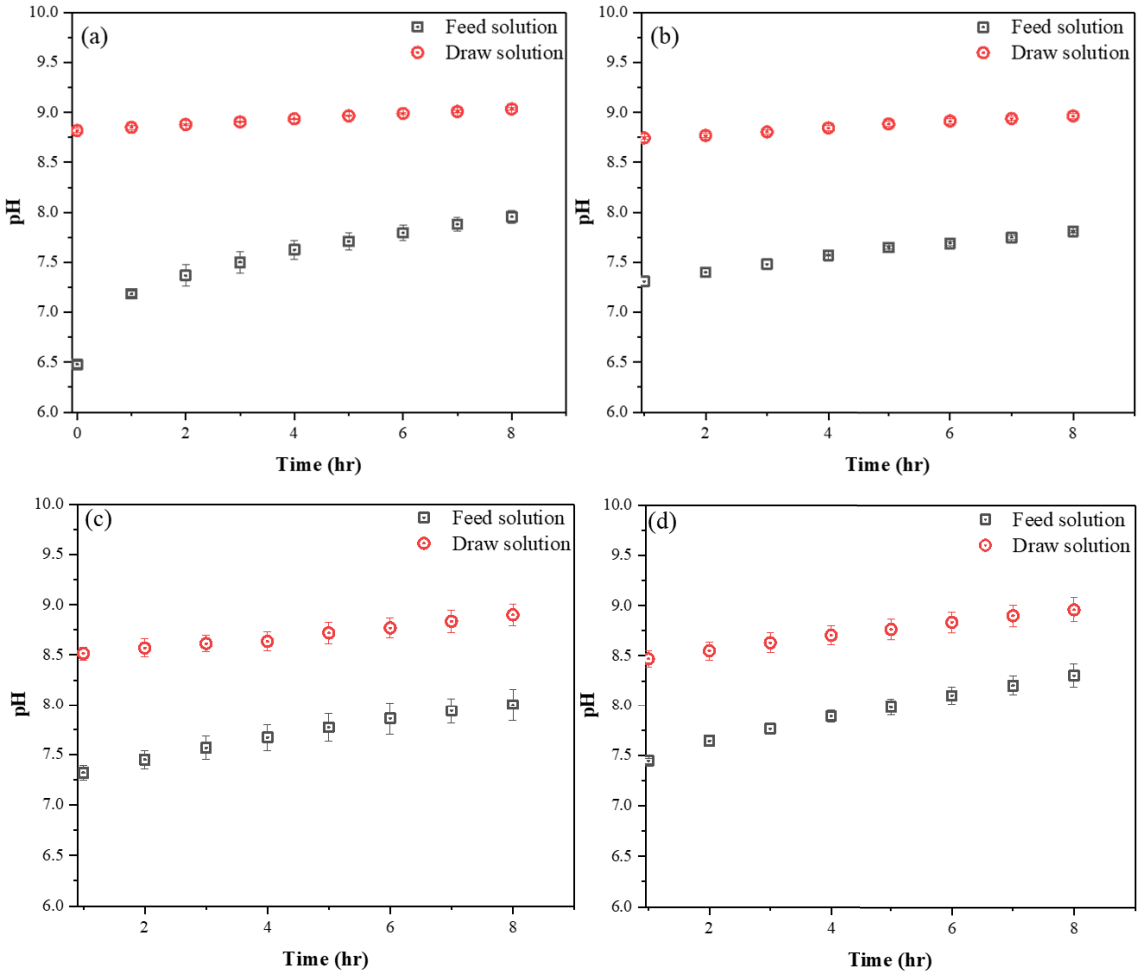

Figure 4.5: Changes in feed solution and draw solution pH as a function of time when (a) DI water was used as a feed with (2x) concentrated saliva solution was as a draw solution (b) rumen fluid was used as a feed with (2x) concentrated saliva solution was as a draw solution (c) rumen fluid was used as a feed with (4x) concentrated saliva solution was as a draw solution (d) rumen fluid was used as a feed with (6x) concentrated saliva solution was as a draw solution. The error bars represent the standard deviation of two replicate experiments.

4.4.4 Effects of temperature and membrane fouling

In ruminant animals, the rumen fluid is maintained at approximately 39 °C to achieve optimum fermentation condition. It is, therefore, necessary to examine the FO process for removing water from the rumen fluid at a similar temperature.

The influence of increasing feed solution temperature on the water flux and the RSF was investigated using a hot water bath and refrigerated water bath for heating and cooling the feed and draw solution, respectively. Rumen fluid was used as a feed solution while artificial saliva (2x concentration) was used as a draw solution. The temperature of the draw solution was kept constant at 20 ± 1 °C while the feed solution temperature was set at 30 ± 1 °C and 40 ± 1 °C. In both cases, increasing the temperature of the feed solution reduced the water flux and the RSF (Figure 4.6). The impacts of reduced water flux and the RSF were also evident from the changes in the pH of the feed and draw solution (Figure 4.7). The pH of feed and draw solution in both cases remained almost the same throughout these experiments.

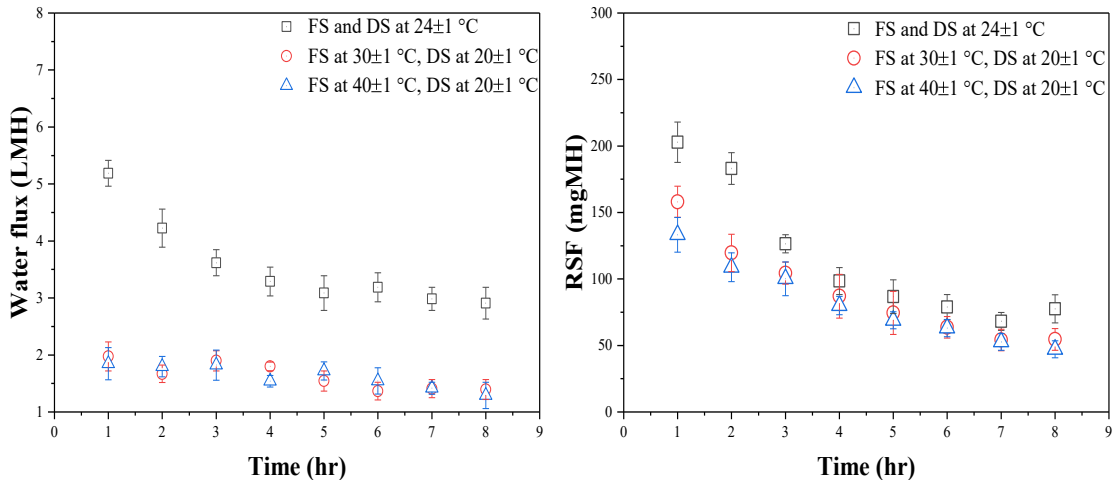

Figure 4.6: Effect of temperature on (a) water flux and (b) RSF with rumen fluid as feed facing the membrane active layer (Note: FS stands for feed solution).

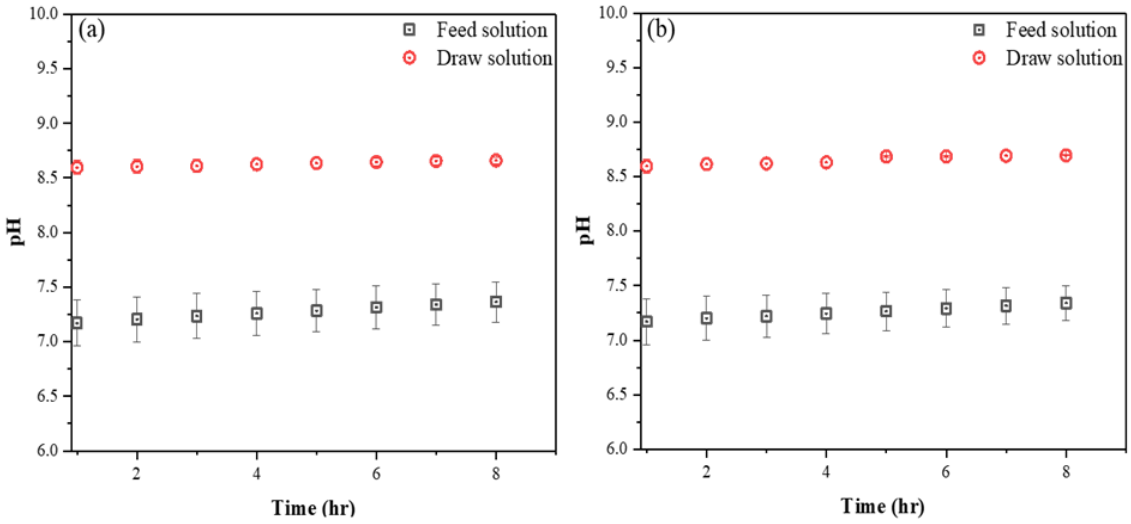

Figure 4.7: Changes in feed solution and draw solution pH as a function of time when (a) feed solution temperature was 30 °C (b) feed solution temperature was 40 °C with (2x) concentrated saliva solution at 20 °C as a draw solution. The error bars represent the standard deviation of two replicate experiments.

There are several possible explanations for this low water flux at high feed solution temperature. It can be attributed to membrane fouling caused by conformational changes of biomolecules in rumen fluid in response to a high temperature. Biomolecules in rumen fluid such as phospholipids, amino acids, carbohydrates, cholesterol esters, and casein are known to be thermally responsive. Increasing the rumen fluid temperature from room temperature to 30 °C and 40 °C may have induced the precipitation of these biomolecules on the membrane surface and within the membrane supporting layer. This was evidenced by a visible change in the colour of the membrane surface from white at the beginning to greenish at the end of the experiment. Another possible reason for the reduced water flux is the increased osmotic pressure of the feed solution at high temperature and therefore the reduced osmotic pressure gradient across the membrane.

When rumen fluid was heated to 30 °C and 40 °C, the water flux and RSF declined with the membrane surface turning from whitish to greenish (Figure 4.8a and Figure 4.8b).

SEM imaging analysis shows a porous fouling layer made of small and uniform particles on the membrane surface (Figure 4.8c). These particles are likely to be folded biomolecules from the rumen fluid. The EDX spectra show two dominant phosphorus and sulphur peaks, suggesting the origin of these particles as biomolecules (Figure 4.8d). The EDX and elemental mapping analyses also show a significant amount of phosphorous and sulphur distributed more uniformly in the fouling layer besides the presence of oxygen, carbon, calcium and some other metals within the fouling layer (Figure 4.8e and Table 4.3).

Table 4.3: EDX elemental composition of the fouling layer

Element	**O**	**C**	**Ca**	**S**	**P**	**Na**	**Mg**	**K**
% atomic composition	55.04	24.06	7.50	5.22	4.89	2.05	1.20	0.04

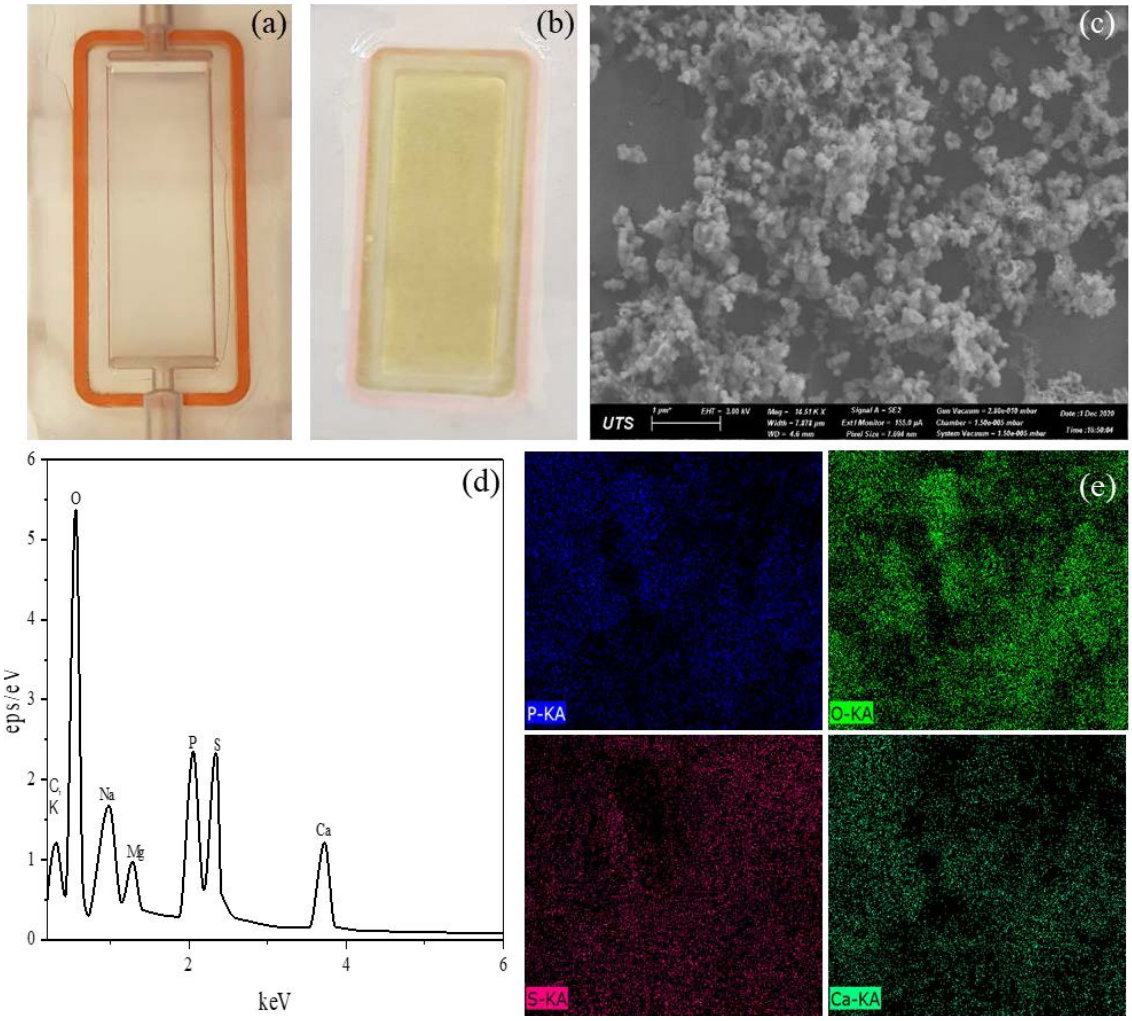

Figure 4.8: Membrane fouling when the feed solution temperature was 30 °C and draw solution temperature was 20 °C (a) camera image (b) SEM image (c) EDX analysis (d) EDX mapping of the membrane fouling layer. Note: Each colour in the elemental mapping image stands for the distribution of a specific element on the fouling layer with blue dots showing phosphorous, bright green dots showing oxygen, dark red dots showing sulphur, and the dark green dots showing the calcium ions.

The organic composition of the membrane fouling layer was confirmed by comparing the FTIR spectra of a pristine membrane and fouled membrane (Figure 4.9). The gap between the two curves shows the level of fouling by different organic compounds. The percentage transmittance in the region of 2800 - 3000 cm^{-1} represents C-H and =C-H based organic

compounds. A peak at 1720 cm^{-1} shows the presence of the carbonyl group (C=O) in the fouling layer. The two peaks at 1637 cm^{-1} and 1540 cm^{-1} confirm the presence of amine groups from proteins while a peak at 1028 cm^{-1} represents the C-O group organic molecules. Additional characteristic peaks include Ca-O and Mg-O bonds (600-700 cm^{-1}), amide III bonds (1245 cm^{-1}), and O-H bonds (3600 cm^{-1}).

Results from SEM-EDX and FTIR analysis reaffirm the possibility of fouling caused by the precipitation of bio-molecules on the membrane surface. FO experiments in this study were conducted ex-situ. In other words, rumen fluid was obtained from a fistulated cow, preserved at low temperature, and then heated up to simulate temperature in the digestive system of ruminant animals. It is recommended that excessive temperature variation is avoided in future experiments.

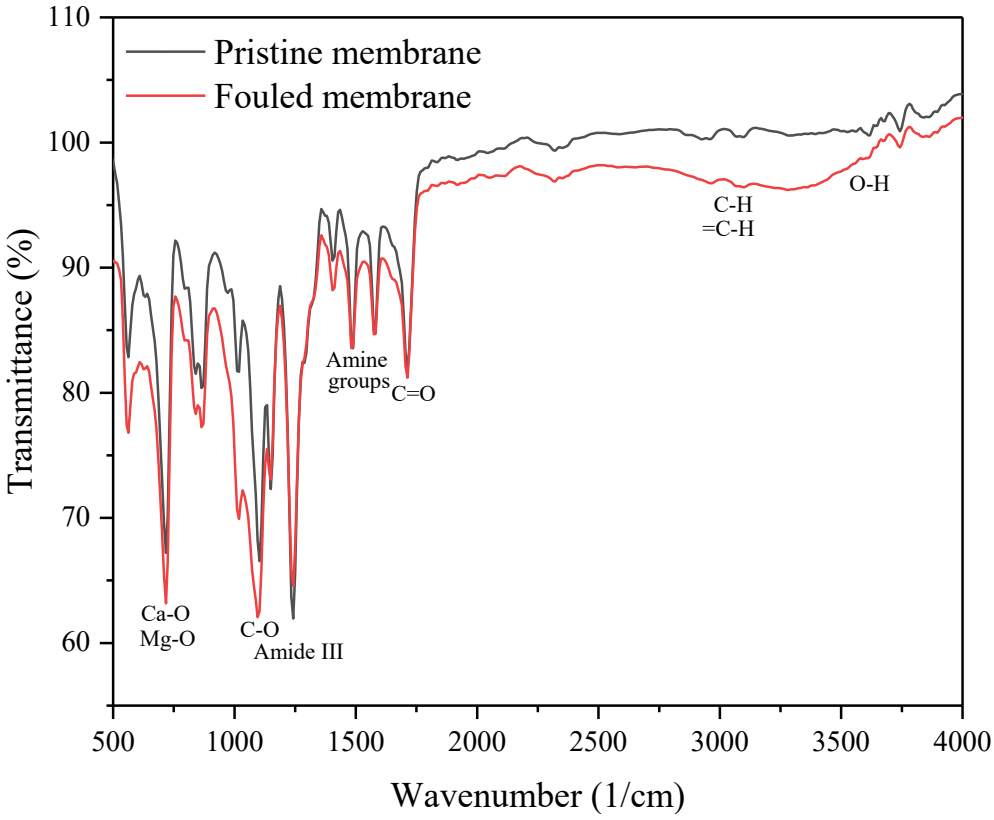

Figure 4.9: FTIR spectra of the membrane fouling layer when the feed solution temperature was 30 °C and draw solution temperature was 20 °C.

4.5 Conclusion

This study validates the potential application of the FO process to remove water from the rumen fluid using artificial saliva as the draw solution. The reference artificial saliva solution was determined by comparing its osmotic pressure to that of the rumen fluid. The concentrated saliva showed good pH buffering capacity with no significant pH changes during FO operation. Excellent water flux and low RSF were demonstrated using a slightly more concentrated saliva solution (double the concentration of the reference) as the draw solution and DI water as the feed. A trade-off between water flux and RSF was also observed. The rumen fluid is however significantly more complex. Thus, the water flux was lower and the RSF was higher when experimenting with rumen fluid. Results from this study highlight membrane fouling as a major challenge to the practical deployment of FO for rumen fluid dewatering. Membrane fouling was evidenced by visual, SEM-EDX, and FTIR examination of the membrane surface. Excessive variation in temperature is likely to aggravate membrane fouling.

Chapter 5 Characterization of Biofouling and Evaluation of Membrane Cleaning Techniques in Forward Osmosis

This thesis chapter has been proposed for a possible publication as the following journal article.

Khan JA, Nguyen AQ, Vu MT, Shon HK, Nghiem LD. Biofouling characterization and evaluation of membrane cleaning techniques in a forward osmosis process to dewater rumen fluid. Journal of Membrane Science (to be submitted).

5.1 Introduction

Fouling is inevitable in all membrane filtration processes. Membrane fouling occurs when the dissolved and/or suspended components from the feed solution are deposited on the membrane surface [185]. The different constituents of feed solution such as organic molecules, inorganic salts, microorganisms, and extracellular polymeric substances (EPS) can accumulate on the membrane surface and cause membrane fouling. These constituents are known as foulants.

Membrane fouling causes an increase in the resistance to water permeation and reverse salt flux (RSF) in the case of forward osmosis (FO) [128]. Membrane fouling can also accelerate the degradation of the membrane, thus, shortening the membrane operational life and increasing the overall operational cost of the membrane process [129]. In general, membrane fouling can be categorized into organic fouling, inorganic fouling or scaling, colloidal fouling or cake formation and biofouling. Different organic and inorganic components along with the microorganisms can interact under a complex mechanism to cause membrane fouling simultaneously [157].

Comparison between an osmotically-driven membrane process like FO and a pressure-driven membrane process such as reverse osmosis (RO) in terms of fouling reversibility

and membrane cleaning efficiency has been extensively discussed in the literature [134]. The fouling tendency in FO is significantly lower than the RO due to the difference in nature and intensity of the pressure difference across the membrane [134]. In RO, water flux is caused by a strong hydraulic pressure generated due to input energy. It results in the formation of a compact fouling layer which is not easy to remove by hydraulic means. On the other hand, FO is driven by osmotic pressure generated naturally due to the concentration gradient across the membrane resulting in a loosely held fouling layer that can be removed by hydraulic means. Lee et al. [135] demonstrated that membrane fouling is almost reversible in FO and is irreversible in the case of RO.

The nature of membrane fouling depends on the composition of the feed solution. For example, membrane biofouling will be more prevalent during the dewatering process of the rumen fluid. Rumen fluid is produced by the biodegradation of lignocellulosic material in an anaerobic environment. The rumen fluid is a complex fluid containing many microbial taxa, VFAs, phospholipids, amino acids, dicarboxylic acids, glycerides, carbohydrates, cholesterol esters, and inorganic ions [184]. Processing rumen fluid for VFAs and water extraction by FO can result in membrane biofouling as rumen fluid microbes can form a biofilm on the membrane surface by thriving on the biodegradable material available in abundance in the rumen fluid. The microbial composition of rumen fluid has been explored in a recent study with the dominant taxa involving *Ruminococcaceae* and *Prevotella* (cellulitic taxa), *Lachnospiraceae* and *Succiniclasticum* (acetogens), *Olsenella* and unassigned *Clostridiales* (fermenters), and *Methanobrevibacter* and *Methanosphaera* (methanogens) [51]. With the known microbial composition of the rumen fluid, it can be expected that the biofilm formed during dewatering of rumen fluid by FO will have some of the rumen fluid microbes

besides the appearance of new microbial taxa due to the FO operation in aerobic conditions.

Biofouling is defined as the accumulation of microorganisms along with their extracellular substances on the membrane surface. Biofouling is the “Achilles heel” of the membrane process due to the ability of the microorganisms to grow and multiply on the membrane surface even after 99.9% of them are removed [157]. It is difficult to remove biofouling due to strong microbial adhesion onto the membrane surface and the formation of a sticky EPS matrix [149]. Biofouling accounts for more than 45% of all membrane fouling and is reported as a major hurdle in pressurized membrane processes like NF and RO [157]. In FO systems, biofouling occurs due to microbial attachment to the membrane surface without hydraulic pressure. Praveen et al. [214] proposed a mechanism of biofouling in FO as the natural diffusion of microbes along with the flow of water from the bulk solution to the membrane surface. Kim et al. [215] suggested the higher tendency of microbes to adhere and grow on the membrane surface is due to the ECP with a higher concentration of nutrients and microbes on the membrane surface than the bulk solution. Moreover, the chemotaxis of motile microbes in search of nutrients tend to move them close to the membrane surface and aggravate the biofouling. Although the work on biofouling in pressure-driven membrane processes has been broadly explored in the literature, the area of actual biofouling in FO has not been sufficiently investigated yet.

Several molecular and microscopic techniques have been employed to characterize the microbial community of a biological system. These techniques include 16S rRNA gene sequencing, fluorescence in situ hybridization (FISH), polymerase chain reaction-denaturing gradient gel electrophoresis (PCR-DGGE), and clone library. The 16S rRNA gene sequencing is an advanced technique to identify, classify and quantify the microbes

in a complex biological system based on variation in the microbial 16S rRNA gene. This technique has been used for rumen fluid microbial community profiling and to track down changes in the microbial community during rumen MBR continuous operation [51]. The FISH is a molecular cytogenetic technique to visualize and map the genetic material using fluorescent probes. Miura et al. [216] found significant differences in the microbial communities between the mixed liquor planktonic biomass and the membrane biofilm layer by using the FISH technique. They found *Betaproteobacteria* through FISH and 16S rRNA gene sequencing as a key microbial taxon responsible for developing the membrane biofilm. Culture-independent techniques such as PCR-DGGE and clone libraries can only identify the most abundant microbial communities and are therefore mostly used to improve the microbial communities characterization in various environments. Liu et al. [45] used the PCR technique to identify *Thauera, Trichococcus*, and *Rhodocyclaceae* in the biofilm of the FO membrane surface during the integrated process of FO membrane and microbial fuel cells.

Both physical and chemical cleaning techniques have been investigated to mitigate membrane fouling. Common physical techniques for cleaning FO membranes include hydraulic cleaning, osmotic backwashing, high cross-flow velocity (CFV), ultrasonication, and air scouring [140]. The basis of all these techniques is to create strong hydrodynamic conditions or disturbances to dislodge the fouling layer from the membrane surface. Chemical cleaning involves the use of one or several chemicals such as sodium hypochlorite [149], hydrogen peroxide [150], EDTA [149], citric acid [151], and sodium hydroxide [152]. Normally, a combined cleaning strategy is adopted which involves the dissolution of fouling matrix by chemicals followed by the removal of foulants by physical cleaning [127]. The selection of physical or chemical cleaning techniques depends on the type of fouling and the cost of the cleaning techniques. For

example, the use of less costly physical cleaning techniques like osmotic backwashing and hydraulic cleaning would be preferred over other physical techniques or the use of chemicals. In the case of membrane biofouling, physical cleaning alone may not be enough, and therefore, the use of chemicals such as sodium hypochlorite or hydrogen peroxide may also be required.

This study focuses on characterizing the actual biofouling in a long term FO operation and its impact on FO performance during a rumen fluid dewatering process. It evaluates the effect of membrane module configurations on biofouling and FO performance. The study also covers the morphology, chemical and microbial composition of the membrane fouling layer. Moreover, various membrane cleaning techniques such as hydraulic cleaning, osmotic backwashing, chemical cleaning, and a combination of osmotic backwashing and chemical cleaning have also been evaluated in terms of flux recovery.

5.2 Materials and methods

5.2.1 Materials

A flat sheet CTA membrane from Hydration Technology Innovation (Albany, OR) was used in this study. This is an asymmetric membrane prepared by phase inversion. Thus, the rejection and support layers are both made of cellulose triacetate. A thin polyester mesh is embedded in the middle to provide additional support [63].

Rumen fluid was obtained from a twelve years old fistulated cow. It was filtered by a two-layered cheesecloth along with a two-layered mesh filter to remove large solid particles. The pre-filtered fluid was stored in the fridge at 4 °C. A synthetic rumen solution was prepared by mixing analytical grade salts with tap water to obtain a solution with an electrolyte composition similar to that of rumen fluid (Table 5.1). It is to resupply organic and nutrients to the system to simulate a realistic condition. The rumen fluid and the

synthetic rumen solution were combined at the volume ratio of 1:9 and used as the feed solution.

Table 5.1: Composition of the synthetic rumen solution.

Chemicals	CH_3COOH	Na_2HPO_4	CH_4N_2O	KCl	$(NH_4)_3PO_4$	$CaCl_2$	$MgSO_4$
Conc. (g/L)	2.86	0.82	0.75	0.66	0.25	0.23	0.20

A concentrated form of artificial saliva, derived from McDougall saliva solution, was employed as a draw solution. Artificial saliva has been recently employed in rumen simulation studies owing to its great buffering ability [51, 209]. The composition of draw solution includes (g/L) $NaHCO_3$ 19.60, Na_2HPO_4 7.37, KCl 1.14, NaCl 0.94, $MgCl_2$ 0.12, and $CaCl_2$ 0.08 dissolved in DI water.

Chemical cleaning of the CTA membrane was performed using 0.1% NaOCl solution. The solution was prepared by mixing analytical grade NaOCl solution (10% strength) with DI water. The pH of the NaOCl cleaning solution was adjusted to 7.0 ± 0.1 by adding a small volume of analytical grade HCl solution.

5.2.2 FO experimental system

A lab-scale FO system was employed in this study (Figure 5.1). A membrane cell consisted of two identical and symmetrical semi-cells having a flow channel with length, width, and depth of 7.6, 2.6, and 0.3 cm, respectively. A flat sheet membrane was sandwiched between the two acrylic semi-cells offering an effective membrane area of 19.76 cm^2. The feed and draw solutions were circulated simultaneously in the FO system with the help of two gear pumps (Cole-Parmer, 75211-15). The flow rate of feed and draw solutions were measured by two acrylic flow meters (Cole-Parmer, 32461-42). The feed solution was placed on the digital balance (Adam Equipment, PGL 8001) and the weight changes were recorded by a computer system after every 10 minutes. A pH/conductivity

meter (Hatch - HQ40D) was used to record the hourly changes in feed solution conductivity.

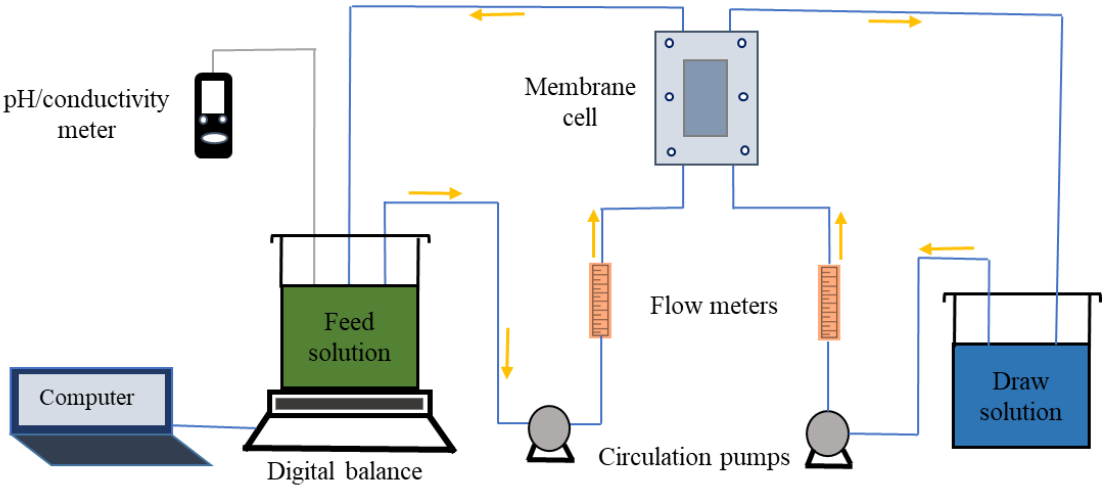

Figure 5.1: Schematic diagram of the FO system.

5.2.3 Experimental methodology

All biofouling experiments were conducted with a lab-scale FO system at room temperature (24 ± 1 °C). The duration of each experiment was 6 days. The initial volumes of feed and draw solutions were 1 L. The circulation flow rate for all the experiments was 500 mL/min with a corresponding CFV of 10.6 cm/min. The system was operated in FO mode with a co-current configuration. Each experiment was comprised of 3 cycles with each cycle lasting for 48 hours. The feed solution was replenished while the draw solution was replaced with a fresh solution two times after the first and second cycle in each experiment. Hourly water flux readings were obtained from the change in mass of feed solution which was recorded automatically by a computer system. Water flux, J_w, was calculated as:

$$J_w = \frac{M_{t-} M_i}{A \times t \times \rho_{water}} \quad (5\text{-}1)$$

Where M_t is the mass of draw solution at time t and M_i is the initial mass of draw solution. A is the effective membrane area, t is the time duration, and ρ_{water} is the water density.

The conductivity of the feed solution was measured regularly to calculate the RSF. The RSF, J_s, was calculated using mass balance equation as:

$$J_s = \frac{C_t \times V_{feed,t} - C_i \times V_{feed,i}}{A \times t} \quad (5\text{-}2)$$

Where C_i is the initial draw solute concentrations in the feed solution and C_t is the draw solute concentration in the feed solution at time t. $V_{feed,i}$ represents the initial feed solution volume and $V_{feed,t}$ shows the feed solution volume at time t.

Biofouling experiments were performed using three membrane module configurations to determine the impact of module orientation on fouling and FO performance (Figure 5.2). In membrane module configuration 1, the feed solution was in the upper semi cell of the membrane module. In membrane module configuration 2, the feed solution flowing in the lower semi cell of the membrane module. In membrane module configurations 1 and 2, the membrane module was horizontal to the surface. In membrane module configuration 3, the membrane module was vertical to the surface, thus, the feed solution and the draw solutions were flowing horizontally parallel to each other.

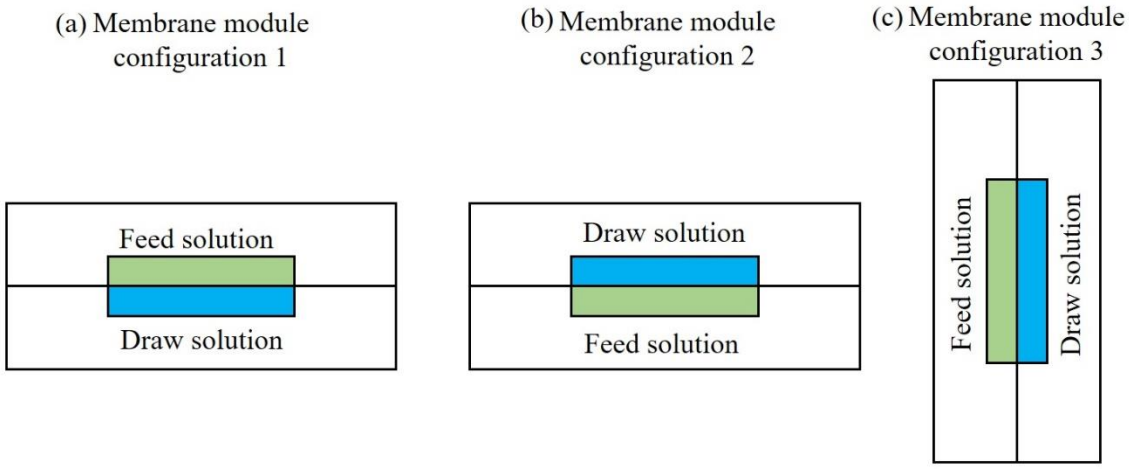

Figure 5.2: Membrane module configurations (a) membrane module configuration 1 - membrane module horizontal with feed solution on top (b) membrane module configuration 2 - membrane module horizontal with feed solution at the bottom (c) membrane module configuration 3 - membrane module vertical.

Membrane cleaning protocol involved hydraulic cleaning, osmotic backwashing, chemical cleaning, and different combinations of these techniques. Each membrane cleaning experiment consisted of the following five steps:

Step 1 - Baseline experiment: To measure the clean water flux and the RSF using DI water as a feed and NaCl 0.5M solution as a draw solution over 1 h of FO experiment with CFV of 10.6 cm/s.

Step 2 - Fouling experiment: To conduct 48 hrs FO experiment with the same experimental protocol as discussed earlier for the biofouling experiment. The membrane active layer was facing upward.

Step 3 - To repeat Step 1 for measuring the change in water flux and the RSF after membrane fouling.

Step 4 - Membrane cleaning experiment for 1 hr.

Step 5 - To repeat Step 1 for measuring the change in water flux and the RSF after membrane cleaning.

Five membrane cleaning strategies were applied to evaluate the effectiveness of each strategy. First, the membrane cleaning was carried out by the hydraulic cleaning method, in which the membrane was flushed with DI water on both feed and draw sides at an increased CFV of 31.8 cm/s (3 times higher than the value used during normal operation). In the second experiment, osmotic backwashing was performed by circulating NaCl 1M solution on the feed side and DI water on the draw side at CFV of 10.6 cm/s to reverse the flow of water through the membrane. The third experiment was conducted with chemical cleaning in which 0.1% NaOCl solution was circulated on both feed and draw sides at a CFV of 10.6 cm/s. The fourth experiment was characterized by a combination of chemical cleaning and osmotic backwashing. The membrane was cleaned by

circulating NaCl 1 M solution on the feed side and 0.1% NaOCl solution on the draw side at a CFV of 10.6 cm/s.

5.2.4 Analytical methods

This study covers the biofouling that occurred on the membrane active layer side only. Therefore, all the analysis results demonstrate the biofilm on the membrane active layer. The membrane coupons were collected at the end of each biofouling experiment. After collecting biofilm samples from multiple locations on the membrane surface, the membrane was dried in a desiccator and coated with the help of a carbon sputter before further analysis. The membrane was analysed by SEM (Zeiss EVO LS15) and EDX (Bruker SDD XFlash 5030) to determine the morphology and elemental composition of the biofilm. FTIR spectra of the pristine and fouled membranes were obtained using an FTIR spectrometer (Bruker V70) under the wavelength range of 500 - 4000 cm^{-1}.

5.2.5 DNA extraction and sequencing

For microbial community profiling, duplicate samples of the inoculum were collected before and after filtration by a two-layered cheesecloth along with a two-layered mesh filter. Three samples of the feed solution were also collected before the experiment. Inoculum and feed solution samples were mixed with 100% v/v ethanol (1:1 v/v). Duplicate samples of the biofilm were collected from the membrane surface at multiple positions at the end of each experiment using cotton swabs (Figure 5.3). These swabs were then submerged in 100% v/v ethanol (1:1 v/v). All samples were stored at -20 ºC before DNA extraction.

Genomic DNA extraction from the above-mentioned samples was carried out using QIAamp DNA Stool Mini Kit (Qiagen) following the manual's instructions. An additional bead-beating step was performed at the beginning of the extraction to enhance DNA yield. The integrity, purity and concentration of the extracted DNA were evaluated

by NanoDrop® spectrophotometer. DNA concentration of all samples was normalized to 10 ng/µl using ultrapure water before sending to the sequencing facility.

The universal primer set 341F (5'-CCTAYGGGRBGCASCAG-3') and 806R (5'-GGACTACNNGGGTATCTAAT-3') was used to amplify 16S rRNA V3 – V4 regions of both bacterial and archaeal communities. Paired-end amplicon sequencing (2 × 300 bp) was carried out on the Illumina MiSeq platform (UTS Next Generation Sequencing Facility, Sydney, Australia).

Raw reads were analysed according to the Quantitative Insights into Microbial Ecology (QIIME) 2 (version 2019.10) pipeline [217]. In brief, reads were denoised using DADA2 with the following parameters: trunc-len-f = 280, trucn-len-r = 280, trim-left-f = 17, trim left-r = 21, min-fold-parent-over-abundance = 8 and all other parameters as the default setting. Taxonomy assignment was performed against the SILVA database (release 132) [218] with a confidence of 0.7. Rarefaction curves of observed amplicon sequence variants at a maximum depth of 70,000 showed that all samples approached a saturation plateau at about 68,500 (Supplementary Information), and this sampling depth was chosen for alpha diversity analysis.

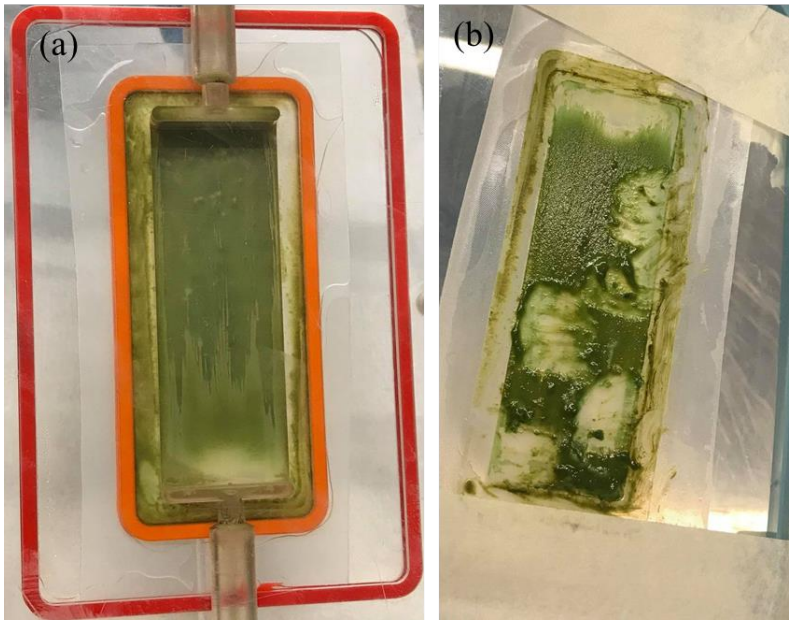

Figure 5.3: Fouled membrane under membrane module configuration 1 with feed solution on top (a) before samples collection (b) after samples collection.

5.3 Results and discussion

5.3.1 Membrane fouling impact on FO performance

The impact of membrane fouling on FO performance was evaluated in terms of water flux and the RSF. The FO was operated in three cycles, each cycle lasted 48 hours (Figure 5.4). High initial water flux and the RSF were recorded in the first cycle in comparison to all subsequent cycles. The initial high flux was due to the clean membrane and no fouling at the start of the experiment. A sharp decline in the water flux and the RSF was observed with time due to membrane fouling and a decrease in concentration gradient across the membrane. After 48 hours, the feed solution was replenished to the initial volume of 1 L while the draw solution was replaced with 1 L of fresh draw solution. The initial water flux and the RSF in the second cycle were much lower than the initial water flux and the RSF in the first cycle due to membrane fouling. Nevertheless, they were significantly higher than the water flux and the RSF values at the end of the first cycle due to the restoration of the concentration gradient between the replenished feed solution

and the undiluted draw solution. A similar trend was observed in the third cycle where initial water flux and the RSF were lower than the initial water flux and the initial RSF in the second cycle but higher than the final water flux and the RSF of the second cycle.

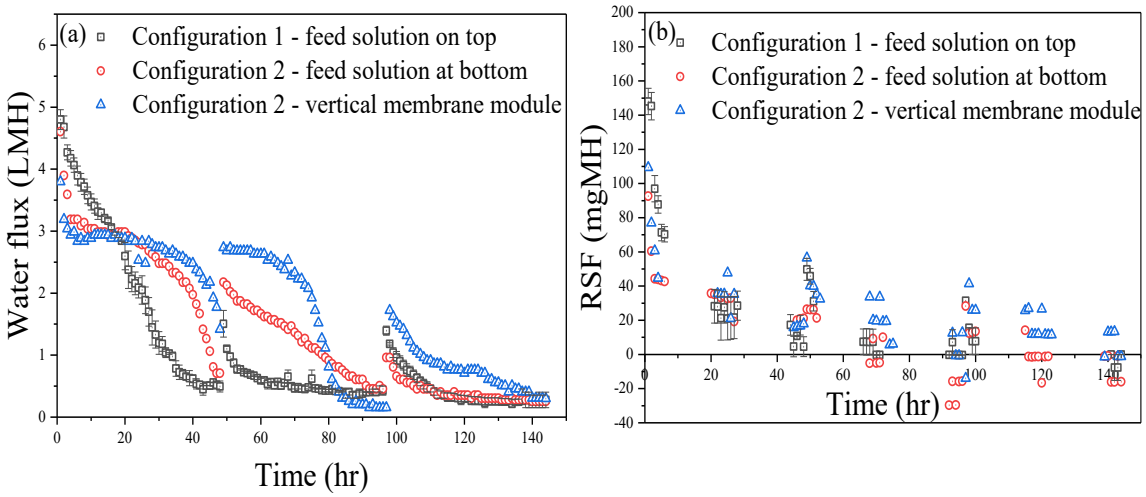

Figure 5.4: Changes in the (a) water flux and the (b) RSF over 6 days (3 cycles) FO operation. The error bars represent the standard deviation of two replicate experiments.

The configuration of the membrane module played a major role in the development of the membrane fouling layer and its impact on FO performance. The worst fouling was observed with the formation of a thick greenish fouling layer on the membrane surface under membrane module configuration 1 (Figure 5.5a). The increased fouling was likely due to a higher tendency of foulants sedimentation under gravity and deposition on the membrane surface. The worst fouling led to the lowest average water flux of 1.04 LMH under membrane module configuration 1 in comparison to the other two membrane module configurations (Figure 5.4a). The water flux in the first, second, and third cycles was 2.13 LMH, 0.55 LMH, and 0.43 LMH, respectively. The sharp decline in water flux after a transition from the first to the second cycle was due to the increased amount of gravity-driven foulants accumulation on the membrane surface.

Less fouling with partial covering of the membrane surface was observed under membrane module configuration 2 than the membrane module configuration 1 (Figure

5.5b). It was due to the absence of gravity-driven deposition of foulants from the feed solution on the membrane surface. However, some fouling material adhered to the membrane surface due to the natural tendency of foulants to approach the membrane surface along with the water content during the dewatering process of rumen fluid. The average water flux under membrane module configuration 2 was 1.42 LMH which was lower than the highest average water flux (1.69 LMH) under membrane module configuration 3 but higher than the lowest average water flux (1.04 LMH) under membrane module configuration 1. The lower value of average water flux under membrane module configuration 2 in comparison to the membrane module configuration 3 could be due to the settling down of salts from the draw solution under gravity to cause fouling on the support layer side of the membrane. The water flux was 2.57 LMH, 1.22 LMH, and 0.46 LMH in the first, second, and third cycle, respectively (Figure 5.4a).

Membrane module configuration 3 (the membrane module was placed vertically to the surface with the feed and draw solutions circulating horizontally parallel to each other) was characterized by minimum fouling. The vertical positioning of the membrane module ruled out the possibility of any gravity-driven accumulation of fouling material on both sides of the membrane surface resulting in minimum covered fouling layer area of the membrane surface (Figure 5.5c). The minimum fouling also resulted in the highest average water flux of 1.69 LMH with 2.69 LMH in the first cycle, 1.60 LMH in the second cycle, and 0.78 LMH in the third cycle (Figure 5.4a).

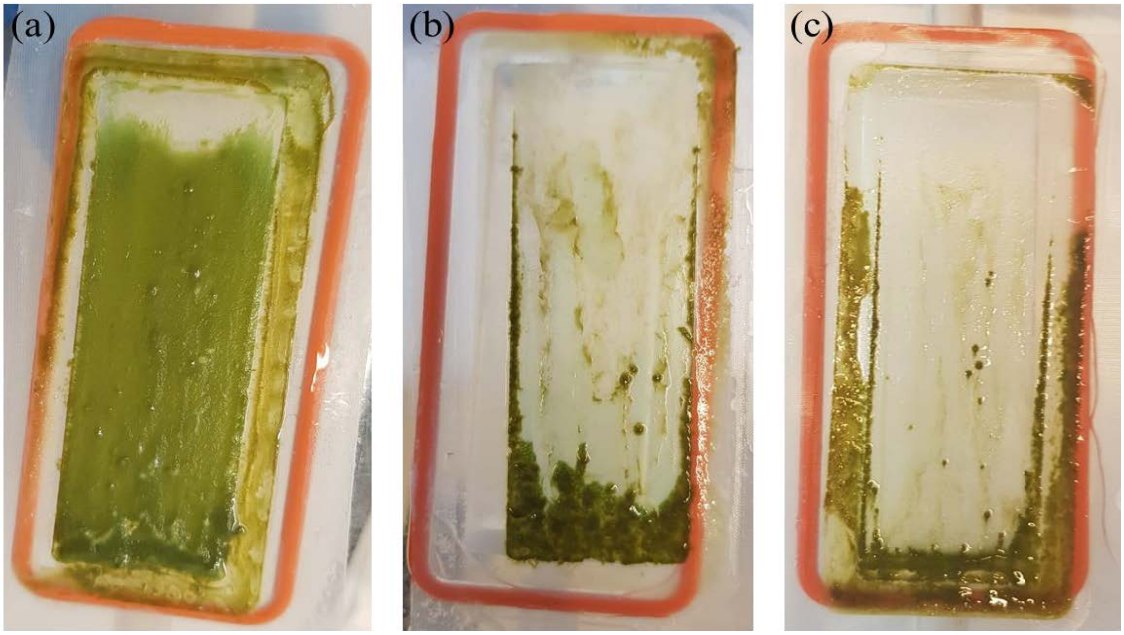

Figure 5.5: Membrane fouling on the active layer side at the end of experiment using (a) feed solution on top in membrane module (b) feed solution at the bottom in membrane module (c) membrane module vertical.

5.3.2 Microbial community composition and diversity

5.3.2.1 Overview of DNA sequencing data

Paired-end Illumina sequencing generated 748,624 sequences from 13 samples. At least 52.2% of input sequences of each sample passed quality filtering, 70.5% of filtered sequences were merged, and 98.4% of merged sequences were non-chimeric. The minimum number of sequences per denoised samples were 18,718, and the maximum number was 38,662. In total, 374,649 denoised sequences were clustered to a total of 2,526 features with a mean frequency per feature of 148.3. Rarefaction curves of observed features at a maximum sequencing depth of 18,700 showed that all samples approached a saturation plateau at a sequencing depth of about 12,000, confirming the sufficient sequencing depth in this study (Figure 5.6).

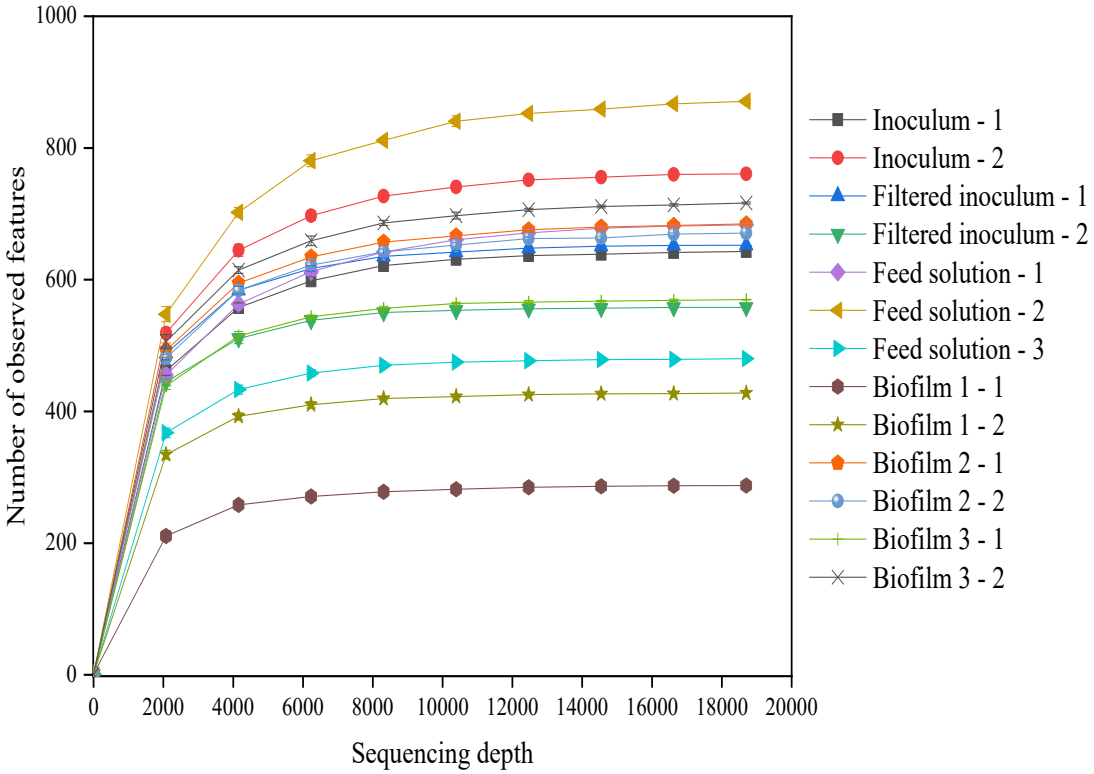

Figure 5.6: Rarefaction curves of 16S rRNA marker gene amplicon sequences at a maximum depth of 18,700 where inoculum-1 and inoculum-2 represent the duplicate samples of the non-filtered rumen fluid; filtered inoculum-1 and filtered inoculum-2 represent the duplicate samples of the filtered rumen fluid; feed solution-1, feed solution-2, and feed solution-3 represent the three feed solution samples taken under the membrane module configurations 1, 2, and 3, respectively; biofilm 1-1 and biofilm 1-2 represent the duplicate biofilm samples under the membrane module configuration 1 with feed solution on top in the membrane module; biofilm 2-1 and biofilm 2-2 represent the duplicate biofilm samples under the membrane module configuration 2 with feed solution at the bottom in the membrane module; biofilm 3-1 and biofilm 3-2 represent the duplicate biofilm samples under the membrane module configuration 3 with vertical membrane module.

5.3.2.2 Membrane module configuration impact on microbial diversity

Microbial diversity including species richness (number of observed species) and species evenness (Shannon index) was similar in the inoculum, filtered inoculum, and feed solution (Figure 5.7). This indicates that the filtration and dilution of rumen fluid did not impact diversity level, and the feed solution was representative of rumen fluid in terms of diversity. Biofilm 1, 2, and 3 corresponds to the membrane module configurations 1, 2, and 3, respectively. It is clear that membrane module configuration 1 significantly reduced biofilm microbial diversity compared to membrane module configurations 2 and 3. The lower diversity of biofilm 1 could be attributed to its maturity compared to biofilm 2 and 3 after 24 hrs. The first step of biofouling development is the attachment of microbes with adhesive capacity (pioneer species) on the membrane surface. In membrane module configuration 1, when the active layer of the membrane was facing upward and the feed solution was flowing in the upper semi cell of the membrane module, gravity made it relatively easy for microorganisms and particles to deposit on the membrane surface. When the biofilm becomes more mature with increased thickness, the number of species can reduce due to the selection for species that thrive in the micro-environment of the biofilm inner side (biofouling succession). Membrane module configurations 2 and 3 led to lower contact chance and time between microorganisms and the membrane surface, thus biofouling was still in the initial development stage, resulting in thin biofilms with a similar diversity level to the rumen fluid inoculum and feed solution.

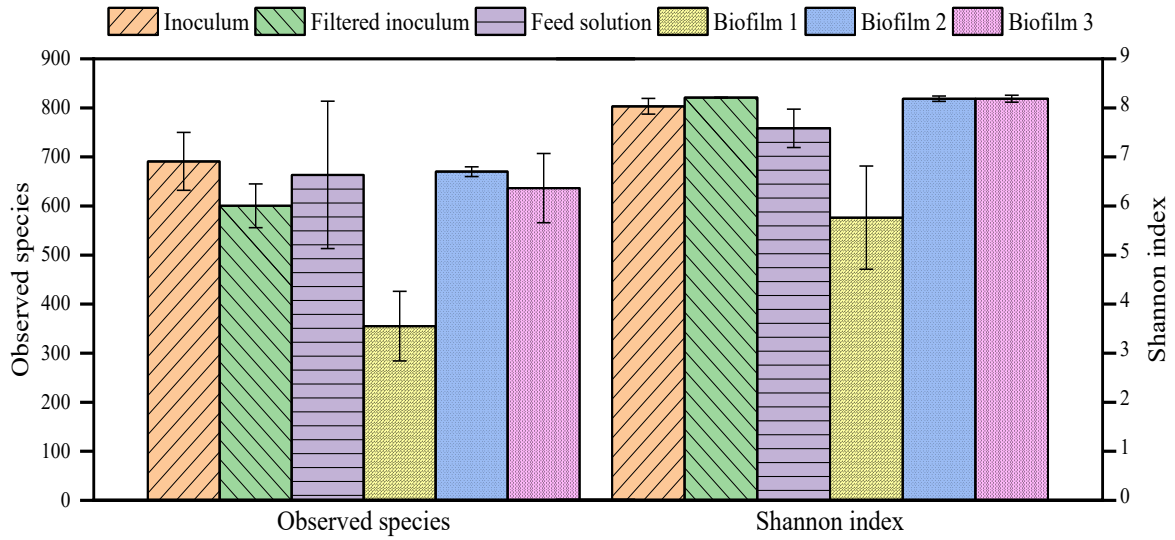

Figure 5.7: Microbial diversity in terms of species richness and Shannon index in the inoculum, filtered inoculum, feed solution and biofilms where biofilm 1 represents the biofilm sample when the feed solution was on top in membrane module, biofilm 2 represents the biofilm sample when the feed solution was at the bottom in membrane module, and biofilm 3 represents the biofilm sample when membrane module was placed vertically on the surface.

5.3.2.3 Membrane module configuration impact on microbial structure

The shift in microbial community structure during the biofouling experiment was revealed in principal coordinates analysis (PcoA) (Figure 5.8). The distance between samples on the plot indicates how similar their microbial communities are to each other. Bray-Curtis dissimilarity metric takes into account both the microbial absence/presence and their relative abundances in the community. PcoA analysis showed that the inoculum and the feed solution are highly diverged from each other, indicating that the feed solution could harbour new taxa that were not presented in the inoculum, or old taxa with relative abundance changed significantly. Membrane module configuration also exerted a strong impact on microbial community structure, with biofilm 1 demonstrated a highly different

structure to biofilm 2 and 3. These results are similar to the microbial diversity result (Section 5.3.2.2), and further confirm that membrane module configuration 1 led to a more mature biofilm where taxa that can thrive in the biofilm anoxic inner side were enriched.

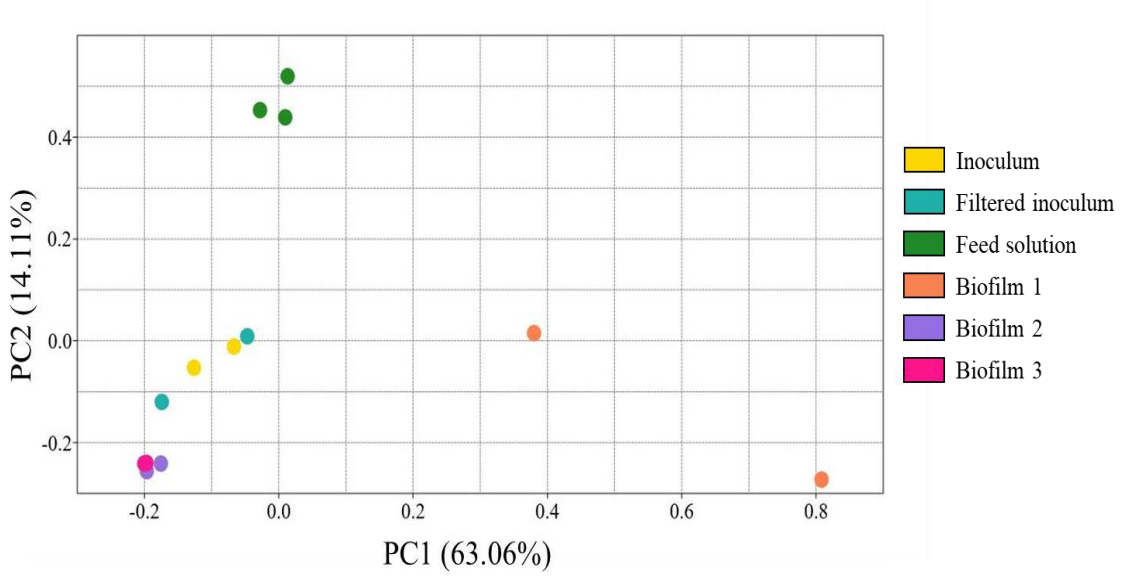

Figure 5.8: Principal coordinates analysis showing the difference in microbial community structure using the Bray–Curtis dissimilarities metric.

5.3.2.4 Membrane module configuration impact on microbial composition

The most dominant taxa in the inoculum (both original and filtered one) were representative of the rumen microbiome with distinct functional groups (Figure 5.9) [51, 219]. Cellulolytic bacteria included *Prevotellaceae*, *Butyrivibrio* (family *Lachnospiraceae*) which attack hemicellulose and pectin [220, 221], and *Ruminococcaceae* which degrades both cellulose and hemicellulose [222]. Abundant fermenters and acetogens were *Veillonellaceae* [223], *Lachnospiraceae* [224], *Succiniclasticum* (family *Acidaminococcaceae*) [225], *Treponema (family Spirochaetaceae*) [226], *Synergistaceae*, *Bacteroidales* UCG-001 and *Muribaculaceae* [227], while *Methanobacteriaceae* was the predominant methanogenic family [228].

Some other taxa presented in inoculum samples (*Rikenellaceae*, *Christensenellaceae*, F082, *Moraxellaceae*) have also been detected in previous studies, though their functions have not been elucidated [51, 219]. The high similarity in microbial composition between the original and the filtered inoculum is also in agreement with PcoA results (Section 2.3).

The microbial composition of the feed solution differed from the inoculum, as several aerobic/facultatively anaerobic taxa emerged due to the exposure of the inoculum to oxygen in the atmosphere. The most enriched taxa were *Pseudomonadaceae*, with relative abundance increased from 0.1 – 0.2% in inoculum to 7.7 – 15.5% in the feed solution. Other taxa that emerged in the feed solution were not detected in the inoculum, including *Shewanellaceae* (facultatively anaerobic), *Aeromonadaceae* (aerobic, facultatively anaerobic), *Nocardiaceae* (aerobic), *Xanthomonadaceae* (facultatively anaerobic), and *Arcobacteraceae* (aerotolerant – cannot utilize oxygen but tolerate its presence).

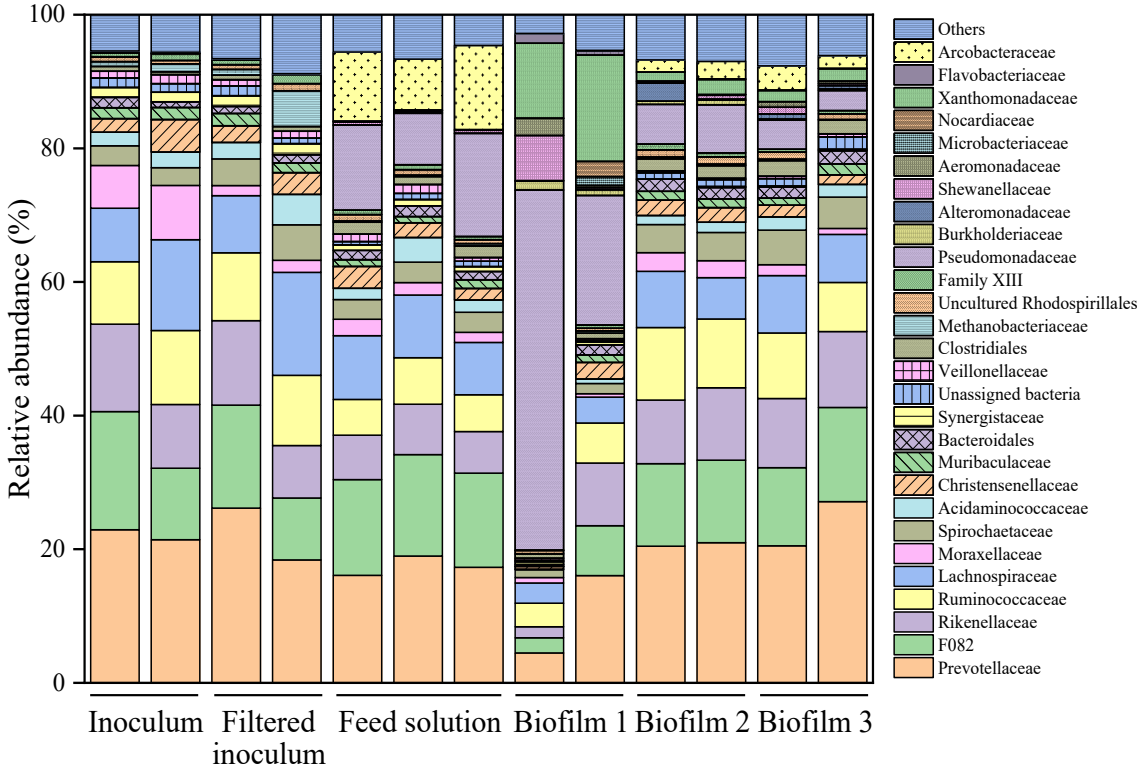

Figure 5.9: Microbial composition of inoculum, filtered inoculum, feed solution and biofilms under different membrane module configurations.

Biofilms harboured highly similar microbial taxa to feed solution, however, their relative abundances were different. It is worth noting that aerobic/facultatively anaerobic taxa which emerged in the feed solution thrived in biofilms. One such taxon was *Xanthomonadaceae*, with abundance increased from 0.03% in feed solution to 1.3 – 15.9% in biofilm samples. *Xanthomonads* are known to possess superior attachment capabilities using type IV pili [229]. Another taxon was *Pseudomonadaceae*, with *Pseudomonas* as the only genus detected in all samples. *Pseudomonas aeruginosa* is widely renowned for its biofilm-forming capacity and is frequently used as a model microorganism to simulate biofouling [230-232]. Vanysacker et al. 2013 reported that the adhesive capacity of *P. aeruginosa* is approximately 100 times more than *E. coli* on polyvinyl difluoride, polyethylene, and polysulfone membranes [233]. *P. aeruginosa* also

possesses polar monotrichous that can propel the bacterium at relatively high speeds towards the membrane (high motility) [233].

Membrane module configuration also impacted the biofilm microbial composition significantly, which is in line with PcoA results (Section 2.3). The most dominant taxa in biofilm 1 were *Pseudomonadaceae* (36.6 ± 17.2%), followed by *Xanthomonadaceae* (13.6 ± 2.4%). Biofilm 1 also fostered a few taxa whose abundance were negligible in other biofilms, including *Shewanellaceae* and *Aeromonadaceae*. *Shewanella* species (*Shewanellaceae* member) can thrive in oxic-anoxic interfaces thanks to their ability to rapidly detect and respond to oxygen fluctuations [234, 235]. The formation and three-dimensional structure of a community (pellicles/aggregates/biofilm) formed by this species are regulated by oxygen concentration [236, 237]. Meanwhile, *Aeromonas* (*Aeromonadaceae* member) possesses several structures and a mechanism and are actively involved in the first step of biofilm formation, such as constitutive polar flagellum (which allows swimming motility), chemotaxis, lipopolysaccharides, and other surface polysaccharides (α-glucan) [238]. Indeed, *Aeromonas* has been reported to colonize multiple biotic and abiotic surfaces, including polyvinyl chloride [239, 240]. In a study on RO membrane biofouling control by nitric oxide treatment, family *Aeromonadaceae* was found to be better integrated into the biofilm than other species [241].

5.3.3 Fouling behaviour of the FO membrane

The membrane fouling layer was characterized by using SEM-EDX and FTIR spectroscopy. The SEM image of the fouling layer showed a dense fouling layer with an irregular pattern of fouling material covering the membrane surface under membrane module configuration 1 (Figure 5.10a). This finding was augmented by the EDX analysis and mapping which demonstrated evenly and densely distributed phosphorous atoms on

the membrane surface beside the presence of other elements like oxygen, sodium, potassium, calcium, and chlorine (Figure 5.10b and Figure 5.11a). The overwhelming presence of elements like oxygen, carbon, phosphorous, and nitrogen having atomic percentage values of 45.19, 23.65, 8.89, and 7.09, respectively hints at the presence of biomolecules in the membrane fouling layer (Table 5.2).

Table 5.2: EDX elemental composition of the fouling layer

Elemental composition (at.%)	**O**	**C**	**P**	**N**	**Na**	**K**	**Ca**	**Cl**
Membrane active layer facing upward	45.19	23.65	8.89	7.06	9.28	0.61	3.27	1.61
Membrane active layer facing downward	59.19	7.57	9.92	-	16.98	0.80	5.35	0.19
Membrane active layer facing sideway	55.01	17.67	9.70	-	12.82	0.67	4.01	0.11

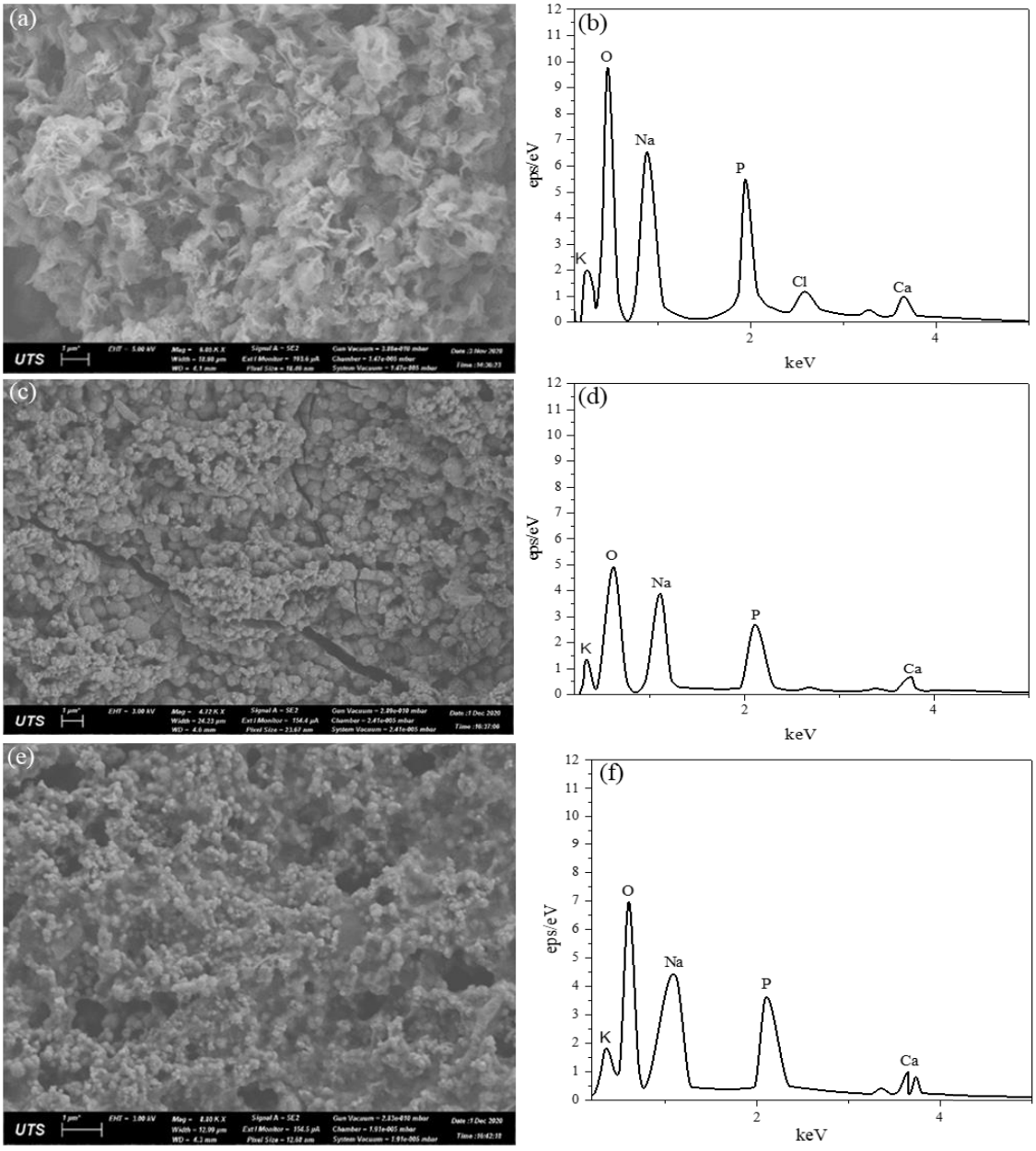

Figure 5.10: SEM and EDX mapping measurements of a fouled membrane surface after 6 days FO operation ((a) and (b)) feed solution on top in membrane module ((b) and (c)) feed solution at the bottom in membrane module ((e) and (f)) membrane module vertical.

The fouling layer became less compact and more porous with the granular form of fouling material under the membrane module configurations 2 and 3 (Figure 5.10c and Figure 5.10e) suggesting less fouling in comparison to Figure 5.10a. The EDX analysis suggests the presence of oxygen, phosphorous, potassium, and calcium in relatively smaller

amounts in the composition of the fouling layer (Figure 5.10d and Figure 5.10f). The EDX mapping confirms the SEM findings and EDX elemental analysis with less dense and uneven distribution of phosphorous atoms on the membrane surface (Figure 5.11b and Figure 5.11c).

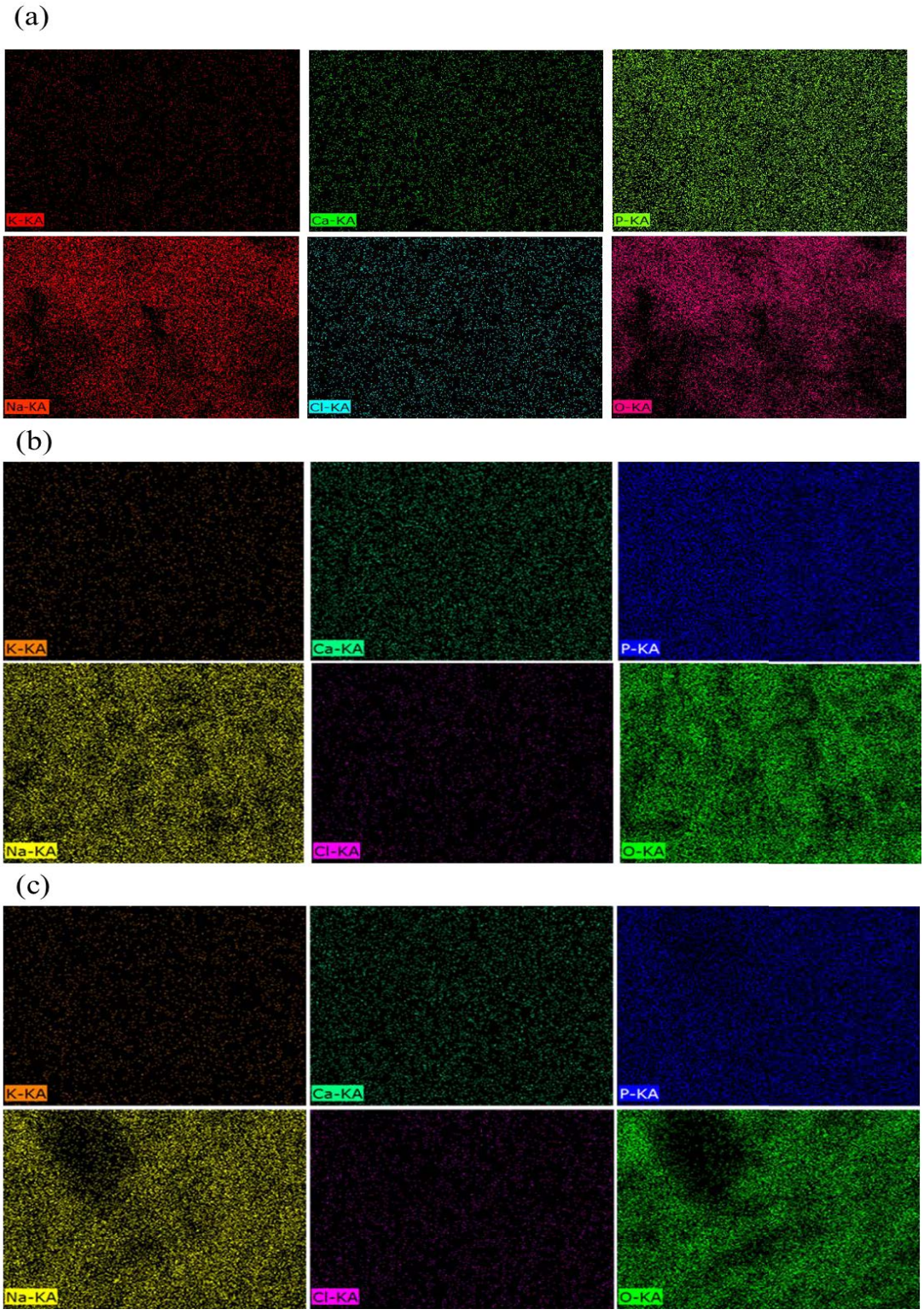

Figure 5.11: EDX mapping of the membrane fouling layer (a) membrane active layer facing upward (b) membrane active layer facing downward (c) membrane active layer facing sideway.

To further investigate the nature of the membrane fouling layer, FTIR analysis was performed on a pristine membrane sample and the three fouled membrane samples. The results demonstrate that the peaks of the fouled membrane were different than the pristine membrane at several positions suggesting the presence of different functional group based molecules (Figure 5.12). The important functional groups in the fouled membrane spectra were aliphatic methylene groups, amide groups, and phosphate groups with their peaks in the bands of 2850-2960 cm^{-1}, 1530-1630 cm^{-1}, and 1086 cm^{-1}, respectively. These functional groups demonstrate the presence of fatty acids, proteins and phospholipids in the membrane fouling layer. Moreover, other prominent peaks in the range of 3000-3400 cm^{-1} symbolize the hydroxyl group (OH^{-1}) presence while peaks around 600-700 cm^{-1} show the presence of Mg-O and Ca-O based molecules.

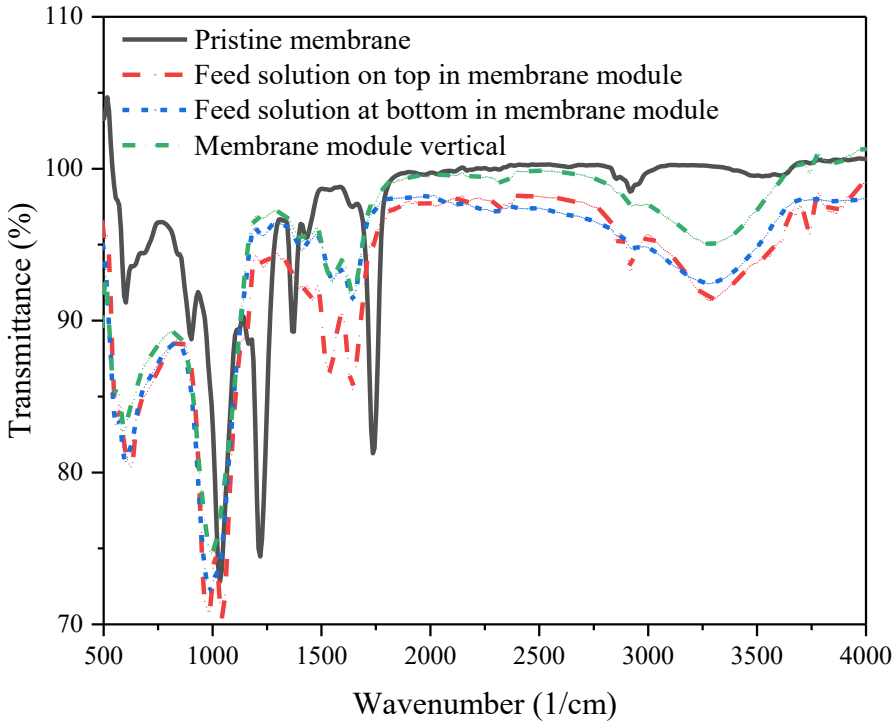

Figure 5.12: FTIR spectra of fouled membrane surfaces after 6 days of FO operation.

5.3.4 Membrane cleaning

The fouling layer formed in an FO process is expected to be loosely held to the membrane surface since FO is based on a naturally occurring osmotic gradient [134]. The low operating pressure can likely reduce the strength of the fouling layer attachment to the membrane surface. However, a long term FO operation involving rumen fluid-based solution as a feed results in the formation of a dense biofouling layer on the membrane surface that involves a variety of microbes and the organic matter sticking to the membrane surface more tightly. The fouling experiment was performed with a feed solution flowing in the upper semi-cell of the membrane module. Both physical and chemical membrane cleaning techniques were applied to evaluate the effectiveness of each cleaning strategy (Figure 5.13).

The physical cleaning techniques involve creating strong hydrodynamic conditions to detach the fouling material from the membrane surface. The average water flux with the pristine membrane was 9.8 LMH. Each membrane cleaning experiment was conducted for one hr at the end of the 48 hrs biofouling simulation experiment. First, the hydraulic cleaning was performed by flushing the fouled membrane with DI water for 1 hr at a high CFV of 31.6 cm after the membrane fouling experiment reduced the flux by 24.6% from 9.8 LMH to 7.2 LMH (Figure 5.13a). The hydraulic cleaning could only recover the flux to 7.6 LMH (14.1% of the lost water flux). This shows that increasing the tangential forces with the increased flow of water are not enough to dislodge the membrane fouling layer. In the case of osmotic backwashing, which involved circulating NaCl 1M solution on the feed side and DI water on the draw side at CFV of 10.6 cm/s, 37.7% of flux recovery was observed at the end of the membrane cleaning experiment (Figure 5.13b). It demonstrates that osmotic backwashing is more effective than hydraulic cleaning to recover the flux as reversing the water flow direction though the membrane is more likely to detach the

fouling material from the membrane surface than simply flushing the fouled membrane with clean water.

The chemical cleaning technique was applied by circulating 0.1% NaOCl solution on both feed and draw sides at a CFV of 10.87 cm/s (Figure 5.13c). The water flux recovery was 55.0% which was significantly higher than what it was for osmotic backwashing. It suggests that the use of an oxidant/disinfectant can be effective in recovering the lost flux as it oxidizes the fouling layer material and facilitates the detachment of the rumen microbes from the membrane surface. After the better performance of osmotic backwashing and chemical cleaning techniques, these two techniques were combined to assess their combined impact on the flux recovery (Figure 5.13d). This strategy employed NaCl 1M solution on the feed side and 0.1% NaOCl solution on the draw side, both circulating at CFV of 10.9 cm/s. A higher flux recovery of 70.0% was observed when the water flux was increased from 5.6 LMH to 8.5 LMH after 1 hr of cleaning operation. These findings suggest that a combination of chemical cleaning and osmotic backwashing can be most effective in recovering the lost flux. While the osmotic backwashing can loosen or detach the fouling material from the membrane surface, the chemical cleaning can specifically target and dislodge the microbes from the membrane surface. This shows that osmotic backwashing augments the effectiveness of chemical cleaning and both should be applied simultaneously to clean the membrane.

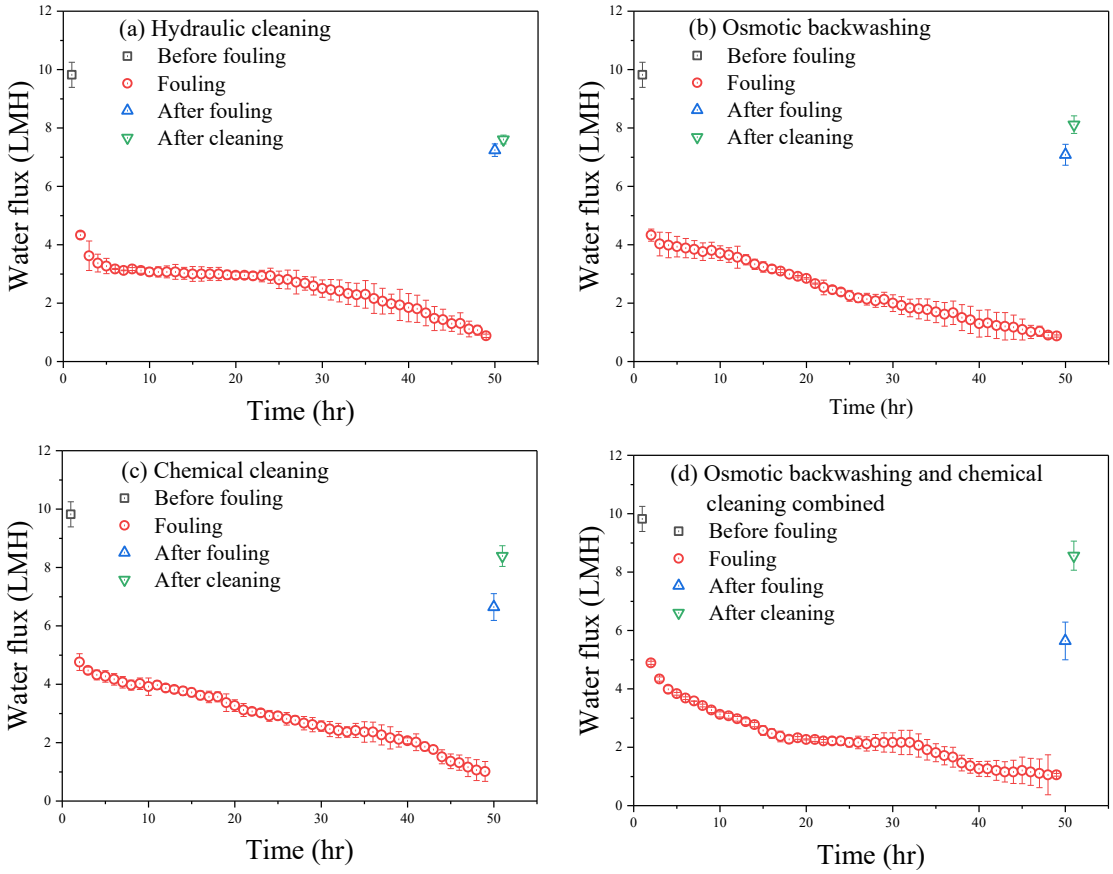

Figure 5.13: Water flux before fouling, during fouling, after fouling, and after cleaning under membrane module configuration 1 with feed solution flowing in the upper semi cell of the membrane module. The error bars represent the standard deviation of two replicate experiments.

The effects of various cleaning techniques were further evaluated by SEM-EDX analysis of the membrane surface. SEM images of a membrane surface before fouling (pristine membrane), after fouling, and after different cleaning techniques are shown in Figure 5.14. It shows that the surface of a pristine membrane (Figure 5.14a) was completely covered with a fouling layer after 48 hours of FO operation (Figure 5.14b). The rumen fluid-based feed solution formed a thick fouling layer on the membrane surface. Some pores were created in the fouling layer after hydraulic cleaning (Figure 5.14c) that helped in recovering 14.1% of water flux. Reversing the flow of water permeation across the membrane using the osmotic backwashing technique weakened the adhesiveness of the

fouling layer to the membrane surface besides developing more pores in the fouling layer (Figure 5.14d). The use of 0.1% NaOCl as a chemical cleaning agent was more effective than physical cleaning techniques that resulted in developing the large cracks in the fouling layer (Figure 5.14e). When chemical cleaning was combined with osmotic backwashing, the holes in the fouling layer became larger that resulted in the maximum flux recovery of 70% (Figure 5.14f).

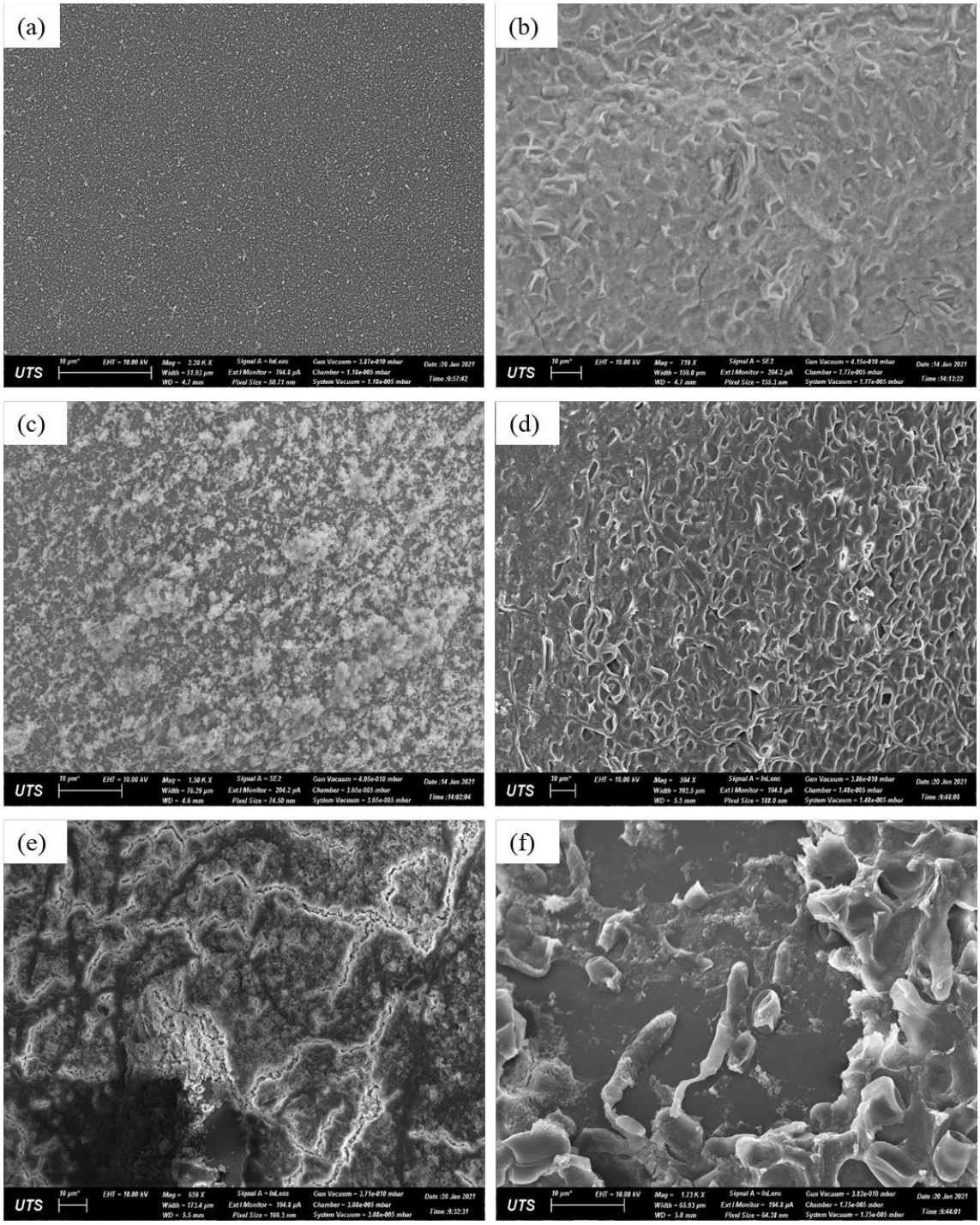

Figure 5.14: SEM images of (a) clean membrane surface (b) after fouling (c) after hydraulic cleaning (d) after osmotic backwashing (e) after chemical cleaning (f) after osmotic backwashing and chemical cleaning combined.

The EDX elemental analysis revealed changes in the elemental composition of the clean and fouled membrane samples (Table 5.3). It can be seen that the pristine CTA membrane

consisted of carbon and oxygen only. After the formation of the fouling layer on the membrane surface, the atomic percentage composition of carbon increased from 61.89 to 65.69 and of oxygen decreased from 38.11 to 31.77 besides the appearance of new elements like sodium, phosphorous, calcium, sulphur, chlorine and potassium in smaller amounts in the fouling layer. This infers the composition of the fouling layer as mostly consisting of biomolecules such as VFAs, phospholipids, proteins and carbohydrates molecules. When the membranes were cleaned using different cleaning techniques, the relative atomic percentage of carbon decreased while that of oxygen increased suggesting the removal of some of the biomolecules from the membrane surface. This claim was verified by the EDX mapping of the carbon and oxygen atoms in the fouling layer which showed the decrease in density and uniformity of carbon atoms distribution in the fouling layer and vice versa for oxygen atoms in the fouling layer (Figure 5.15). It is also noteworthy that chemical cleaning and especially in combination with osmotic backwashing was most effective in reducing the relative atomic percentage of carbon in the fouling layer. This suggests that chemical cleaning can influence the removal of carbon-based molecules more than physical cleaning techniques.

Table 5.3: EDX elemental composition of clean and fouled membranes

Elemental composition (atomic %)	**O**	**C**	**Na**	**P**	**Ca**	**S**	**Cl**	**K**
Pristine membrane	38.11	61.89	-	-	-	-	-	-
Fouled membrane	31.77	65.69	0.57	0.76	0.24	0.17	0.04	0.42
After hydraulic cleaning	40.55	57.86	0.22	0.60	0.02	0.12	0.05	0.41
After osmotic backwashing	38.53	58.43	1.47	0.71	0.20	0.12	0.49	0.05
After chemical cleaning	45.97	50.86	0.78	1.17	1.14	0.01	0.03	0.03
After osmotic backwashing and chemical cleaning combined	54.81	35.84	5.71	2.51	0.39	0.14	0.54	0.05

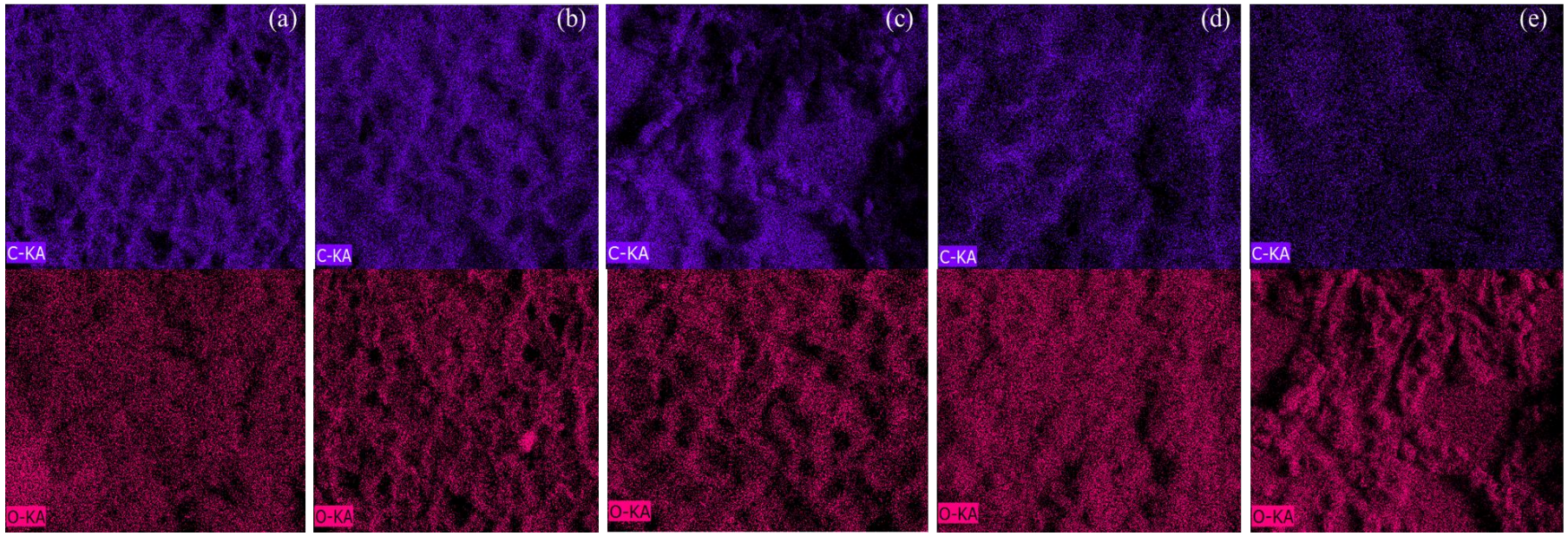

Figure 5.15: EDX carbon and oxygen mapping of (a) fouled membrane (b) membrane after hydraulic cleaning (c) membrane after osmotic backwashing (d) membrane after chemical cleaning (e) membrane after osmotic backwashing and chemical cleaning combined.

5.4 Conclusion

This study provides new insights into membrane biofouling, its effect on FO performance, and the effectiveness of various membrane cleaning techniques in a water extraction process from rumen fluid. The main finding of this study is that the fouling phenomenon is mostly gravity-driven as it was influenced significantly by the membrane module configuration. The most severe membrane fouling condition with the lowest water flux of 1.04 LMH was observed for membrane module configuration 1 when the feed solution was circulated through the upper semi-cell of the membrane module. Under membrane module configurations 2 and 3, there was an increase in the water flux to 1.42 LMH and 1.69 LMH, respectively with a significant reduction in membrane fouling. These findings were endorsed by the visual, SEM-EDX, and FTIR analysis of the fouled membranes. The SEM-EDX and FTIR analysis also confirmed the presence of biomolecules based elements and functional groups in the membrane fouling layer hinting at the occurrence of biofouling. The biofouling phenomenon was further endorsed by the DNA sequencing of the fouling layer samples which revealed the presence of several microbial taxa such as *Prevotellaceae*, *Ruminococcaceae*, and *Acidaminococcaceae* that were also present in the rumen fluid. The diversity of microbial taxa was less with *Pseudomonadaceae* as the most dominant taxa in the thick and more mature fouling layer under membrane module configuration 1 in comparison to membrane module configurations 2 and 3. Different membrane cleaning strategies such as hydraulic cleaning, osmotic backwashing, chemical cleaning, and their combinations were assessed for flux recovery. The combination of osmotic backwashing and chemical fouling was found to be more effective with 70.0% flux recovery while hydraulic cleaning was the least effective cleaning technique that could recover only 14.1% of water flux.

Chapter 6 Conclusions and Recommendations for Future Work

6.1 Conclusions

This thesis signified the potential of FO as a platform for resource recovery from rumen fluid by following the natural separation processes that take place inside the ruminant animal digestive system. The findings demonstrated the promising capability of FO in extracting acetic acid and water from rumen fluid. Moreover, the thesis explored the membrane biofouling phenomenon in a long term FO operation and evaluates its impact on FO performance. Besides, various membrane cleaning strategies were assessed in terms of their effectiveness for flux recovery.

Chapter 2 reviewed the comprehensive literature available on FO. It highlighted the current barriers in the transition of scaling up this process from laboratory to full-scale applications. Both research and review papers available on FO were studied rigorously to compose an updated literature review. The literature review suggested that FO offers more promising prospects than other membrane-based separation technologies. Contents including membrane development, draw solution, transport phenomena, membrane fouling and its mitigation were thoroughly investigated. Moreover, critical challenges like membrane fouling and the development of improved membranes and suitable draw solutes were identified. The review accentuated several research gaps and insisted to further investigate the issues like actual membrane biofouling.

Chapter 3 evaluated the FO potential to extract acetic acid from rumen fluid and the effects of several process parameters such as membrane type, pH of the stripping solution, and membrane orientation on the extraction process. It introduced a novel approach to encourage solutes transport through the FO membrane with minimum water flux for acetic acid extraction from rumen fluid into a clean matrix. Two types of membranes were used to compare their performance in terms of solutes permeation through the membrane.

The CTA membrane allowed more acetic acid to permeation than the TFC-PA membrane. This result was in accordance with the membrane characterization of the two membranes, which showed that solute flux was significantly higher with the CTA membrane in comparison to the TFC-PA membrane. Moreover, increased permeation of acetic acid was observed with an increase in the pH of the stripping solution for both membranes. The results showed that maximum acetic acid recovery of 27% was obtained when the CTA membrane was used in FO mode configuration at stripping solution pH of 9.0 - 10.0. In Chapter 4, the effectiveness of FO was investigated for the dewatering of rumen fluid. A novel draw solution in the form of artificial saliva was introduced that showed excellent results in terms of high water flux and low RSF with DI water as feed. However, replacing the DI water with real rumen fluid resulted in lowering of water flux owing to the complex nature of the rumen fluid. Results showed that increasing the artificial saliva concentration increased the water extraction rate from the rumen fluid. Furthermore, the results suggested that excessive temperature variation can exacerbate membrane fouling. Chapter 5 focussed on characterizing the membrane biofouling in a long term FO process to dewater the rumen fluid besides evaluating various membrane cleaning strategies. The membrane module configuration played a crucial role in determining the severity of the membrane fouling. Membrane fouling was maximum with minimum water flux when the feed solution was circulated in the upper chamber of the membrane module. The membrane fouling reduced significantly with a subsequent increase in the water flux for the other two membrane module configurations. These findings demonstrated the connection of membrane fouling with the gravity-driven sedimentation of the foulants. Membrane fouling was identified as biofouling due to the presence of biomolecules based elements and functional groups identified by SEM-EDX and FTIR analysis. The DNA sequencing of the fouling layer samples further endorsed the biofouling phenomenon with

the presence of several rumen fluid microbial taxa such as *Prevotellaceae*, *Ruminococcaceae*, and *Acidaminococcaceae*. The membrane cleaning was performed using hydraulic cleaning, osmotic backwashing, chemical cleaning, and their combinations. The combination of osmotic backwashing and chemical cleaning was the most effective cleaning technique which was able to achieve 70.0% water flux recovery.

6.2 Recommendations

This thesis has demonstrated the potential of FO as an effective membrane-based separation process to extract acetic acid and water from the rumen fluid. It provides an insight to better understand membrane biofouling and evaluates the effectiveness of various membrane cleaning techniques in a water recovery process from rumen fluid. However, there remain several challenges and unexplored areas that need to be investigated further. Recommendations for future research work are as below.

1- This thesis work has demonstrated potential techniques to improve acetic acid extraction to a clean matrix such as regulating the pH difference between the feed and stripping solutions. Further research to increase acetic acid flux may include the development of new FO membranes with large pore sizes. This thesis work has shown negligible water flux during acetic acid extraction since there is no osmotic gradient between the feed and stripping solution for water transport.

2- Rumen fluid is a complex fluid with a variety of organic and inorganic substances in its composition that generated almost the same osmotic pressure as artificial saliva. It also offered more resistance to allow acetic acid permeation through the FO membrane in comparison to the synthetic acetic acid solution. Rumen fluid needs to be further studied to understand and predict its behaviour during a resource recovery process.

3- The effect of feed and draw solutions temperature on acetic acid extraction from rumen fluid has not been explored yet. It is recommended for future research work.

4- Although increasing the feed solution temperature aggravated membrane fouling and caused a decline in water flux, further research may explore the effect of an increase in draw solution temperature and the simultaneous increase in the feed and draw solution temperatures on FO performance.

5- Membrane biofouling is still one of the least understood phenomena in FO. Long term experiments are recommended to understand the actual biofouling that can pave the way for its control and mitigation strategies.

References

1. Balatsky AV, Balatsky GI, Borysov SS. Resource demand growth and sustainability due to increased world consumption. Sustainability. 2015;7(3):3430-40.

2. Tilman D, Socolow R, Foley JA, Hill J, Larson E, Lynd L, et al. Beneficial biofuels—the food, energy, and environment trilemma. Science. 2009;325(5938):270-71.

3. Lynd LR, Woods J. Perspective: A new hope for Africa. Nature. 2011;474(7352):S20-S21.

4. Gírio FM, Fonseca C, Carvalheiro F, Duarte LC, Marques S, Bogel-Łukasik R. Hemicelluloses for fuel ethanol: a review. Bioresource technology. 2010;101(13):4775-800.

5. Clark JH, Luque R, Matharu AS. Green chemistry, biofuels, and biorefinery. Annual review of chemical and biomolecular engineering. 2012;3:183-207.

6. Zhang L, Peng X, Zhong L, Chua W, Xiang Z, Sun R. Lignocellulosic biomass derived functional materials: synthesis and applications in biomedical engineering. Current Medicinal Chemistry. 2019;26(14):2456-74.

7. Hendriks A, Zeeman G. Pretreatments to enhance the digestibility of lignocellulosic biomass. Bioresource technology. 2009;100(1):10-18.

8. Yue Z-B, Yu H-Q, Harada H, Li Y-Y. Optimization of anaerobic acidogenesis of an aquatic plant, Canna indica L., by rumen cultures. Water research. 2007;41(11):2361-70.

9. Thanakoses P, Black AS, Holtzapple MT. Fermentation of corn stover to carboxylic acids. Biotechnology and Bioengineering. 2003;83(2):191-200.

10. Mood SH, Golfeshan AH, Tabatabaei M, Jouzani GS, Najafi GH, Gholami M, et al. Lignocellulosic biomass to bioethanol, a comprehensive review with a focus on pretreatment. Renewable and Sustainable Energy Reviews. 2013;27:77-93.

11. Limayem A, Ricke SC. Lignocellulosic biomass for bioethanol production: current perspectives, potential issues and future prospects. Progress in energy and combustion science. 2012;38(4):449-67.

12. Lee H, Hamid SBA, Zain S. Conversion of lignocellulosic biomass to nanocellulose: structure and chemical process. The Scientific World Journal. 2014;2014.

13. Himmel ME, Ding S-Y, Johnson DK, Adney WS, Nimlos MR, Brady JW, et al. Biomass recalcitrance: engineering plants and enzymes for biofuels production. science. 2007;315(5813):804-07.

14. Bozell JJ, O'Lenick C, Warwick S. Biomass fractionation for the biorefinery: heteronuclear multiple quantum coherence–nuclear magnetic resonance investigation of lignin isolated from solvent fractionation of switchgrass. Journal of agricultural and food chemistry. 2011;59(17):9232-42.

15. Yue Z-B, Li W-W, Yu H-Q. Application of rumen microorganisms for anaerobic bioconversion of lignocellulosic biomass. Bioresource technology. 2013;128:738-44.

16. Sha Y, Hu J, Shi B, Dingkao R, Wang J, Li S, et al. Characteristics and Functions of the Rumen Microbial Community of Cattle-Yak at Different Ages. BioMed Research International. 2020;2020.

17. Brulc JM, Antonopoulos DA, Miller MEB, Wilson MK, Yannarell AC, Dinsdale EA, et al. Gene-centric metagenomics of the fiber-adherent bovine rumen microbiome reveals forage specific glycoside hydrolases. Proceedings of the National Academy of Sciences. 2009;106(6):1948-53.

18. Forsberg CW, Cheng K-J, White BA. Polysaccharide degradation in the rumen and large intestine. Gastrointestinal microbiology: Springer; 1997. p. 319-79.

19. Sauer M, Marx H, Mattanovich D. From rumen to industry. Microbial Cell Factories. 2012;11(1):121.

20. An X, Hu Y, Wang N, Zhou Z, Liu Z. Continuous juice concentration by integrating forward osmosis with membrane distillation using potassium sorbate preservative as a draw solute. Journal of Membrane Science. 2019;573:192-99.

21. Ansari AJ, Hai FI, Price WE, Nghiem LD. Phosphorus recovery from digested sludge centrate using seawater-driven forward osmosis. Separation and Purification Technology. 2016;163:1-7.

22. Vu MT, Price WE, He T, Zhang X, Nghiem LD. Seawater-driven forward osmosis for pre-concentrating nutrients in digested sludge centrate. Journal of Environmental Management. 2019;247:135-39.

23. Chen G, Wang Z, Nghiem LD, Li X-M, Xie M, Zhao B, et al. Treatment of shale gas drilling flowback fluids (SGDFs) by forward osmosis: Membrane fouling and mitigation. Desalination. 2015;366:113-20.

24. Nguyen CN, Duong HC, Chen S-S, Thi Nguyen H, Hao Ngo H, Guo W, et al. Water and nutrient recovery by a novel moving sponge – Anaerobic osmotic membrane

bioreactor – Membrane distillation (AnOMBR-MD) closed-loop system. Bioresource Technology. 2020;312:123573.

25. Saini JK, Saini R, Tewari L. Lignocellulosic agriculture wastes as biomass feedstocks for second-generation bioethanol production: concepts and recent developments. 3 Biotech. 2015;5(4):337-53.

26. Kuhad RC, Singh A. Lignocellulose biotechnology: current and future prospects. Critical Reviews in Biotechnology. 1993;13(2):151-72.

27. Nguyen AQ, Nguyen LN, Johir MAH, Ngo H-H, Chaves AV, Nghiem LD. Derivation of volatile fatty acid from crop residues digestion using a rumen membrane bioreactor: a feasibility study. Bioresource Technology. 2020:123571.

28. Mirmohamadsadeghi S, Karimi K, Zamani A, Amiri H, Horváth IS. Enhanced solid-state biogas production from lignocellulosic biomass by organosolv pretreatment. BioMed research international. 2014;2014.

29. Saleem F, Bouatra S, Guo AC, Psychogios N, Mandal R, Dunn SM, et al. The bovine ruminal fluid metabolome. Metabolomics. 2013;9(2):360-78.

30. Whiting A, Azapagic A. Life cycle environmental impacts of generating electricity and heat from biogas produced by anaerobic digestion. Energy. 2014;70:181-93.

31. [Available from: https://archive.epa.gov/region02/webinars/web/pdf/3-24-10_1.pdf.

32. Jenifer C. Beddoes KSB, Robert T. Burns, and William F. Lazarus. An Analysis of Energy Production Costs from Anaerobic Digestion Systems on U.S. Livestock Production Facilities: United States Department of Agriculture; 2007 [Available from: https://directives.sc.egov.usda.gov/OpenNonWebContent.aspx?content=22533.wba.

33. Baruah J, Nath BK, Sharma R, Kumar S, Deka RC, Baruah DC, et al. Recent trends in the pretreatment of lignocellulosic biomass for value-added products. Frontiers in Energy Research. 2018;6:141.

34. Mehta D, Gupta L, Dhingra R. Forward osmosis in India: Status and comparison with other desalination technologies. International scholarly research notices. 2014;2014.

35. Elimelech M, Phillip WA. The future of seawater desalination: energy, technology, and the environment. science. 2011;333(6043):712-17.

36. Ahmed FE, Hashaikeh R, Hilal N. Solar powered desalination–Technology, energy and future outlook. Desalination. 2019;453:54-76.

37. Misdan N, Lau W, Ismail A. Seawater Reverse Osmosis (SWRO) desalination by thin-film composite membrane—Current development, challenges and future prospects. Desalination. 2012;287:228-37.

38. Akther N, Sodiq A, Giwa A, Daer S, Arafat H, Hasan S. Recent advancements in forward osmosis desalination: a review. Chemical Engineering Journal. 2015;281:502-22.

39. Ibrar I, Altaee A, Zhou JL, Naji O, Khanafer D. Challenges and potentials of forward osmosis process in the treatment of wastewater. Critical Reviews in Environmental Science and Technology. 2020;50(13):1339-83.

40. Rood B, Zhang C, Inniss E, Hu Z. Forward osmosis with an algal draw solution to concentrate municipal wastewater and recover resources. Water Environment Research. 2020;92(5):689-97.

41. Haupt A, Lerch A. Forward osmosis application in manufacturing industries: A short review. Membranes. 2018;8(3):47.

42. Li Z, Linares RV, Sarp S, Amy G. Direct and Indirect Seawater Desalination by Forward Osmosis. Membrane-Based Salinity Gradient Processes for Water Treatment and Power Generation: Elsevier; 2018. p. 245-72.

43. Achilli A, Cath TY, Marchand EA, Childress AE. The forward osmosis membrane bioreactor: a low fouling alternative to MBR processes. Desalination. 2009;239(1-3):10-21.

44. Chekli L, Kim Y, Phuntsho S, Li S, Ghaffour N, Leiknes T, et al. Evaluation of fertilizer-drawn forward osmosis for sustainable agriculture and water reuse in arid regions. Journal of environmental management. 2017;187:137-45.

45. Liu J, Wang X, Wang Z, Lu Y, Li X, Ren Y. Integrating microbial fuel cells with anaerobic acidification and forward osmosis membrane for enhancing bio-electricity and water recovery from low-strength wastewater. Water research. 2017;110:74-82.

46. Loo S-L, Fane AG, Krantz WB, Lim T-T. Emergency water supply: a review of potential technologies and selection criteria. Water research. 2012;46(10):3125-51.

47. Hickenbottom KL, Hancock NT, Hutchings NR, Appleton EW, Beaudry EG, Xu P, et al. Forward osmosis treatment of drilling mud and fracturing wastewater from oil and gas operations. Desalination. 2013;312:60-66.

48. Ibrar I, Yadav S, Altaee A, Samal AK, Zhou JL, Nguyen TV, et al. Treatment of biologically treated landfill leachate with forward osmosis: Investigating membrane performance and cleaning protocols. Science of The Total Environment. 2020;744:140901.

49. Vu MT, Ansari AJ, Hai FI, Nghiem LD. Performance of a seawater-driven forward osmosis process for pre-concentrating digested sludge centrate: Organic enrichment and membrane fouling. Environmental Science: Water Research & Technology. 2018;4(7):1047-56.

50. Zhao S, Zou L, Tang CY, Mulcahy D. Recent developments in forward osmosis: opportunities and challenges. Journal of membrane science. 2012;396:1-21.

51. Nguyen AQ, Nguyen LN, Johir MAH, Ngo H-H, Chaves AV, Nghiem LD. Derivation of volatile fatty acid from crop residues digestion using a rumen membrane bioreactor: A feasibility study. Bioresource Technology. 2020;312:123571.

52. Makinde O, Sonaiya E. A simple technology for production of vegetable-carried blood or rumen fluid meals from abattoir wastes. Animal feed science and technology. 2010;162(1-2):12-19.

53. Roy M, Karmakar S, Debsarcar A, Sen PK, Mukherjee J. Application of rural slaughterhouse waste as an organic fertilizer for pot cultivation of solanaceous vegetables in India. International Journal of Recycling of Organic Waste in Agriculture. 2013;2(1):6.

54. Zacharof M-P, Mandale SJ, Williams PM, Lovitt RW. Nanofiltration of treated digested agricultural wastewater for recovery of carboxylic acids. Journal of Cleaner Production. 2016;112:4749-61.

55. Mostafa N. Production and recovery of volatile fatty acids from fermentation broth. Energy conversion and management. 1999;40(14):1543-53.

56. Reyhanitash E, Kersten SR, Schuur B. Recovery of volatile fatty acids from fermented wastewater by adsorption. ACS sustainable chemistry & engineering. 2017;5(10):9176-84.

57. Reyhanitash E, Zaalberg B, Kersten SR, Schuur B. Extraction of volatile fatty acids from fermented wastewater. Separation and purification technology. 2016;161:61-68.

58. Choudhari SK, Cerrone F, Woods T, Joyce K, O'Flaherty V, O'Connor K, et al. Pervaporation separation of butyric acid from aqueous and anaerobic digestion (AD) solutions using PEBA based composite membranes. Journal of Industrial and Engineering Chemistry. 2015;23:163-70.

59. Pan X-R, Li W-W, Huang L, Liu H-Q, Wang Y-K, Geng Y-K, et al. Recovery of high-concentration volatile fatty acids from wastewater using an acidogenesis-electrodialysis integrated system. Bioresource technology. 2018;260:61-67.

60. Bóna Á, Bakonyi P, Galambos I, Bélafi-Bakó K, Nemestóthy N. Separation of Volatile Fatty Acids from Model Anaerobic Effluents Using Various Membrane Technologies. Membranes. 2020;10(10):252.

61. Jung K, Lee D, Seo C, Lee J, Lee SY, Chang HN, et al. Permeation characteristics of volatile fatty acids solution by forward osmosis. Process Biochemistry. 2015;50(4):669-77.

62. Ruprakobkit T, Ruprakobkit L, Ratanatamskul C. Carboxylic acid concentration by forward osmosis processes: Dynamic modeling, experimental validation and simulation. Chemical Engineering Journal. 2016;306:538-49.

63. Cath TY, Childress AE, Elimelech M. Forward osmosis: principles, applications, and recent developments. Journal of membrane science. 2006;281(1-2):70-87.

64. Jafarinejad S. Forward osmosis membrane technology for nutrient removal/recovery from wastewater: Recent advances, proposed designs, and future directions. Chemosphere. 2020:128116.

65. Goh PS, Ismail AF, Ng BC, Abdullah MS. Recent progresses of forward osmosis membranes formulation and design for wastewater treatment. Water. 2019;11(10):2043.

66. Wang C-Y, Ho H-O, Lin L-H, Lin Y-K, Sheu M-T. Asymmetric membrane capsules for delivery of poorly water-soluble drugs by osmotic effects. International journal of pharmaceutics. 2005;297(1-2):89-97.

67. Gerstandt K, Peinemann K-V, Skilhagen SE, Thorsen T, Holt T. Membrane processes in energy supply for an osmotic power plant. Desalination. 2008;224(1-3):64-70.

68. Wang KY, Ong RC, Chung T-S. Double-skinned forward osmosis membranes for reducing internal concentration polarization within the porous sublayer. Industrial & Engineering Chemistry Research. 2010;49(10):4824-31.

69. Zhang S, Wang KY, Chung T-S, Chen H, Jean Y, Amy G. Well-constructed cellulose acetate membranes for forward osmosis: minimized internal concentration polarization with an ultra-thin selective layer. Journal of Membrane Science. 2010;360(1-2):522-35.

70. Sairam M, Sereewatthanawut E, Li K, Bismarck A, Livingston A. Method for the preparation of cellulose acetate flat sheet composite membranes for forward osmosis—Desalination using MgSO4 draw solution. Desalination. 2011;273(2-3):299-307.

71. Tiraferri A, Yip NY, Phillip WA, Schiffman JD, Elimelech M. Relating performance of thin-film composite forward osmosis membranes to support layer formation and structure. Journal of Membrane Science. 2011;367(1-2):340-52.

72. Widjojo N, Chung T-S, Weber M, Maletzko C, Warzelhan V. The role of sulphonated polymer and macrovoid-free structure in the support layer for thin-film composite (TFC) forward osmosis (FO) membranes. Journal of Membrane Science. 2011;383(1-2):214-23.

73. Zhang S, Wang KY, Chung T-S, Jean Y, Chen H. Molecular design of the cellulose ester-based forward osmosis membranes for desalination. Chemical engineering science. 2011;66(9):2008-18.

74. Song X, Liu Z, Sun DD. Nano gives the answer: breaking the bottleneck of internal concentration polarization with a nanofiber composite forward osmosis membrane for a high water production rate. Advanced materials. 2011;23(29):3256-60.

75. Qiu C, Setiawan L, Wang R, Tang CY, Fane AG. High performance flat sheet forward osmosis membrane with an NF-like selective layer on a woven fabric embedded substrate. Desalination. 2012;287:266-70.

76. Ma N, Wei J, Qi S, Zhao Y, Gao Y, Tang CY. Nanocomposite substrates for controlling internal concentration polarization in forward osmosis membranes. Journal of membrane science. 2013;441:54-62.

77. Li X, He T, Dou P, Zhao S. 2.5 Forward Osmosis and Forward Osmosis Membranes. 2017.

78. Yanar N, Son M, Yang E, Kim Y, Park H, Nam S-E, et al. Investigation of the performance behavior of a forward osmosis membrane system using various feed spacer materials fabricated by 3D printing technique. Chemosphere. 2018;202:708-15.

79. Wang Y-N, Wei J, She Q, Pacheco F, Tang CY. Microscopic characterization of FO/PRO membranes–a comparative study of CLSM, TEM and SEM. Environmental science & technology. 2012;46(18):9995-10003.

80. Ong RC, Chung T-S, Helmer BJ, de Wit JS. Novel cellulose esters for forward osmosis membranes. Industrial & engineering chemistry research. 2012;51(49):16135-45.

81. Yip NY, Tiraferri A, Phillip WA, Schiffman JD, Elimelech M. High performance thin-film composite forward osmosis membrane. Environmental science & technology. 2010;44(10):3812-18.

82. Wang R, Shi L, Tang CY, Chou S, Qiu C, Fane AG. Characterization of novel forward osmosis hollow fiber membranes. Journal of membrane science. 2010;355(1-2):158-67.

83. Qasim M, Darwish NA, Sarp S, Hilal N. Water desalination by forward (direct) osmosis phenomenon: A comprehensive review. Desalination. 2015;374:47-69.

84. Wang Y-N, Goh K, Li X, Setiawan L, Wang R. Membranes and processes for forward osmosis-based desalination: Recent advances and future prospects. Desalination. 2018;434:81-99.

85. Zheng L, Price WE, Nghiem LD. Effects of fouling on separation performance by forward osmosis: the role of specific organic foulants. Environmental Science and Pollution Research. 2018:1-12.

86. Sahebi S, Phuntsho S, Woo YC, Park MJ, Tijing LD, Hong S, et al. Effect of sulphonated polyethersulfone substrate for thin film composite forward osmosis membrane. Desalination. 2016;389:129-36.

87. Amini M, Jahanshahi M, Rahimpour A. Synthesis of novel thin film nanocomposite (TFN) forward osmosis membranes using functionalized multi-walled carbon nanotubes. Journal of membrane science. 2013;435:233-41.

88. Emadzadeh D, Lau WJ, Matsuura T, Rahbari-Sisakht M, Ismail AF. A novel thin film composite forward osmosis membrane prepared from PSf–TiO2 nanocomposite substrate for water desalination. Chemical Engineering Journal. 2014;237:70-80.

89. Setiawan L, Wang R, Li K, Fane AG. Fabrication of novel poly (amide–imide) forward osmosis hollow fiber membranes with a positively charged nanofiltration-like selective layer. Journal of Membrane Science. 2011;369(1-2):196-205.

90. Balogun HA, Sulaiman R, Marzouk SS, Giwa A, Hasan SW. 3D printing and surface imprinting technologies for water treatment: A review. Journal of Water Process Engineering. 2019;31:100786.

91. Fu F-J, Zhang S, Sun S-P, Wang K-Y, Chung T-S. POSS-containing delamination-free dual-layer hollow fiber membranes for forward osmosis and osmotic power generation. Journal of membrane science. 2013;443:144-55.

92. Liu X, Ng HY. Fabrication of layered silica–polysulfone mixed matrix substrate membrane for enhancing performance of thin-film composite forward osmosis membrane. Journal of membrane science. 2015;481:148-63.

93. Achilli A, Cath TY, Childress AE. Selection of inorganic-based draw solutions for forward osmosis applications. Journal of membrane science. 2010;364(1-2):233-41.

94. Ng HY, Tang W, Wong WS. Performance of forward (direct) osmosis process: membrane structure and transport phenomenon. Environmental science & technology. 2006;40(7):2408-13.

95. Su J, Chung T-S, Helmer BJ, de Wit JS. Enhanced double-skinned FO membranes with inner dense layer for wastewater treatment and macromolecule recycle using Sucrose as draw solute. Journal of membrane science. 2012;396:92-100.

96. Bowden KS, Achilli A, Childress AE. Organic ionic salt draw solutions for osmotic membrane bioreactors. Bioresource technology. 2012;122:207-16.

97. Zou S, Gu Y, Xiao D, Tang CY. The role of physical and chemical parameters on forward osmosis membrane fouling during algae separation. Journal of Membrane Science. 2011;366(1-2):356-62.

98. Phuntsho S, Shon HK, Hong S, Lee S, Vigneswaran S. A novel low energy fertilizer driven forward osmosis desalination for direct fertigation: evaluating the performance of fertilizer draw solutions. Journal of Membrane Science. 2011;375(1-2):172-81.

99. Sato N, Sato Y, Yanase S. Forward osmosis using dimethyl ether as a draw solute. Desalination. 2014;349:102-05.

100. Inada A, Yumiya K, Takahashi T, Kumagai K, Hashizume Y, Matsuyama H. Development of thermoresponsive star oligomers with a glycerol backbone as the draw solute in forward osmosis process. Journal of membrane science. 2019;574:147-53.

101. Li D, Zhang X, Simon GP, Wang H. Forward osmosis desalination using polymer hydrogels as a draw agent: Influence of draw agent, feed solution and membrane on process performance. Water research. 2013;47(1):209-15.

102. Ng HY, Tang W. Forward (direct) osmosis: A novel and prospective process for brine control. Proceedings of the Water Environment Federation. 2006;2006(8):4345-52.

103. Nguyen NC, Nguyen HT, Ho S-T, Chen S-S, Ngo HH, Guo W, et al. Exploring high charge of phosphate as new draw solute in a forward osmosis–membrane distillation hybrid system for concentrating high-nutrient sludge. Science of the Total Environment. 2016;557:44-50.

104. Neff RA. Solvent extractor. Google Patents; 1964.

105. McGinnis RL, McCutcheon JR, Elimelech M. A novel ammonia–carbon dioxide osmotic heat engine for power generation. Journal of membrane science. 2007;305(1-2):13-19.

106. Chen Q, Xu W, Ge Q. Synthetic draw solutes for forward osmosis: status and future. Reviews in Chemical Engineering. 2017.

107. Zhao D, Wang P, Zhao Q, Chen N, Lu X. Thermoresponsive copolymer-based draw solution for seawater desalination in a combined process of forward osmosis and membrane distillation. Desalination. 2014;348:26-32.

108. Kim J-j, Kang H, Choi Y-S, Yu YA, Lee J-C. Thermo-responsive oligomeric poly (tetrabutylphosphonium styrenesulfonate) s as draw solutes for forward osmosis (FO) applications. Desalination. 2016;381:84-94.

109. McGinnis RL, Hancock NT, Nowosielski-Slepowron MS, McGurgan GD. Pilot demonstration of the NH3/CO2 forward osmosis desalination process on high salinity brines. Desalination. 2013;312:67-74.

110. Phuntsho S, Kim JE, Johir MA, Hong S, Li Z, Ghaffour N, et al. Fertiliser drawn forward osmosis process: Pilot-scale desalination of mine impaired water for fertigation. Journal of Membrane Science. 2016;508:22-31.

111. Kim Y, Lee JH, Kim YC, Lee KH, Park IS, Park S-J. Operation and simulation of pilot-scale forward osmosis desalination with ammonium bicarbonate. Chemical Engineering Research and Design. 2015;94:390-95.

112. Corzo B, de la Torre T, Sans C, Ferrero E, Malfeito JJ. Evaluation of draw solutions and commercially available forward osmosis membrane modules for wastewater reclamation at pilot scale. Chemical Engineering Journal. 2017;326:1-8.

113. Wang Z, Zheng J, Tang J, Wang X, Wu Z. A pilot-scale forward osmosis membrane system for concentrating low-strength municipal wastewater: performance and implications. Scientific reports. 2016;6:21653.

114. Hancock NT, Xu P, Heil DM, Bellona C, Cath TY. Comprehensive bench-and pilot-scale investigation of trace organic compounds rejection by forward osmosis. Environmental science & technology. 2011;45(19):8483-90.

115. Zhao S, Zou L. Relating solution physicochemical properties to internal concentration polarization in forward osmosis. Journal of membrane science. 2011;379(1-2):459-67.

116. Hancock NT, Cath TY. Solute coupled diffusion in osmotically driven membrane processes. Environmental science & technology. 2009;43(17):6769-75.

117. Suh C, Lee S. Modeling reverse draw solute flux in forward osmosis with external concentration polarization in both sides of the draw and feed solution. Journal of membrane science. 2013;427:365-74.

118. Coday BD, Xu P, Beaudry EG, Herron J, Lampi K, Hancock NT, et al. The sweet spot of forward osmosis: treatment of produced water, drilling wastewater, and other complex and difficult liquid streams. Desalination. 2014;333(1):23-35.

119. Lutchmiah K, Verliefde A, Roest K, Rietveld LC, Cornelissen ER. Forward osmosis for application in wastewater treatment: a review. Water research. 2014;58:179-97.

120. Ansari AJ, Hai FI, Price WE, Drewes JE, Nghiem LD. Forward osmosis as a platform for resource recovery from municipal wastewater-A critical assessment of the literature. Journal of membrane science. 2017;529:195-206.

121. Zou S, Qin M, He Z. Tackle reverse solute flux in forward osmosis towards sustainable water recovery: reduction and perspectives. Water research. 2018.

122. Huang L, Bui N-N, Meyering MT, Hamlin TJ, McCutcheon JR. Novel hydrophilic nylon 6, 6 microfiltration membrane supported thin film composite membranes for engineered osmosis. Journal of membrane science. 2013;437:141-49.

123. Zou S, Smith ED, Lin S, Martin SM, He Z. Mitigation of bidirectional solute flux in forward osmosis via membrane surface coating of zwitterion functionalized carbon nanotubes. Environment international. 2019;131:104970.

124. Gray GT, McCutcheon JR, Elimelech M. Internal concentration polarization in forward osmosis: role of membrane orientation. Desalination. 2006;197(1-3):1-8.

125. Choi Y, Hwang T-M, Jeong S, Lee S. The use of ultrasound to reduce internal concentration polarization in forward osmosis. Ultrasonics sonochemistry. 2018;41:475-83.

126. AlSawaftah N, Abuwatfa W, Darwish N, Husseini G. A Comprehensive Review on Membrane Fouling: Mathematical Modelling, Prediction, Diagnosis, and Mitigation. Water. 2021;13(9):1327.

127. Chun Y, Mulcahy D, Zou L, Kim IS. A short review of membrane fouling in forward osmosis processes. Membranes. 2017;7(2):30.

128. Shaffer DL, Werber JR, Jaramillo H, Lin S, Elimelech M. Forward osmosis: where are we now? Desalination. 2015;356:271-84.

129. Guo W, Ngo H-H, Li J. A mini-review on membrane fouling. Bioresource technology. 2012;122:27-34.

130. Khan MMT, Stewart PS, Moll DJ, Mickols WE, Burr MD, Nelson SE, et al. Assessing biofouling on polyamide reverse osmosis (RO) membrane surfaces in a laboratory system. Journal of Membrane Science. 2010;349(1-2):429-37.

131. Alzahrani S, Mohammad AW. Challenges and trends in membrane technology implementation for produced water treatment: A review. Journal of Water Process Engineering. 2014;4:107-33.

132. Flemming H-C, Wingender J. The biofilm matrix. Nature Reviews Microbiology. 2010;8(9):623.

133. Chen D. Ultrasonic control of ceramic membrane fouling caused by silica particles and dissolved organic matter: The Ohio State University; 2005.

134. Lee S, Boo C, Elimelech M, Hong S. Comparison of fouling behavior in forward osmosis (FO) and reverse osmosis (RO). Journal of membrane science. 2010;365(1-2):34-39.

135. Mi B, Elimelech M. Gypsum scaling and cleaning in forward osmosis: measurements and mechanisms. Environmental science & technology. 2010;44(6):2022-28.

136. Linares RV, Yangali-Quintanilla V, Li Z, Amy G. Rejection of micropollutants by clean and fouled forward osmosis membrane. Water research. 2011;45(20):6737-44.

137. Khan JA, Vu MT, Nghiem LD. A preliminary assessment of forward osmosis to extract water from rumen fluid for artificial saliva. Case Studies in Chemical and Environmental Engineering. 2021:100095.

138. Cagnetta C, D'Haese A, Coma M, Props R, Buysschaert B, Verliefde A, et al. Increased carboxylate production in high-rate activated A-sludge by forward osmosis thickening. Chemical Engineering Journal. 2017;312:68-78.

139. Chun Y, Zaviska F, Cornelissen E, Zou L. A case study of fouling development and flux reversibility of treating actual lake water by forward osmosis process. Desalination. 2015;357:55-64.

140. Nguyen NC, Nguyen HT, Chen S-S, Nguyen NT, Li C-W. Application of forward osmosis (FO) under ultrasonication on sludge thickening of waste activated sludge. Water Science and Technology. 2015;72(8):1301-07.

141. Kim C, Lee S, Hong S. Application of osmotic backwashing in forward osmosis: mechanisms and factors involved. Desalination and Water Treatment. 2012;43(1-3):314-22.

142. Blandin G, Verliefde AR, Comas J, Rodriguez-Roda I, Le-Clech P. Efficiently combining water reuse and desalination through forward osmosis—reverse osmosis (FO-RO) hybrids: a critical review. Membranes. 2016;6(3):37.

143. Li J, Sanderson R, Jacobs E. Ultrasonic cleaning of nylon microfiltration membranes fouled by Kraft paper mill effluent. Journal of Membrane Science. 2002;205(1-2):247-57.

144. Zhang Q, Jie YW, Loong WLC, Zhang J, Fane AG, Kjelleberg S, et al. Characterization of biofouling in a lab-scale forward osmosis membrane bioreactor (FOMBR). Water research. 2014;58:141-51.

145. Chun Y, Kim S-J, Millar GJ, Mulcahy D, Kim IS, Zou L. Forward osmosis as a pre-treatment for treating coal seam gas associated water: Flux and fouling behaviour. Desalination. 2017;403:144-52.

146. Oviedo C, Rodríguez J. EDTA: The chelating agent under environmental scrutiny. Quimica Nova. 2003;26(6):901-05.

147. Li Q, Elimelech M. Organic fouling and chemical cleaning of nanofiltration membranes: measurements and mechanisms. Environmental science & technology. 2004;38(17):4683-93.

148. Majeed T, Phuntsho S, Chekli L, Lee S-H, Kim K, Shon HK. Role of various physical and chemical techniques for hollow fibre forward osmosis membrane cleaning. Desalination and Water Treatment. 2016;57(17):7742-52.

149. Yoon H, Baek Y, Yu J, Yoon J. Biofouling occurrence process and its control in the forward osmosis. Desalination. 2013;325:30-36.

150. Wang X, Hu T, Wang Z, Li X, Ren Y. Permeability recovery of fouled forward osmosis membranes by chemical cleaning during a long-term operation of anaerobic osmotic membrane bioreactors treating low-strength wastewater. Water research. 2017;123:505-12.

151. Guillen-Burrieza E, Ruiz-Aguirre A, Zaragoza G, Arafat HA. Membrane fouling and cleaning in long term plant-scale membrane distillation operations. Journal of Membrane Science. 2014;468:360-72.

152. Saleh TA, Gupta VK. Nanomaterial and polymer membranes: synthesis, characterization, and applications: Elsevier; 2016.

153. Madaeni SS, Sharifnia S, Moradi G. Chemical cleaning of microfiltration membranes fouled by whey. Journal of the Chinese Chemical Society. 2001;48(2):179-91.

154. Lee J, Johir M, Chinu K, Shon H, Vigneswaran S, Kandasamy J, et al. Hybrid filtration method for pre-treatment of seawater reverse osmosis (SWRO). Desalination. 2009;247(1-3):15-24.

155. Liu Y. Fouling in forward osmosis membrane processes: Chracterization, mechanisms, and mitigation [Dissertation]: University of Maryland; 2013.

156. Park C, Lee YH, Lee S, Hong S. Effect of cake layer structure on colloidal fouling in reverse osmosis membranes. Desalination. 2008;220(1-3):335-44.

157. Nguyen T, Roddick FA, Fan L. Biofouling of water treatment membranes: a review of the underlying causes, monitoring techniques and control measures. Membranes. 2012;2(4):804-40.

158. Gogate PR. Application of cavitational reactors for water disinfection: current status and path forward. Journal of environmental management. 2007;85(4):801-15.

159. Nguyen TPN, Jun B-M, Kwon Y-N. The chlorination mechanism of integrally asymmetric cellulose triacetate (CTA)-based and thin film composite polyamide-based forward osmosis membrane. Journal of Membrane Science. 2017;523:111-21.

160. Polanska M, Huysman K, Van Keer C. Investigation of assimilable organic carbon (AOC) in flemish drinking water. Water Research. 2005;39(11):2259-66.

161. Hammes F, Meylan S, Salhi E, Köster O, Egli T, Von Gunten U. Formation of assimilable organic carbon (AOC) and specific natural organic matter (NOM) fractions during ozonation of phytoplankton. Water research. 2007;41(7):1447-54.

162. Lehtola MJ, Miettinen IT, Vartiainen T, Rantakokko P, Hirvonen A, Martikainen PJ. Impact of UV disinfection on microbially available phosphorus, organic carbon, and microbial growth in drinking water. Water Research. 2003;37(5):1064-70.

163. Ali S, Rimassa SM, Auzerais FM, Boney CL, Li L. Method for treating fracturing water. Google Patents; 2013.

164. Ye Y, Ngo HH, Guo W, Liu Y, Li J, Liu Y, et al. Insight into chemical phosphate recovery from municipal wastewater. Science of the Total Environment. 2017;576:159-71.

165. Schmidt JJ, Gagnon GA, Jamieson RC. Microalgae growth and phosphorus uptake in wastewater under simulated cold region conditions. Ecological engineering. 2016;95:588-93.

166. Jacobs JF, Hasan MN, Paik KH, Hagen WR, van Loosdrecht MC. Development of a bionanotechnological phosphate removal system with thermostable ferritin. Biotechnology and bioengineering. 2010;105(5):918-23.

167. Peng L, Dai H, Wu Y, Peng Y, Lu X. A comprehensive review of phosphorus recovery from wastewater by crystallization processes. Chemosphere. 2018;197:768-81.

168. Karaca S, Gürses A, Ejder M, Açıkyıldız M. Adsorptive removal of phosphate from aqueous solutions using raw and calcinated dolomite. Journal of hazardous materials. 2006;128(2-3):273-79.

169. Vasudevan S, Sozhan G, Ravichandran S, Jayaraj J, Lakshmi J, Sheela M. Studies on the removal of phosphate from drinking water by electrocoagulation process. Industrial & Engineering Chemistry Research. 2008;47(6):2018-23.

170. González JE, Keshavan ND. Messing with bacterial quorum sensing. Microbiology and Molecular Biology Reviews. 2006;70(4):859-75.

171. Kim S, Lee S, Hong S, Oh Y, Kweon J, Kim T. Biofouling of reverse osmosis membranes: microbial quorum sensing and fouling propensity. Desalination. 2009;247(1-3):303-15.

172. Ponnusamy K, Paul D, Kim YS, Kweon JH. 2 (5H)-Furanone: a prospective strategy for biofouling-control in membrane biofilm bacteria by quorum sensing inhibition. Brazilian Journal of Microbiology. 2010;41(1):227-34.

173. Kappachery S, Paul D, Yoon J, Kweon JH. Vanillin, a potential agent to prevent biofouling of reverse osmosis membrane. Biofouling. 2010;26(6):667-72.

174. Yeon K-M, Cheong W-S, Oh H-S, Lee W-N, Hwang B-K, Lee C-H, et al. Quorum sensing: a new biofouling control paradigm in a membrane bioreactor for advanced wastewater treatment. Environmental science & technology. 2008;43(2):380-85.

175. Mc Grath S, van Sinderen D. Bacteriophage: genetics and molecular biology: Horizon Scientific Press; 2007.

176. Barraud N, Storey MV, Moore ZP, Webb JS, Rice SA, Kjelleberg S. Nitric oxide-mediated dispersal in single-and multi-species biofilms of clinically and industrially relevant microorganisms. Microbial biotechnology. 2009;2(3):370-78.

177. He L, Dumée LF, Feng C, Velleman L, Reis R, She F, et al. Promoted water transport across graphene oxide–poly (amide) thin film composite membranes and their antibacterial activity. Desalination. 2015;365:126-35.

178. Van der Bruggen B. Chemical modification of polyethersulfone nanofiltration membranes: a review. Journal of Applied Polymer Science. 2009;114(1):630-42.

179. Bae T-H, Tak T-M. Effect of TiO2 nanoparticles on fouling mitigation of ultrafiltration membranes for activated sludge filtration. Journal of Membrane Science. 2005;249(1-2):1-8.

180. Liu P-S, Chen Q, Wu S-S, Shen J, Lin S-C. Surface modification of cellulose membranes with zwitterionic polymers for resistance to protein adsorption and platelet adhesion. Journal of Membrane Science. 2010;350(1-2):387-94.

181. Church M. Forward Water demonstration plant begins operations 2019, August 23 [Available from: https://www.canadianbiomassmagazine.ca/forward-water-demonstration-plant-begins-operations/.

182. Wang Z, Zheng J, Tang J, Wang X, Wu Z. A pilot-scale forward osmosis membrane system for concentrating low-strength municipal wastewater: performance and implications. Scientific reports. 2016;6(1):1-11.

183. Creevey CJ, Kelly WJ, Henderson G, Leahy SC. Determining the culturability of the rumen bacterial microbiome. Microbial biotechnology. 2014;7(5):467-79.

184. Artegoitia VM, Foote AP, Lewis RM, Freetly HC. Rumen Fluid Metabolomics Analysis Associated with Feed Efficiency on Crossbred Steers. Scientific Reports. 2017;7(1):2864.

185. Khan JA, Shon HK, Nghiem LD. From the Laboratory to Full-Scale Applications of Forward Osmosis: Research Challenges and Opportunities. Current Pollution Reports. 2019;5(4):337-52.

186. Fujioka T, Nguyen KH, Hoang AT, Ueyama T, Yasui H, Terashima M, et al. Biofouling Mitigation by Chloramination during Forward Osmosis Filtration of Wastewater. International Journal of Environmental Research and Public Health. 2018;15(10):2124.

187. Zheng L, Price WE, McDonald J, Khan SJ, Fujioka T, Nghiem LD. New insights into the relationship between draw solution chemistry and trace organic rejection by forward osmosis. Journal of Membrane Science. 2019;587:117184.

188. Kim DI, Gwak G, Zhan M, Hong S. Sustainable dewatering of grapefruit juice through forward osmosis: Improving membrane performance, fouling control, and product quality. Journal of Membrane Science. 2019;578:53-60.

189. Pătruț C, Udrea EC, Bildea CS. Separation of water-Acetic acid mixtures by cyclic distillation. UPB Scientific Bulletin, Series B: Chemistry and Materials Science. 2018;80(4):49-66.

190. Ijmker H, Gramblička M, Kersten SR, van der Ham AG, Schuur B. Acetic acid extraction from aqueous solutions using fatty acids. Separation and purification technology. 2014;125:256-63.

191. Choi WS, Kim K-J. Separation of acetic acid from acetic acid-water mixture by crystallization. Separation Science and Technology. 2013;48(7):1056-61.

192. Wang X, Zhao Y, Yuan B, Wang Z, Li X, Ren Y. Comparison of biofouling mechanisms between cellulose triacetate (CTA) and thin-film composite (TFC) polyamide forward osmosis membranes in osmotic membrane bioreactors. Bioresource Technology. 2016;202:50-58.

193. Fam W, Phuntsho S, Lee JH, Shon HK. Performance comparison of thin-film composite forward osmosis membranes. Desalination and Water Treatment. 2013;51(31-33):6274-80.

194. Nguyen LN, Nguyen AQ, Johir MAH, Guo W, Ngo HH, Chaves AV, et al. Application of rumen and anaerobic sludge microbes for bio harvesting from lignocellulosic biomass. Chemosphere. 2019;228:702-08.

195. Cath TY, Elimelech M, McCutcheon JR, McGinnis RL, Achilli A, Anastasio D, et al. Standard Methodology for Evaluating Membrane Performance in Osmotically Driven Membrane Processes. Desalination. 2013;312:31-38.

196. Luo W, Xie M, Song X, Guo W, Ngo HH, Zhou JL, et al. Biomimetic aquaporin membranes for osmotic membrane bioreactors: Membrane performance and contaminant removal. Bioresource technology. 2018;249:62-68.

197. Luo W, Xie M, Hai FI, Price WE, Nghiem LD. Biodegradation of cellulose triacetate and polyamide forward osmosis membranes in an activated sludge bioreactor: Observations and implications. Journal of Membrane Science. 2016;510:284-92.

198. Madsen HT, Bajraktari N, Hélix-Nielsen C, Van der Bruggen B, Søgaard EG. Use of biomimetic forward osmosis membrane for trace organics removal. Journal of membrane science. 2015;476:469-74.

199. Zhao S, Zou L, Mulcahy D. Effects of membrane orientation on process performance in forward osmosis applications. Journal of membrane science. 2011;382(1-2):308-15.

200. Caushi D, Martens H. Absorption of bicarbonate in sheep omasum. Research in veterinary science. 2018;118:324-30.

201. Masot A, Franco A, Redondo E. Morphometric and immunohistochemical study of the abomasum of red deer during prenatal development. Journal of Anatomy. 2007;211(3):376-86.

202. Sklan D, Hurwitz S. Movement and absorption of major minerals and water in ovine gastrointestinal tract. Journal of dairy science. 1985;68(7):1659-66.

203. Piccione G, Foà A, Bertolucci C, Caola G. Daily rhythm of salivary and serum urea concentration in sheep. Journal of Circadian Rhythms. 2006;4(1):16.

204. Llamas M, Magdalena JA, González-Fernández C, Tomás-Pejó E. Volatile fatty acids as novel building blocks for oil-based chemistry via oleaginous yeast fermentation. Biotechnology and bioengineering. 2020;117(1):238-50.

205. Lukitawesa, Patinvoh RJ, Millati R, Sárvári-Horváth I, Taherzadeh MJ. Factors influencing volatile fatty acids production from food wastes via anaerobic digestion. Bioengineered. 2020;11(1):39-52.

206. Righetti E, Nortilli S, Fatone F, Frison N, Bolzonella D. A Multiproduct Biorefinery Approach for the Production of Hydrogen, Methane and Volatile Fatty Acids from Agricultural Waste. Waste and Biomass Valorization. 2020:1-8.

207. Khan JA, Nguyen LN, Duong HC, Nghiem LD. Acetic acid extraction from rumen fluid by forward osmosis. Environmental Technology & Innovation. 2020;20:101083.

208. Kim B, Gwak G, Hong S. Review on methodology for determining forward osmosis (FO) membrane characteristics: Water permeability (A), solute permeability (B), and structural parameter (S). Desalination. 2017;422:5-16.

209. Ramos AF, Terry SA, Holman DB, Breves G, Pereira LG, Silva AG, et al. Tucumã oil shifted ruminal fermentation, reducing methane production and altering the microbiome but decreased substrate digestibility within a RUSITEC fed a mixed hay–concentrate diet. Frontiers in microbiology. 2018;9:1647.

210. Cath TY, Elimelech M, McCutcheon JR, McGinnis RL, Achilli A, Anastasio D, et al. Standard methodology for evaluating membrane performance in osmotically driven membrane processes. Desalination. 2013;312:31-38.

211. Martin JT, Kolliopoulos G, Papangelakis VG. An improved model for membrane characterization in forward osmosis. Journal of Membrane Science. 2020;598:117668.

212. Wei J, Qiu C, Tang CY, Wang R, Fane AG. Synthesis and characterization of flat-sheet thin film composite forward osmosis membranes. Journal of Membrane Science. 2011;372(1-2):292-302.

213. Artegoitia VM, Foote AP, Lewis RM, Freetly HC. Rumen fluid metabolomics analysis associated with feed efficiency on crossbred steers. Scientific Reports. 2017;7(1):1-14.

214. Praveen P, Nguyen DTT, Loh K-C. Biodegradation of phenol from saline wastewater using forward osmotic hollow fiber membrane bioreactor coupled chemostat. Biochemical Engineering Journal. 2015;94:125-33.

215. Kim C-M, Kim S-J, Kim LH, Shin MS, Yu H-W, Kim IS. Effects of phosphate limitation in feed water on biofouling in forward osmosis (FO) process. Desalination. 2014;349:51-59.

216. Miura Y, Watanabe Y, Okabe S. Membrane biofouling in pilot-scale membrane bioreactors (MBRs) treating municipal wastewater: impact of biofilm formation. Environmental science & technology. 2007;41(2):632-38.

217. Bolyen E, Rideout JR, Dillon MR, Bokulich NA, Abnet CC, Al-Ghalith GA, et al. Reproducible, interactive, scalable and extensible microbiome data science using QIIME 2. Nature Biotechnology. 2019;37(8):852-57.

218. Glöckner FO, Yilmaz P, Quast C, Gerken J, Beccati A, Ciuprina A, et al. 25 years of serving the community with ribosomal RNA gene reference databases and tools. Journal of Biotechnology. 2017;261:169-76.

219. Xin J, Chai Z, Zhang C, Zhang Q, Zhu Y, Cao H, et al. Comparing the Microbial Community in Four Stomach of Dairy Cattle, Yellow Cattle and Three Yak Herds in Qinghai-Tibetan Plateau. Frontiers in Microbiology. 2019;10(1547).

220. Krause DO, Denman SE, Mackie RI, Morrison M, Rae AL, Attwood GT, et al. Opportunities to improve fiber degradation in the rumen: microbiology, ecology, and genomics. FEMS Microbiology Reviews. 2003;27(5):663-93.

221. Palevich N, Kelly WJ, Leahy SC, Denman S, Altermann E, Rakonjac J, et al. Comparative Genomics of Rumen Butyrivibrio spp. Uncovers a Continuum of Polysaccharide-Degrading Capabilities. Applied and Environmental Microbiology. 2019;86(1):e01993-19.

222. Flint HJ, Bayer EA, Rincon MT, Lamed R, White BA. Polysaccharide utilization by gut bacteria: potential for new insights from genomic analysis. Nature Reviews Microbiology. 2008;6(2):121-31.

223. Kishimoto A, Ushida K, Phillips GO, Ogasawara T, Sasaki Y. Identification of Intestinal Bacteria Responsible for Fermentation of Gum Arabic in Pig Model. Current Microbiology. 2006;53(3):173-77.

224. Gagen EJ, Padmanabha J, Denman SE, McSweeney CS. Hydrogenotrophic culture enrichment reveals rumen Lachnospiraceae and Ruminococcaceae acetogens and hydrogen-responsive Bacteroidetes from pasture-fed cattle. FEMS Microbiology Letters. 2015;362(14).

225. Van Gylswyk NO. Succiniclasticum ruminis gen. nov., sp. nov., a Ruminal Bacterium Converting Succinate to Propionate as the Sole Energy-Yielding Mechanism. International Journal of Systematic and Evolutionary Microbiology. 1995;45(2):297-300.

226. Deusch S, Camarinha-Silva A, Conrad J, Beifuss U, Rodehutscord M, Seifert J. A Structural and Functional Elucidation of the Rumen Microbiome Influenced by Various Diets and Microenvironments. Frontiers in microbiology. 2017;8:1605-05.

227. Sun Z, Yu Z, Wang B. Perilla frutescens Leaf Alters the Rumen Microbial Community of Lactating Dairy Cows. Microorganisms. 2019;7(11):562.

228. Janssen PH, Kirs M. Structure of the Archaeal Community of the Rumen. Applied and Environmental Microbiology. 2008;74(12):3619.

229. Nagaraj V, Skillman L, Ho G, Li D, Gofton A. Characterisation and comparison of bacterial communities on reverse osmosis membranes of a full-scale desalination plant by bacterial 16S rRNA gene metabarcoding. npj Biofilms and Microbiomes. 2017;3(1):13.

230. Yang Y, Kitajima M, Pham TPT, Yu L, Ling R, Gin KYH, et al. Using Pseudomonas aeruginosa PAO1 to evaluate hydrogen peroxide as a biofouling control agent in membrane treatment systems. Letters in Applied Microbiology. 2016;63(6):488-94.

231. Curtin AM, Thibodeau MC, Buckley HL. The Best-Practice Organism for Single-Species Studies of Antimicrobial Efficacy against Biofilms Is Pseudomonas aeruginosa. Membranes. 2020;10(9).

232. Yu C, Wu J, Contreras AE, Li Q. Control of nanofiltration membrane biofouling by Pseudomonas aeruginosa using d-tyrosine. Journal of Membrane Science. 2012;423-424:487-94.

233. Vanysacker L, Denis C, Declerck P, Piasecka A, Vankelecom IFJ. Microbial adhesion and biofilm formation on microfiltration membranes: a detailed characterization using model organisms with increasing complexity. BioMed research international. 2013;2013:470867-67.

234. Wu C, Cheng Y-Y, Yin H, Song X-N, Li W-W, Zhou X-X, et al. Oxygen promotes biofilm formation of Shewanella putrefaciens CN32 through a diguanylate cyclase and an adhesin. Scientific Reports. 2013;3(1):1945.

235. Zhou G, Yuan J, Gao H. Regulation of biofilm formation by BpfA, BpfD, and BpfG in Shewanella oneidensis. Frontiers in Microbiology. 2015;6(790).

236. Liang Y, Gao H, Chen J, Dong Y, Wu L, He Z, et al. Pellicle formation in Shewanella oneidensis. BMC Microbiol. 2010;10:291-91.

237. McLean JS, Pinchuk GE, Geydebrekht OV, Bilskis CL, Zakrajsek BA, Hill EA, et al. Oxygen-dependent autoaggregation in Shewanella oneidensis MR-1. Environmental Microbiology. 2008;10(7):1861-76.

238. Talagrand-Reboul E, Jumas-Bilak E, Lamy B. The Social Life of Aeromonas through Biofilm and Quorum Sensing Systems. Frontiers in Microbiology. 2017;8(37).

239. Balasubramanian V, Palanichamy S, Subramanian G, Rajaram R. Development of polyvinyl chloride biofilms for succession of selected marine bacterial populations. J Environ Biol. 2012;33(1):57-60.

240. Mizan MFR, Jahid IK, Ha S-D. Microbial biofilms in seafood: A food-hygiene challenge. Food Microbiology. 2015;49:41-55.

241. Oh H-S, Constancias F, Ramasamy C, Tang PYP, Yee MO, Fane AG, et al. Biofouling control in reverse osmosis by nitric oxide treatment and its impact on the bacterial community. Journal of Membrane Science. 2018;550:313-21.